



THE HONG KONG  
POLYTECHNIC UNIVERSITY

香港理工大學

Pao Yue-kong Library

包玉剛圖書館

---

## Copyright Undertaking

This thesis is protected by copyright, with all rights reserved.

**By reading and using the thesis, the reader understands and agrees to the following terms:**

1. The reader will abide by the rules and legal ordinances governing copyright regarding the use of the thesis.
2. The reader will use the thesis for the purpose of research or private study only and not for distribution or further reproduction or any other purpose.
3. The reader agrees to indemnify and hold the University harmless from and against any loss, damage, cost, liability or expenses arising from copyright infringement or unauthorized usage.

### IMPORTANT

If you have reasons to believe that any materials in this thesis are deemed not suitable to be distributed in this form, or a copyright owner having difficulty with the material being included in our database, please contact [lbsys@polyu.edu.hk](mailto:lbsys@polyu.edu.hk) providing details. The Library will look into your claim and consider taking remedial action upon receipt of the written requests.

Pao Yue-kong Library, The Hong Kong Polytechnic University, Hung Hom, Kowloon, Hong Kong

<http://www.lib.polyu.edu.hk>

**QUANTITATIVE PERFORMANCE  
ASSESSMENT AND OPTIMAL DESIGN  
OF MICROGRID SYSTEMS  
CONSIDERING SUPPLY-DEMAND  
UNCERTAINTIES**

**LUO JIANING**

**PhD**

**The Hong Kong Polytechnic University**

**2023**

The Hong Kong Polytechnic University

Department of Building Environment and Energy Engineering

**QUANTITATIVE PERFORMANCE  
ASSESSMENT AND OPTIMAL DESIGN  
OF MICROGRID SYSTEMS  
CONSIDERING SUPPLY-DEMAND  
UNCERTAINTIES**

**LUO JIANING**

**A thesis submitted in partial fulfillment of the requirements for the  
degree of Doctor of Philosophy**

Oct 2022

## **CERTIFICATE OF ORIGINALITY**

I hereby declare that this thesis is my own work and that, to the best of my knowledge and belief, it reproduces no materials previously published or written, nor material that has been accepted for the award of any other degree or diploma, except where due acknowledgement has been made in the text.

\_\_\_\_\_ (Signed)

LUO Jianing (Name of student)

# ABSTRACT

Abstract of thesis entitled: Quantitative performance assessment and optimal design of microgrid systems considering supply-demand uncertainties

Submitted by : LUO Jianing

For the degree of : Doctor of Philosophy

at The Hong Kong Polytechnic University in September 2022

Reducing carbon emissions and achieving carbon neutrality are urgent tasks for sustainable development. High renewable energy penetration in power generation is increasingly recognized as a solution to current environmental challenges and energy crises. Microgrids, as efficient means, have received increasing attention due to their potential to achieve high renewable energy penetration. Microgrid quantitative assessment and optimal design play significant roles in achieving high renewable energy penetration in power generation. However, quantitative approaches for the microgrid performance assessment and some key indexes to quantify the microgrid performance are still absent to provide the support and guideline for optimal microgrid design. In addition, existing microgrid optimal design methods optimize microgrids with simple assumptions for the demand-side variables. These methods are simple to implement but may result in reduced security/reliability and higher investment cost as the impacts of the demand-side systems on microgrid overall performance are not quantitatively considered. A trade-off between system reliability and the overall cost cannot be achieved.

This study, therefore, aims to develop assessment approaches to quantify microgrid performance, including the economics, reliability (i.e., system adequacy and security),

and renewable energy penetration, and to develop effective and comprehensive optimal design methods considering the supply-demand sides simultaneously.

The contributions to the development of the microgrid quantitative assessment approaches are listed below.

1. A multi-dimensional performance assessment approach for the convenient assessment of microgrids is developed concerning their key performance indicators (i.e., economics, reliability, and renewable energy penetration). An empirical cost model is developed based on the Latin hypercube sampling (LHS) method, which can effectively reduce the computation cost and achieve acceptable accuracy compared with the conventional exhaustive method. The outputs of this work can effectively quantify the multi-dimensional performance of the microgrid.

2. A quantitative approach is proposed to assess the security of microgrids' dynamic load of power consumers. Two simplified generic transient models are developed based on the ANOVA (analysis of variance) method to quantify chiller motor startup performance, including inrush current and startup time. The microgrid blackout risk and system wear potential can be effectively quantified using the proposed quantitative approach and models. The quantitative approach and the utilization of the simplified generic transient startup power models are tested and verified using a hotel microgrid on a remote island. The outputs of this work can effectively quantify the system security and system wear potential in the real application of the microgrid design and chiller size determination.

3. A novel uncertainty-based reliability assessment approach is developed for microgrids considering uncertainties at both supply and demand sides. A new reliability index (named power inadequacy risk) is proposed, and a risk quantification

method is developed to measure the risk/probability of power inadequacy under uncertainties. The uncertainties at both supply and demand sides are detailedly quantified using a bottom-up approach.

As for developing the optimal microgrid design, we proposed two methods to enhance and trade off the microgrid reliability and economics, as summarized below.

1. A coordinated optimal design method is proposed for enhanced reliability and economics of microgrids. The designs of supply and demand systems are optimized simultaneously. Microgrid security is assessed quantitatively by considering the impacts of demand-side systems and considered as the optimization constraints together with the power supply adequacy. On the premise of ensuring power supply adequacy, the system security is enhanced significantly while achieving 5% of overall cost savings.

2. A robust optimal design method is proposed to obtain a trade-off between reliability enhancement and cost saving. As for enhancement of reliability, a novel indicator named power inadequacy risk is introduced by considering the supply-demand uncertainties simultaneously to quantify the probability of power supply inadequacy, which is used as a cost penalty in the optimization objective. In addition, the applicability and difference of two commonly-used robust optimal objective functions are analyzed, and their design solutions are compared with conventional optimization methods. The maximum overall cost saving is up to 16.5%, and power inadequacy risk is reduced by over 220 times maximum compared to existing optimal design methods.

## PUBLICATIONS ARISING FROM THIS THESIS

### Journal Papers

[1] **Jianing Luo**, Hangxin Li, Shengwei Wang. (2022). A quantitative approach and simplified generic transient motor startup power models for microgrids security assessment. *Sustainable Cities and Society*, 83,103998.

[2] **Jianing Luo**, Hangxin Li, Gongsheng Huang, Shengwei Wang. (2022). A multi-dimensional performance assessment framework for microgrids concerning renewable penetration, reliability, and economics. *Journal of Building Engineering*. 63, 105508.

[3] **Jianing Luo**, Hangxin Li, Shengwei Wang. (2022). A quantitative reliability assessment and risk quantification method for microgrids considering supply and demand uncertainties. *Applied Energy*, 328,120130.

[4] **Jianing Luo**, Hangxin Li, Shengwei Wang. (2022). Coordinated optimal design of islanded microgrids for enhanced reliability and economics based on a quantitative security assessment. *Renewable energy*. (Under review).

[5] **Jianing Luo**, Hangxin Li, Shengwei Wang. (2022). Robust optimal design of microgrids to enhance the reliability and economics considering the quantified power inadequacy risk. Preparation.

## **Conference Papers**

[1] **Jianing Luo**, Shengwei Wang, Hangxin Li. (2020). Taguchi-based sensitivity analysis of the price fluctuations, CO2 penalty and system reliability quantification in microgrid design. *11th International Conference on Applied Energy*. Paper ID 329. December 01 to 10, 2020, Bangkok / Virtual, Thailand.

[2] **Jianing Luo**, Shengwei Wang, Hangxin Li. (2021). A quantitative approach of microgrid performance assessment at the planning stage. *7th Applied Energy Symposium 2021: Low carbon cities and urban energy system*. Paper ID 79. September 04 to 08. Matsue, Japan.

## ACKNOWLEDGEMENTS

First and foremost, I would like to express my deepest gratitude to my supervisor, Professor Shengwei Wang, my supervisor, I benefited greatly from his excellent guidance throughout my graduate studies. His readily available supervision, extensive expertise, and charismatic personality enabled me to learn a lot during the research period. I would also like to thank my co-supervisors, Dr. Hangxin Li, and Professor Fu Xiao, for their suggestions and support throughout my Ph.D. study.

I would also like to express my heartfelt appreciation to all colleagues in the BEAR research group, especially Dr. Kui Shan, Dr. Xiuming Li, Dr. Chaoqun Zhuang, Dr. Chong Zhang, Dr. Zhuang Zheng, and Dr. Huilong Wang. Their talents and diligence always inspire and encourage me to be better.

Finally, I am truly grateful for my family's love, support, and patience. Without them, I would not have been able to thrive in my doctoral program. I am incredibly grateful for those friends who have provided tacit and powerful support over the past three years. Without their love and support, this research work would not have been finished possible. This thesis is dedicated to them.

# TABLE OF CONTENTS

<b>CERTIFICATE OF ORIGINALITY.....</b>	<b>i</b>
<b>ABSTRACT .....</b>	<b>ii</b>
<b>PUBLICATIONS ARISING FROM THIS THESIS .....</b>	<b>v</b>
<b>ACKNOWLEDGEMENTS.....</b>	<b>vii</b>
<b>TABLE OF CONTENTS.....</b>	<b>viii</b>
<b>LIST OF FIGURES .....</b>	<b>i</b>
<b>LIST OF TABLES .....</b>	<b>vi</b>
<b>NOMENCLATURE.....</b>	<b>i</b>
<b>CHAPTER 1 INTRODUCTION .....</b>	<b>1</b>
1.1 Background and motivation.....	1
1.2 Aim and objectives.....	4
1.3 Organization of this thesis.....	5
<b>CHAPTER 2 LITERATURE REVIEW .....</b>	<b>9</b>
2.1 Overview of microgrid investigation .....	9
2.1.1 Microgrid definition and operation modes.....	9
2.1.2 Worldwide development .....	11
2.2 Microgrid assessment approaches and reliability analysis .....	13
2.2.1 Microgrid assessment approaches.....	13
2.2.2 Reliability definition and classification.....	14

2.2.3	Reliability solutions and challenges .....	15
2.2.4	Reliability assessment approaches and summary of the reliability indexes .....	19
2.3	Optimal design of microgrids .....	21
2.3.1	Supply-demand profiles considered in optimal design .....	21
2.3.2	Optimal design of microgrid considering the reliability impacts.....	22
2.3.3	Energy efficiency consideration in design optimization.....	24
2.4	Uncertainty quantitation analysis and robust optimal design .....	25
2.4.1	Uncertainties quantification methods and analysis .....	25
2.4.2	Robust optimal design methods concerning the uncertainties .....	25
2.5	Summary .....	27
<b>CHAPTER 3 REFERENCE HOTEL MICROGRID AND HOTEL MICROGRID SIMULATION MODEL.....</b>		<b>30</b>
3.1	Description of the reference hotel microgrid .....	30
3.1.1	Basic information of the hotel.....	30
3.1.2	Configuration of hotel microgrid energy system .....	32
3.2	Microgrid simulation model.....	32
3.2.1	Power generation models .....	32
3.2.2	Demand-side energy system model .....	34
3.2.3	Energy storage model.....	35
3.3	Microgrid system control mechanism.....	36



4.4.3	Reliability vs economics .....	53
4.5	Summary .....	55
<b>CHAPTER 5 A QUANTITATIVE APPROACH AND SIMPLIFIED GENERIC</b>		
<b>TRANSIENT MOTOR STARTUP POWER MODELS FOR MICROGRIDS</b>		
<b>SECURITY ASSESSMENT.....56</b>		
5.1	Procedure and method of quantitative security assessment .....	56
5.1.1	Outline of security assessments quantification procedure and method...56	
5.1.2	Determination of microgrid transient load capacity.....58	
5.1.3	Introduction of equivalent overloaded load .....	59
5.1.4	Formulation of the quantitative approach .....	60
5.2	Development and validation of transient startup power models for chillers/motors	
	63	
5.2.1	Basic assumption and feature of models, and the model development procedure .....	63
5.2.2	Identification of input variables of significance and model inputs .....	66
5.2.3	Inrush current model and startup time model developed .....	66
5.2.4	Identification of inputs for inrush current and startup time models.....	68
5.2.5	Identification of model coefficients and fitness verification.....	70
5.2.6	Model validation .....	73
5.3	Security assessment and assessment results.....	74
5.3.1	Overview of the microgrid assessed and estimation of annual inrush load- embedded dynamic load profile.....	74

5.3.2	Results of risk-based microgrid capacity quantification and analysis ....	77
5.3.3	Results of microgrid system wear potential quantification and analysis	79
5.4	Summary .....	80
<b>CHAPTER 6 COORDINATED OPTIMAL DESIGN OF ISLANDED MICROGRIDS FOR ENHANCED RELIABILITY AND ECONOMICS BASED ON QUANTITATIVE SECURITY ASSESSMENT .....</b>		
<b>81</b>		
6.1	Procedure and objectives of coordinated optimal design.....	81
6.1.1	Procedure and the major steps.....	81
6.1.2	Optimization objectives for microgrid optimal design .....	84
6.1.3	Constraints for microgrid system design.....	86
6.2	Overview of the design case study and the microgrid system models.....	88
6.2.1	Description of the microgrid and its control strategies .....	88
6.2.2	Basic information of the design variables and their search ranges .....	88
6.3	Results of optimization case studies and performance analysis .....	91
6.3.1	Overview of the optimization cases .....	91
6.3.2	Results of microgrid design optimization .....	92
6.3.3	Performance analysis and comparison .....	93
6.4	Summary .....	97
<b>CHAPTER 7 A QUANTITATIVE RELIABILITY ASSESSMENT AND RISK QUANTIFICATION METHOD FOR MICROGRIDS CONSIDERING SUPPLY AND DEMAND UNCERTAINTIES .....</b>		
<b>99</b>		

7.1	Uncertainty-based quantitative approach for microgrid reliability assessment..	99
7.1.1	Outline of the proposed reliability assessment approach .....	99
7.1.2	Quantification of uncertainties in power generation and consumption.	101
7.1.3	Uncertainty-based power inadequacy risk quantification for microgrid reliability assessment .....	103
7.1.4	Reliability performance assessment using the commonly-used indexes .....	105
7.2	Basic information and its distributions of the main uncertain parameters concerned for the test case .....	106
7.2.1	Basic information for the test case .....	106
7.2.2	Distributions of the main uncertain parameters concerned.....	107
7.3	Test results and reliability performance analysis .....	108
7.3.1	Distributions of power generation and consumption under uncertainties .....	108
7.3.2	Results of power inadequacy risk quantification .....	111
7.3.3	Results of reliability performance assessment using commonly-used indexes .....	116
7.3.4	Impacts of backup power generator capacity on microgrid reliability performance .....	117
7.4	Summary .....	119

<b>CHAPTER 8 ROBUST OPTIMAL DESIGN OF MICROGRIDS TO ENHANCE THE RELIABILITY AND ECONOMICS CONSIDERING THE QUANTIFIED POWER INADEQUACY RISK.....</b>	<b>120</b>
8.1 Procedure and objectives of robust optimal design .....	120
8.1.1 Approach and steps of robust design optimization .....	120
8.1.2 Optimization objectives for microgrid optimal design .....	122
8.1.3 Quantification of uncertainties in power generation and consumption.....	123
8.1.4 Reliability constraints and power inadequacy risk quantification .....	124
8.2 Basic information of the microgrid and model development .....	125
8.2.1 Design variables concerned and basic data of energy system parameters .....	125
8.2.2 Parameter uncertainty quantifications.....	127
8.3 Results of optimization case studies and performance analysis .....	128
8.3.1 Basic information of the proposed cases and their design results.....	128
8.3.2 Comparison and analysis of the economic performance.....	130
8.3.3 Comparison and analysis of the reliability performance.....	133
8.3.4 Energy use efficiency performance comparison and analysis .....	136
8.4 Discussion on microgrid optimization developments considering different reliability requirements .....	138
8.5 Summary .....	139
<b>CHAPTER 9 CONCLUSIONS AND FUTURE WORK.....</b>	<b>140</b>

9.1 Summary of main contributions.....	140
9.2 Conclusions.....	141
9.3 Recommendations for future work .....	147
<b>REFERENCES.....</b>	<b>149</b>

## LIST OF FIGURES

Figure 3.1 Overview of the building microgrid location .....	31
Figure 3.2 Annual solar radiation and wind velocity in this location .....	31
Figure 3.3 Configuration of the hotel microgrid energy systems. ....	32
Figure 3.4 Relative COP of chillers at different load ratios.....	35
Figure 3.5 Flowchart of the Microgrid system control mechanism.....	37
Figure 4.1 The framework of the microgrid quantitative assessment.....	39
Figure 4.2 R-squared values of empirical cost model concerning different powers of the input variables .....	45
Figure 4.3 A comparison between accuracy and computation cost of the empirical cost models .....	49
Figure 4.4 Correlation among three microgrid performance indicators .....	50
Figure 4.5 The correlations between REP and economics of the different microgrid energy portfolios under different reliabilities .....	51
Figure 4.6 Monthly microgrid power and load profiles under two renewable energy penetration scenarios.....	53
Figure 4.7 Quantification results of the reliability and the economics .....	53
Figure 4.8 Monthly microgrid power and load profiles under two reliability requirements.....	54
Figure 5.1 Outline of the proposed security assessment .....	58
Figure 5.2 Schematic representation of the microgrid operation states .....	59

Figure 5.3 Functions of the failure probabilities in different partial load ratios .....	62
Figure 5.4 Schematic representation of inrush current waveform and basic assumption of inrush current calculation .....	64
Figure 5.5 Procedure of the model development .....	65
Figure 5.6 Identification of inrush current model inputs of significance.....	69
Figure 5.7 Identification of startup time model inputs of significance .....	70
Figure 5.8 Actual residuals (a) and standardized residuals (b) of linear and nonlinear inrush current models.....	71
Figure 5.9 Fitness verification of the two inrush current models .....	72
Figure 5.10 Actual residual and standardized residual for the startup time model....	72
Figure 5.11 Fitness verification of the startup time model .....	73
Figure 5.12 The profile of the annual dynamic cooling load (a) and dynamic electrical load (b) in the hotel microgrid .....	75
Figure 5.13 Three scenarios of the monthly number of the chillers in operation and their inrush load-embedded dynamic load profiles of the microgrid employing three different sizes of chillers .....	77
Figure 5.14 The microgrid blackout risk quantification in the overloaded cases among the different motor capacity ratios .....	79
Figure 5.15 System wear potential quantification among the different motor capacity ratios.....	80

Figure 6.1 Outline of the conventional optimal design method and the proposed coordinated optimal design method for power generation and demand-side systems of microgrids .....	84
Figure 6.2 The unit price of the chiller under different sizes.....	91
Figure 6.3 Cost of the optimal microgrid system designs given by the coordinated and the conventional optimization.....	94
Figure 6.4 Transient load ratios during the chiller startup and the number of the chiller startup times in these two design cases.....	95
Figure 6.5 Annual COP profiles of the optimized chillers given by the coordinated and the conventional optimization.....	96
Figure 7.1 Procedure of the proposed uncertainty-based reliability assessment approach.....	101
Figure 7.2 Schematic microgrid supply-demand profiles in the conventional reliability assessment (a) and uncertainty-based reliability assessment (b) .....	104
Figure 7.3 Distribution of hourly renewable power generation and its cumulative density function.....	109
Figure 7.4 Distribution of the hourly microgrid load and its cumulative density function .....	110
Figure 7.5 Hourly minimum and maximum available generation capacity and power consumption generated using the proposed approach.....	111
Figure 7.6 Hourly available generation capacity and power consumption generated using the conventional approach.....	111
Figure 7.7 Distribution of outage power and its cumulative density function.....	112

Figure 7.8 Average hourly power inadequacy risk of the test microgrid under uncertainties ..... 113

Figure 7.9 Average monthly power inadequacy risk of the test microgrid under uncertainties ..... 114

Figure 7.10 24-hour average power inadequacy risk of the test microgrid under uncertainties ..... 115

Figure 7.11 ELF values under different backup power generator capacities when uncertainties are considered ..... 118

Figure 7.12 Power inadequacy risks under different backup power generator capacities when uncertainties are considered ..... 119

Figure 8.1 Outline of the proposed robust optimal design method of the microgrid ..... 122

Figure 8.2 The optimization process for the proposed optimization cases ..... 129

Figure 8.3 Cost results of different items among the different optimization cases.. 132

Figure 8.4 Results of the overall cost and the comparison ratios among these optimization cases ..... 133

Figure 8.5 Power inadequacy risk performance among four cases..... 135

Figure 8.6 Quantification of the impacts of the power inadequacy risk on microgrid economics..... 136

Figure 8.7 Comparison results of the COP profiles between Case 1 and Reference case R2 and the corresponding cooling load profile ..... 137

Figure 8.8 Overall cost results under different average operation COP values ..... 138

Figure 8.9 Summary of the microgrid optimization developments considering different reliability requirements ..... 139

## LIST OF TABLES

Table 2.1 Summary characteristics of four representative projects in USA .....	12
Table 2.2 Categories of peak current, its causes and solutions (Hwang and Lou, 1998) .....	17
Table 2.3 Summary of the commonly used reliability indexes.....	21
Table 4.1 Microgrid variables and their range at the planning stage .....	42
Table 4.2 Basic data of microgrid hybrid power generation system* .....	43
Table 4.1 Microgrid variables concerned with the reference model development ....	46
Table 4.4 The detailed specifications of the adopted computer.....	47
Table 4.5 Accuracy and computation cost of empirical cost models.....	48
Table 5.1 List of motor specifications and model inputs .....	66
Table 5.2 Detailed information of the inrush current model.....	67
Table 5.3 Detailed information of the startup time model .....	67
Table 5.4 Model validation results.....	74
Table 6.1 Design parameters to be optimized and their searching ranges .....	89
Table 6.2 Basic performance and cost data of the main microgrid facilities* .....	90
Table 6.3 Optimal design solutions given by the two optimal design methods.....	93
Table 6.4 Renewable energy penetration in the optimized microgrid systems given by the coordinated and the conventional optimization .....	97
Table 7.1 Sizes of the hotel microgrid system components.....	107
Table 7.2 Main uncertain parameters and their distributions concerned .....	108

Table 7.3 Results of reliability performance assessment using commonly-used indexes .....	117
Table 8.1 Key microgrid design parameters and their searching ranges .....	126
Table 8.2 Basic information and cost data of the microgrid and its energy systems * .....	127
Table 8.3 Parameter uncertainty distributions in the microgrid robust optimal design .....	128
Table 8.4 Basic information of the proposed cases .....	129
Table 8.5 Optimal design results of the microgrid between Case 1 and Case 2 .....	129
Table 8.6 Optimal design results of the microgrid among these cases .....	130
Table 8.7 Reliability performance for these optimization cases .....	134
Table 8.8 Results of the energy efficiency among the different optimization cases	136

# NOMENCLATURE

$A_{PV}$	Total area of PV panels
$Con_{BPG}$	Natural gas consumption
$Cap_{chi}$	Chiller capacity
$Cap_{mic}$	Microgrid capacity
$C_{fac,k}$	The initial cost of the kth facility
$C_{ov}$	Microgrid overall cost
$C_{ini}$	Initial cost
$C_{opt}$	Operation cost
$C_{emi}$	Carbon emission cost
$CL$	Cooling load
$COP$	Coefficient of performance
$D$	Total of days
$d_t$	Validated values from the actual performance data
$E_{bat}$	Battery storage
$E_R$	Relative error of the model
$F_{ove}$	Function of the overall objective
$F_{cos}$	Function of the cost
$F_{emi}$	Function of the carbon emission
$FP$	Failure probability
$G_i$	Distribution of the $i^{\text{th}}$ uncertain parameter
$H$	The number of the total steps
$I_{current}$	Inrush current
$ICS$	Inrush current shock
$K_{PV}$	Temperature coefficient
$L_{equ}$	The equivalent overloaded load
$L_{ove}$	The overloaded load
$\bar{m}$	The Average value of the validated values
MA	Model accuracy
$N_{tot}$	Number of total data points
$N_{ove}$	Number of overloaded cases
$N^t$	The number of the chiller startup at the time t
$p_{dch}$	Battery power discharging

$P_{EC}$	Power consumption of electrical chiller
$Prb$	Occurrence probabilities
$pi_{t,s}$	Power inadequacy occurrence index
$P_{ren}$	Renewable power usage
$P_{CL}$	Power consumption of chillers
$P_{dem,t}$	Power consumption at time step $t$
$P_{sup,t}$	Power generation at time step $t$
$P_{WT}$	Power generated from wind source
$P_{PV}$	Power generated from solar radiation
$P_{BPG}$	Backup power generation from natural gas
$Pr_{BPG}$	Primary energy consumption price
$p_{ch}$	Battery power charging
$p$	Number of the adjustable model parameters
$Re$	Reliability
$R_{pi}$	Power inadequacy risk
$Rad$	Solar radiation per area
$R_{pi,ave}$	Average power inadequacy risk
$R_{WAT}$	Risk of system wear and tear
$R_{acom}$	Accumulated annual number of the microgrid blackout times
$R_{av}$	Annual average failure probability of overloaded cases
$s_t$	Validated values from prediction by the models
$t$	Timestep
$T_{amb}$	Ambient temperature
$T_{ref}$	PV panels reference temperatures
$T_{startup}$	Startup time
$\Delta T$	The reference duration
$UP_{gas}$	Unit price of the gas generator
$\Delta V_{upper}$	Upper boundary difference
$\Delta V_{lower}$	Lower boundary difference
$v_{wind}$	Wind speeds
$x_n$	$n^{\text{th}}$ uncertain parameters/inputs
$Y$	Distribution of outputs
$Y_k$	The total years of the life cycle

## ***Subscripts***

<i>ANOVA</i>	Analysis of variance
<i>CAIFI</i>	Customer Average Interruption Frequency Index
<i>CDF</i>	Cumulative density function
<i>CVRMSE</i>	Coefficient of Variance of the Root Mean Square Error
<i>EENS</i>	Expected Energy not Supplied
<i>ELF</i>	Equivalent Loss Factor
<i>FMEA</i>	Failure mode and effects analysis
<i>GA</i>	Genetic algorithm
<i>HVAC</i>	Heating, ventilation, and air conditioning
<i>ICS</i>	Inrush current shock
<i>LHS</i>	Latin hypercube sampling
<i>LOEE</i>	Loss of Energy Expected
<i>LOLE</i>	Loss of Load Expected
<i>LPSP</i>	Loss of Power Supply Probability
<i>MCS</i>	Monte Carlo simulation
<i>MBR</i>	Microgrid blackout risk
<i>NMBE</i>	Normalized Mean Bias Error
<i>REP</i>	Renewable energy penetration
<i>SAIDI</i>	System Average Interruption Duration Index
<i>SAIFI</i>	System Average Interruption Frequency Index
<i>SaF</i>	Safety factor
<i>SuF</i>	Surge factor
<i>SWP</i>	System wear potential
<i>TMY</i>	Typical meteorological year
<i>ave</i>	average
<i>amb</i>	ambient
<i>bat</i>	battery
<i>c</i>	cooling system
<i>dem</i>	demand
<i>emi</i>	carbon emission
<i>fac</i>	facility
<i>max</i>	the maximum value
<i>min</i>	the minimum value
<i>ov</i>	overall
<i>ref</i>	reference
<i>sup</i>	supply

### ***Greek symbols***

$\eta_{BPG}$	Backup power generator efficiency
$\eta_{PV}$	Overall efficiency of PV panels
$\eta_{ch}$	Charging efficiency
$\eta_{dch}$	Discharging efficiency
$\alpha_{COP}$	Relative COP
$\omega$	Weight ratio
$\Delta$	Standard deviation

# CHAPTER 1 INTRODUCTION

## 1.1 Background and motivation

Currently, the world is facing significant challenges of energy crisis and environmental pollution due to the increasing consumption of fossil fuels. Yearly carbon emissions have grown continuously from 1.3% to 2.2% in the last thirty years (IPCC, 2014). Urgent measures, such as energy-efficient technologies and essential policy support, are necessary to address these critical energy and environmental issues.

Global governments are setting ambitious goals toward carbon neutrality. China will scale up its contribution to these issues and aims to reach peak CO<sub>2</sub> emissions by 2030 and achieve carbon neutrality before 2060 (IEA, 2020). Besides, the Committee on Industry, Research and Energy (ITRE) of the European Union (EU) announced in 2022 that the EU aims to become the first climate-neutral continent by 2050 (EEA, 2022). To deliver on this ambition, the different measures and technologies in the energy sector are investigated and tested.

In addition to government policies, renewable resources provide a promising means to address these critical energy and environmental issues. Renewable energy technologies, particularly solar and wind energy, are studied. The deployments of the renewable energy system in different forms and scales are investigated and tested. Among different types of renewable energy systems, microgrids have gained great interest in academia and practical engineering due to their enormous potential to secure a sustainable power supply with high renewable energy penetration.

As a new type of power generation system, a microgrid can be used as an effective supplement to the traditional power system. Power generation from renewable

resources is used to meet the demand, which can significantly decrease the consumption of fossil fuels.

Due to their advantages, microgrid technologies are experiencing an increasing application as a sustainable power generation system worldwide. For instance, a physical microgrid integrated with a virtual community energy market platform is developed in Brooklyn, New York (Mengelkamp et al., 2018). Renewable power generators and backup power generators, as the critical components of the physical microgrid, are used to provide the power supply. Both power consumers and prosumers can achieve economic profits from microgrid technologies. The microgrid system can provide incentives for investments and effectively decrease the consumption of fossil fuels.

In the future, the microgrid system will be more widely applied than the traditional fossil-fuel-fired power generation system with the progress made in new technologies and the increased costs of traditional fossil fuels. However, the development of microgrids at the planning and design stages is still faced with many technical challenges:

Firstly, microgrid performance assessment methods and tools at the planning and design stages are essential. These methods are valuable in providing insights for decision-makers regarding their multiple key performance indicators, including renewable penetration, reliability, and economics. However, most existing studies focus on or are limited to assessing the impacts using a single performance indicator, or the performance indicators are considered separately. The interactions among multiple performance indicators have not been considered due to the high computation costs. There is a need for an effective and simple multi-dimensional microgrid

performance assessment method with relatively lower computation costs in the quantitative calculation process while considering three key indicators (i.e., renewable penetration, reliability, and economics) together.

Secondly, enhancement of the security of the microgrids is another significant measure to secure the system's reliable operation. The ability of microgrids to cope with internal disruptions (e.g., peak inrush current, short-circuit current, etc.) is usually much weaker than the main grid due to the smaller capacity. Here, the microgrid capacity is the maximum load that can be carried by the system (Khodaei and Shahidehpour, 2012; Miner et al., 2018), which is associated with the capacities of the main electrical equipment and devices (e.g., inverters, rectifiers, electrical cables, etc.). Expanding capacity and setting peak current limits are effective solutions. However, expanding microgrid capacity on the supply side is costly. Setting a peak current limit can reduce the magnitude of the peak current but requires careful design and operation on the demand side. Currently, the microgrid capacity is determined using safety and surge factors to meet the security requirement. It is a simple solution but may result in reduced security and higher investment costs as the impacts of the demand-side systems on microgrid security are not quantitatively considered. An effective security indicator is needed considering the demand-side impacts, and it should provide support and guideline in microgrid optimal design. In addition, using the new security indicator as the optimization constraint, a novel coordinated optimal design method of microgrids is needed to enhance security and economics simultaneously.

Thirdly, microgrid renewable energy generations such as wind turbines and solar photovoltaics (PV) can be considered as promising solutions to supply power with low emissions. However, their intermittent and fluctuating features threaten the system's reliability (i.e., power supply adequacy). Especially in an islanded microgrid, the

reliability issue is more critical due to no power charging from the main grids. The conventional solutions are conducting the microgrid reliability assessment and setting the reliability indexes as a constraint in the design optimization. However, the power supply inadequacy risk due to uncertainties is commonly ignored. The development of an effective, robust microgrid optimal design method considering both uncertainty-based risk quantitation and reliability constraint is needed.

## **1.2 Aim and objectives**

This study aims to provide essential and quantitative microgrid assessment methods and develop effective and comprehensive microgrid optimal design methods based on assessment results from the proposed assessment methods. It is accomplished by addressing the following objectives:

1. Construct a dynamic simulation platform for an islanded hotel microgrid system and simulate the microgrid system performance dynamically and accurately in the islanded mode for testing and validating the assessment and design methods developed in this thesis.
2. Develop and validate a novel multi-dimensional (i.e., renewable penetration, reliability, and economics) performance assessment approach for the microgrid systems. The assessment method is expected to reduce the computation costs while meeting the accuracy requirement.
3. Develop a quantitative approach to assess the security of microgrid dynamic load of power consumers and propose a simplified method to quantify chiller motor startup performance, including inrush current and startup time. The assessment method is expected to quantify the system security and wear potential in the real application of

the microgrid design and chiller size determination, which can provide a guideline to enhance the system security in further microgrid optimal design.

4. Develop a coordinated optimal design method for microgrids to enhance their security and economics. The method is expected to obtain the global optimal design solution, which needs to simultaneously optimize microgrid supply and demand systems.

5. Develop a quantitative reliability assessment and risk quantification method for microgrids with consideration of system uncertainties. The assessment method is expected to consider the supply and demand uncertainties together. The proposed novel risk index (named power inadequacy risk) can effectively quantify the risk of power supply inadequacy due to uncertainties. The impacts of uncertainties on system power supply adequacy can be quantified, and the system reliability can be enhanced.

6. Develop a robust optimal design method for microgrids to enhance their reliability and economics based on the quantified power inadequacy risk. The method is expected to effectively avoid the impacts of uncertain microgrid supply-demand variables on microgrid power supply adequacy and enhance the system's performance under uncertain operating conditions.

### **1.3 Organization of this thesis**

**Chapter 1** introduces the background and the motivation of this study on microgrid systems. The critical challenges for the microgrid quantitative assessment and its optimal design are presented and discussed, as well as the research aim and objectives.

**Chapter 2** presents a comprehensive literature review of related existing studies, including an overview of quantitative assessment, reliability analysis, and optimal

design for microgrid systems. The assessment approaches are introduced, which mainly include two main categories, i.e., the deterministic approach and the stochastic approach. Then the reliability analysis, including the reliability definition, categories, and existing quantitative indexes, is presented. Next, the design optimizations are introduced in terms of the design optimization methods and reliability considerations. Besides, the uncertainty analysis for microgrids is reviewed, including the uncertainty quantification methods on the supply and demand sides and the robust optimal design methods. This chapter also elaborates on the research gaps addressed in this thesis.

**Chapter 3** describes the development of the microgrid model, the energy system configurations, and its operating principles. A hotel microgrid is selected as the reference microgrid in this study. The microgrid model consists of power generation models (i.e., renewable power generation models and a backup power generation model), a battery storage model, and demand-side power generation models.

**Chapter 4** presents a multi-dimensional performance assessment approach for microgrids concerning renewable energy penetration, reliability, and economics. An empirical cost model is developed based on the Latin hypercube sampling (LHS) method, which can effectively reduce the computation costs while meeting the accuracy requirement. The proposed assessment method is validated on the developed hotel microgrid. Its performance in deviation and computation costs is evaluated by comparing it with the exhaustive searching method (ESM).

**Chapter 5** presents a quantitative security assessment approach concerning the microgrid dynamic load of power consumers. Two simplified generic transient models are developed based on the ANOVA (analysis of variance) method to quantify chiller motor startup performance, including inrush current and startup time. The proposed

quantitative approach can effectively quantify the microgrid blackout risk and system wear potential. The quantitative method and the utilization of the simplified generic transient startup power models are tested and verified using a hotel microgrid on a remote island.

**Chapter 6** presents a novel uncertainty-based reliability assessment approach for microgrids considering uncertainties at both supply and demand sides. A new reliability index is proposed, and a risk quantification method is developed to measure the risk/probability of power inadequacy under uncertainties. The uncertainties at both supply and demand sides are detailedly quantified using a bottom-up approach. The proposed reliability assessment approach and risk quantification method are tested on the developed hotel microgrid.

**Chapter 7** presents a coordinated microgrid optimal design method for enhancing the security and economics of microgrids. The design of supply and demand systems is optimized simultaneously. The microgrid security is assessed quantitatively, considering the impacts of demand-side systems and considered as the optimization constraints together with the power supply adequacy. The proposed coordinated microgrid optimal design method is tested on the developed hotel microgrid.

**Chapter 8** presents a robust optimal design method considering the supply-demand side uncertainties together. A novel index named power inadequacy risk is introduced to quantify the uncertainty-based power supply inadequacy risk and enhance reliability. Two typical robust optimization objective functions are selected, and their optimal design solutions are compared and analyzed. The energy use efficiency is considered in the optimization, and the impact of energy use efficiency on overall cost is analyzed.

**Chapter 9** summarizes the main contributions and conclusions of the Ph.D. study and gives recommendations for future research.

## CHAPTER 2 LITERATURE REVIEW

This chapter presents a comprehensive literature review on the concept, quantitative assessment methods, performance indicators, and optimal design of microgrids. The research background and research significance of the microgrids have been summarized.

*Section 2.1* presents an overview of microgrids, including their definitions, operating modes, and worldwide development.

*Section 2.2* presents a review of the microgrid assessment approaches and reliability investigations. Two typical microgrid assessment approaches are introduced. The definition, categories, solutions, and challenges of reliability are reviewed.

*Section 2.3* reviews the optimal designs of microgrid systems, including the microgrid supply-demand profiles, reliability, and energy efficiency considerations.

*Section 2.4* reviews the robust optimal designs of microgrid systems, including the uncertainty quantification and robust microgrid optimal design methods under uncertainties.

*Section 2.5* presents conclusive remarks on the reviews in the above research areas.

### **2.1 Overview of microgrid investigation**

#### ***2.1.1 Microgrid definition and operation modes***

Different microgrids definitions are developed by different investigations and energy departments. For instance, “*microgrids are local energy networks that are able to separate from the larger electrical grid during extreme weather events or emergencies, providing power to individual customers and crucial public services such as hospitals,*

*first responders, and water treatment facilities”* from Powering a New York State Energy Research and Development Authority (NY Prize, 2015) and *“A microgrid usually consists of multiple distributed energy generations (including renewable resources) and interconnected loads as well as the system controllers”* (Lasseter and Paigi, 2004).

The Office of Electricity Delivery and Energy Reliability within the Department of Energy (DOE) gave the widely accepted definition of microgrids in 2010. A microgrid refers to *“a group of interconnected loads and distributed energy resources within clearly defined electrical boundaries that acts as a single controllable entity with respect to the grid. a microgrid can connect and disconnect from the grid to enable it to operate in both grid-connected and/or island-mode”* (DOE, 2017)

Under the definition, the microgrids can work with two operating modes, i.e., grid-connected mode and islanded mode (i.e., isolated mode). The operating modes significantly impact microgrid reliability in terms of power supply adequacy. The grid-connected microgrid is easier to maintain the system reliability compared to the operating microgrid with solely islanded mode. The main grid, as strong support, can provide the power supply to avoid microgrid power outages. This typical mode is mostly applied in cities or locations where the microgrid is not far from the main grid.

On the other hand, for remote sites, the long-distance power transmission carried from the main grid would cause high energy loss and need high investment for the electrical facilities (Babazadeh et al., 2013). The islanded mode could be the only practical solution for the power supply in those remote areas or islands. In the islanded microgrid, the power generation is solely provided by itself without the backup of extra power from the main grid. Battery storage and/or local backup power generators

(mostly driven by fossil fuels) are necessarily considered in the design of islanded microgrids. The use of battery storage may lead to increased investment and pose a safety threat, while backup power generations would also lead to increased investment and carbon emissions.

### ***2.1.2 Worldwide development***

Different countries/regions have made efforts to develop microgrids in terms of feasibility, funding sources, technologies, and primary functions to combat climate change and the energy crisis. Four representative projects in the USA are summarized as shown in Table 2.1. These projects consider and test different types of power generators under diverse landscapes. Different departments, such as corporations, universities, and so on, have begun to make many efforts to promote this technology into practice in the future.

Besides, China began its microgrid investigation and development in the 12<sup>th</sup> Five-Year Plan. A total of 28 microgrid demonstration projects have been planned and/or constructed since 2015. Among these demonstration projects, the Tianjin Eco-City microgrid is one of the most successful demonstration projects (Yu et al., 2018). Their microgrid power generators consist of combined cooling heating power generators and PV panels, and the capacity has already been up to 39.6 MW since 2016.

Table 2.1 Summary characteristics of four representative projects in the USA

Project Funders	Location	Power generators	Energy storage
DOE and Alameda Country	Alameda Country, California	PV panels and diesel power generators	Battery storage
University of California, Irvine	Southern California Edison	Gas turbines and steam turbines	Battery and thermal storage
San Diego Gas and Electric and California Energy Commission	Borrego Springs, California	Diesel power generators	Battery storage
Philadelphia Industrial Development Corp	Philadelphia, Pennsylvania	Gas turbines and diesel power generators	Battery and thermal storage

Japan has also conducted many microgrid demonstration projects, such as Aichi Microgrid, Hachinohe Microgrid, Miyako Island Microgrid, and so on. The capacities range from 300 kW to 33 MW, and the power generators consist of PV panels, wind turbines, gas turbines, and fuel cell power generators (Ton and Smith, 2012).

In Europe, eight pilot microgrids were developed by different manufacturers and power distribution utilities, with research teams from 12 European countries (EEA, 2022). In these projects, the control technologies of the microgrids are tested, and their performance is quantified and analyzed.

In summary, many achievements in microgrid investigations have been obtained due to the efforts of different researchers from different countries/regions. However, many critical challenges still exist, which have been analyzed and reviewed in the following sections of this chapter.

## **2.2 Microgrid assessment approaches and reliability analysis**

### ***2.2.1 Microgrid assessment approaches***

Quantitative assessment, as an effective solution, can examine the performance of alternative design options and provide preliminary guidelines for the decision-makers at the planning stage, as reported by Aghajani et al. (2017) and Sabzehgar et al. (2020).

Currently, three main dimensions of microgrid systems are concerned at the planning stage: economics, reliability, and renewable power generation (Tayal, 2017). For the economics of microgrids, the overall cost is the most crucial evaluation indicator. For the reliability of microgrids, the different assessment methods, testbeds, and indexes are used as reported in the literature reviews by Akhtar and Saqib (2016) and Morato et al. (2021), which are reviewed detailedly in Section 2.2.4. For renewable power generation in microgrids, renewable energy penetration is often used to represent the ratio of renewable power generation. Piwko et al. (2012) assessed the impacts of renewable energy penetration on the overall costs of power generation systems, where several cases in Europe, China, and North America were presented and analyzed. Sarkar and Ajjarapu (2011) assessed the resource benefits of renewable energy penetration, including investments in renewable power generators and reserve requirements for the effective utilization of renewable energy.

Different approaches or frameworks have been proposed in the existing literature for assessing the performance of microgrids according to their scales and the complexity of systems. Çetinbaş et al. (2021) compared different modeling algorithms and proposed a quantitative method to assess the system's complexity. For small-scale microgrid systems, the system complexity is relatively low (Gómez-Hernández et al., 2019), and thus the computation costs of the systems are low (Florio et al., 2021).

Commonly, for small-scale microgrid systems, the quantification assessment at the planning stage and the system's optimal design at the design stage are considered together, such as the joint planning and design frameworks proposed by Kiptoo et al. (2020) and Mohanty et al. (2012). On the other hand, for those large-scale complex microgrid systems, the system performance assessments at the planning stage are conducted first due to the high computation costs.

### ***2.2.2 Reliability definition and classification***

System reliability is one of the most vital issues with microgrid systems. It refers to *“the ability to meet the electricity needs of end-use customers, even when unexpected equipment failures or other conditions reduce the amount of available power supply”* (Shaaban et al., 2015). According to the definition, system reliability is commonly divided into system adequacy and security.

The adequacy represents the ability of the power generation that can meet the anticipated energy demand without considering device disruptions (Jimada-Ojuolape and Teh, 2020). To enhance the system adequacy, the optimizations of the system design have been investigated by Elkadeem et al. (2020) and Florio et al. (2021), where the capacities and specifications of the different electrical equipment could be determined. During the optimization process, a few indexes (such as Loss of Power Supply Probability, Loss of Energy Expected, etc.) are introduced to assess the system's adequacy. They are mostly used as the constraints in the optimizations of the system design, as reported by Ganjehlou et al. (2020), Mohammed et al. (2021), and Suman et al. (2021).

On the other hand, security represents the ability of the microgrid to respond to sudden and uncertain disruptions. The security of microgrid systems was generally

investigated in terms of security protection (Hemmati et al., 2021). System security protection is an effective measure to defend against internal disruptions, where the internal sudden and uncertain disruptions are mainly caused by the peak current/power. System security protection is set mainly according to the power grid's capacity. Generally, a system with a larger capacity can get more support from security protection. Therefore, the ability of microgrids to cope with internal disruptions is usually much weaker compared with main grids due to the smaller capacity.

As for these two reliability performances, the former has attracted more attention since the intermittent and random characteristics of power generation from renewable sources are considered more. Actually, security is also important in system reliability. Especially for microgrids, the smaller capacity has a higher risk when facing sudden and uncertain disruptions e.g., peak current. Thus both these are should be considered in future studies.

### ***2.2.3 Reliability solutions and challenges***

#### **System adequacy**

Although carbon emissions can be reduced effectively by increasing the microgrids' renewable energy penetration, it also risks power supply inadequacy due to the unpredictable and uncontrollable nature of renewable power generation (Tomin et al., 2022). The grid-connected microgrids can address this problem by power charging from the main grids. With respect to the islanded microgrids, due to the lack of power charging from main grids, battery storage (Zhou and Cao, 2019) and backup power generation systems (Bracco and Delfino, 2017) are often used to enhance their reliability in terms of the system adequacy. Simply increasing the capacities of the backup power generators and battery storage is expensive, though it can directly

enhance the power supply adequacy and ensure the power supply. An accurate adequacy assessment approach is needed to address this issue, and the effective microgrid optimal design method should be developed based on the support and guidelines from the accurate assessment.

### **System security**

Expanding capacity and setting peak current limits are considered simple and effective solutions to enhance system security. Expanding microgrid capacity strengthens the ability of microgrids to cope with peak current, especially in facing surge current. However, expanding microgrid capacity on the supply side is costly. Setting a peak current limit reduces the strength of the peak current but requires careful design and operation on the demand side. To effectively reduce the impact of the peak current on system security, the peak current is investigated and classified into two main states, whose causes and solutions are listed in Table 2.2.

Table 2.2 Categories of peak current, its causes, and solutions (Hwang and Lou, 1998)

Peak current categories		Causes	Solutions
Steady state (O'Shaughnessy et al., 2018)		High power consumption	Increase system capacity Adopt proper control strategies Increase the power storage capacity Adopt dynamic electricity pricing
Transient state (Baimel et al. 2021)	Short-circuit current	Faulty circuit wire insulation Loose wire connection Faulty appliance wiring	Adopt system protections (breakers/fuses, ground-fault circuit interrupters, arc-fault circuit interrupters, etc.)
	Inrush current (Khederzadeh, 2010)	Multiple-step capacitor bank switching Chiller and lift motors startup Transformers energized	Adjust startup modes Adopt surge protections Increase system capacity

Steady-state peak current refers to the peak load over relatively long periods, i.e., hours or minutes. Extended operation at peak current can cause outages. Existing studies achieved load shifting/shaving for addressing it by optimizing system design (Luo et al., 2020) and system control (Sun et al., 2013), power scheduling (Sun et al., 2020), etc. Besides, steady-state peak current can be limited to an acceptable range by the control strategies implemented, as stated by Fontenot and Dong (2019) in a review paper on demand response technologies used in microgrid systems.

The transient peak current is another crucial factor affecting system security. The transient peak current can be further grouped into short-circuit current and inrush current, as shown in Table 2.2. Short-circuit current occurs typically due to equipment malfunction, while inrush current mostly appears during the startup periods of electrical equipment. Setting the protections, regular inspection, and maintenance services are necessary to avoid the short-circuit current. Inrush current appears more frequently and is, therefore, more harmful to system security (Faiz et al., 2008).

Adjusting the motor startup mode, adopting surge protection, and increasing microgrid capacity are all conventional methods to reduce the impact of inrush current (Rashid, 2011).

During the startup periods of electrical equipment, the inrush current shock (ICS) can threaten the system's security and increase the wear potential of the system. High wear potential causes a high risk of microgrid blackouts. The large electrical equipment is also a big threat to microgrid security, and it also increases the wear potential of the system, requiring more maintenance in operation (Shuai et al., 2016). Maintenance is needed to decrease the microgrid system's wear potential.

Among the electrical equipment, the frequent start/stop of chillers in centralized air-conditioning systems can significantly increase the risk of microgrid blackouts. Therefore, investigation of chiller startup performance, including inrush current quantification, is important to avoid microgrid blackouts. Existing studies on chiller startup performance are concerned with energy efficiency and cost-saving (Campanari et al., 2014; Zhuang et al., 2021). For example, a mathematical model (Fan and Ding, 2019) and an ANN model (Bechtler et al., 2001) were developed to improve energy efficiency and save costs during the chiller startup periods. These studies focused on chiller startup performance during relatively long periods, such as a few minutes or dozens of minutes, and increasing energy efficiency and/or cost saving were the objectives. Studies on chiller startup performance during a very short period, i.e., seconds or even less, are missing in the literature. In fact, it is reasonable to neglect the inrush current if the study does not focus on chiller startups in a very short period (Jia et al., 1995). As for the existing studies on chiller startup performance concerning chillers and their compressor motors, timely satisfying the cooling demand was their main concern, and few of them have considered the impact of the startup current of

the chiller induction motors on the system security. Besides, no generic and simplified transient startup power model of chillers is available for such an application. Using the safety/surge factors and decreasing the inrush current from the motor and chiller startup are the conventional methods to ensure microgrid reliability and avoid voltage dips and system damage (Xu et al., 2016; Akinyele and Rayudu, 2016). However, the microgrid capacity can only be determined roughly using safety/surge factors, which may result in a redundant capacity as the actual need is not precisely assessed.

#### ***2.2.4 Reliability assessment approaches and summary of the reliability indexes***

Existing microgrid reliability assessment approaches can be classified into two main categories, i.e., the deterministic approach and the stochastic approach (Jin and Jimenez, 2010; Luo et al., 2022a). The *deterministic approach* is a simple assessment approach, where the power generation and consumption of the microgrid are assumed as fixed and deterministic profiles/values. Usually, the typical supply profile and demand profile (Amir and Azimian, 2020; Sabzehgar et al., 2020; Xu et al., 2014) or the peak load obtained under typical weather conditions (Adefarati and Bansal, 2019; Luo et al., 2020; Muhtadi et al., 2021) are used for system reliability assessment. However, the actual renewable generation and energy demand are stochastic. The microgrid reliability performance may be overestimated/underestimated using the deterministic assessment approach, which may make the system design unreliable or conservative. The *stochastic approach* treats power generation and/or consumption as uncertain parameters. The stochastic characteristics of renewable energy resources and/or energy demands are considered quantitatively. The design solution identified using this approach can make the system operation more reliable, especially when the fluctuations in power generation and consumption are significant.

Different indexes have been proposed and used in the literature to evaluate the microgrid reliability performance. Sarkar et al. (2019) used the Loss of Power Supply Probability (LPSP) index in the reliability assessment for a PV-wind-biogas hybrid microgrid system. LPSP is defined as the ratio of the power not supplied to the total power that the power generation system can produce. It can be used to measure the magnitude of power outages. Song et al. (2019) adopted the System Average Interruption Duration Index (SAIDI) and System Average Interruption Frequency Index (SAIFI) to assess the reliability of a microgrid integrated with PV panels and an energy storage system. They are commonly used to quantify the average frequency of sustained interruptions per customer account occurring during the analysis period. Sekhar et al. (2016) used various indexes, such as SAIFI, SAIDI, and Customer Average Interruption Frequency Index (CAIFI), to assess the microgrid reliability performance. The Loss of Energy Expected (LOEE) index was used by Kuznetsova et al. (2014) to assess the microgrid reliability performance under different energy management strategies. LOEE as another commonly-used reliability index is used to calculate the expected amount of energy losses. Table 2.3 lists the commonly-used reliability indexes where the outage duration, outage frequency, and outage load are all quantified (Maleki and Askarzadeh, 2014; Garcia and Weisser, 2006; Pecenak et al., 2020; Wu and Sansavini, 2020; Adefarati et al., 2017; Adefarati and Bansal, 2019).

Table 2.3 Summary of the commonly used reliability indexes

Index	Abbreviation	Quantified object	Reliability enhancement direction
Loss of Load Expected	LOLE	Outage duration	Smaller LOLE
Loss of Energy Expected	LOEE	Outage energy	Smaller LOEE
Loss of Power Supply Probability	LPSP	Outage load ratio	Smaller LPSP
Equivalent Loss Factor	ELF	Outage duration & load	Smaller ELF
System Average Interruption Duration Index	SAIDI	Outage duration	Smaller SAIDI
System Average Interruption Frequency Index	SAIFI	Outage frequency	Smaller SAIFI
Customer Average Interruption Frequency Index	CAIFI	Outage frequency	Smaller CAIFI
Customer Average Interruption Duration Index	CAIDI	Outage duration	Smaller CAIDI
Average Service Availability Index	ASAI	Service duration ratio	Larger ASAI

## 2.3 Optimal design of microgrids

### 2.3.1 Supply-demand profiles considered in optimal design

Supply-demand profiles have a significant impact on the optimal microgrid design. The deterministic supply-demand profiles are used in the optimal microgrid design (Jin and Jimenez, 2010). For example, Sabzehgar et al. (2020) minimized the cost by optimizing the microgrid design based on four 12-hour supply-demand profiles. Baghaee et al. (2016) proposed a cost-based optimization method for microgrid design, where the supply-demand profiles of the typical year are considered in the optimization.

Besides, to further enhance the reliability and achieve the requirements of meeting load timely, the peak load should be considered in the optimal microgrid design (Thomas et al. 2016). Sarkar et al. (2019) and Quashie et al. (2018) proposed a

microgrid optimal design method using peak load, where the microgrid economics, including the initial cost, operation cost, and maintenance cost, is set as the objective function. The results show that using peak load can effectively ensure the zero loss of power supply probability for the optimal microgrid design, but it may increase the total cost due to the load being overestimated. In summary, this kind of optimal design method is relatively simple with low computation costs. However, it is probable to endanger the continuity and quality of the power supply, as renewable power generation and power consumption may be overestimated or underestimated (Polleux et al., 2022).

### ***2.3.2 Optimal design of microgrid considering the reliability impacts***

In previous studies on microgrid optimal design, the capacities of power generation and energy storage systems of microgrids are usually optimized based on the assumption that the demand-side loads are known (Ayodele et al., 2019; Barbaro and Castro, 2020; Blair and Mabee, 2020; Ding et al., 2020; Mashayekh et al., 2018; Mehleri et al., 2013), and the power supply adequacy is commonly considered as one of the optimization constraints. A trade-off is made in optimizing power supply adequacy and economics (Adefarati and Bansal, 2019; Baghaee et al., 2016; Cattaneo et al., 2018). For instance, Mashayekh et al. (2018) developed a reliability-constrained microgrid design method, where the mix of the hybrid power generations and their sizes are optimized, and the economic benefits are obtained. Barbaro and Castro (2020) developed a microgrid optimal design method to minimize the overall cost, where the sizes of the wind, PV, geothermal, and diesel generators, as well as battery energy storage systems, are all optimized. The requirements of the power supply adequacy are met by setting the reliability indexes in the optimization. Obara et al. (2018) explored a 3D topographical map to analyze and assess renewable energy layout and

further optimized the design of the renewable power generators and the electrical facilities (e.g., inverters, transformers, and controllers) for a microgrid, while the requirement of the power supply inadequacy is met by the backup power generators. The results show that the minimum cost can be achieved when renewable energy penetration is up to 40%. Tomin et al. (2022) and Fioriti et al. (2020) developed optimal design methods to optimize the mix and sizes of the microgrid power generators and battery storage capacity considering the impacts of the flexible renewable energy resources and different economic indicators respectively, where good economics are achieved. Balderrama et al. (2019) proposed a two-stage linear programming microgrid design optimization method to optimize the sizes of the power generators and battery storage capacity by considering the power imbalance as a cost penalty. The results show that good economics can be achieved as the renewable energy penetration at 29.7% for their case study.

It can be observed that existing academic studies on microgrid optimal design mainly aim to secure power supply adequacy, while microgrid security is rarely concerned. In practice, setting a safety factor (SaF) and a surge factor (SuF) in the microgrid capacity determination after the microgrid design optimization is the common method to meet the security requirement (Isatezde et al., 2018; Xu et al., 2016). This method is simple to implement but may result in reduced security/reliability as the impacts of the demand-side systems (e.g., the startup of the large chillers in buildings) on microgrid security are not quantitatively considered. Besides, higher investment costs are probably required to increase the microgrid capacity to meet the security requirement without making a trade-off between system reliability and overall costs. The cost due to increased capacity usually accounts for a large percentage of the microgrid's overall costs (Domenech et al., 2015; Her et al., 2021; Shi et al., 2020).

Therefore, it is necessary to consider the impacts of demand-side system design on microgrid security and make a better trade-off between microgrid reliability and overall costs, which is still absent in existing studies.

### ***2.3.3 Energy efficiency consideration in design optimization***

Increasing energy efficiency in microgrid design optimization is another potential solution to achieve good microgrid energy and economic performance. Wouters et al. (2016) quantified and analyzed the impacts of weather conditions on the renewable power generation efficiency of the microgrid, which can provide support in the robust optimization to increase overall power generation efficiency and decrease the operation cost. Mehleri et al. (2013) discussed the impacts of fixed efficiency for combined heating power (CHP) system and combined cooling, heating power (CCHP) system on the optimal microgrid design, where the fixed efficiency assumption can effectively maintain linearity of the model formulation while the error introduced by this assumption is solely acceptable for the lower-level optimal design models. Blair and Mabee (2020) quantified the impacts of CHP efficiency on the economics of the microgrid system optimal design. Results show that the CO<sub>2</sub> abatement costs are reduced significantly when the microgrid CHP system is under high efficiency (from the range of 600–900 CAD/ton to the range of 40–150 CAD/ton). However, in the microgrid field, few works investigated the impacts of energy use efficiency on microgrid performance.

## **2.4 Uncertainty quantitation analysis and robust optimal design**

### ***2.4.1 Uncertainties quantification methods and analysis***

A series of stochastic approaches have been developed for microgrids to quantify the uncertainties of power generation and/or consumption. For instance, Recalde and Alvarez (2020) and Yamchi et al. (2019) proposed a Monte-Carlo-based quantitative approach to obtain a probabilistic annual power supply profile. Chen et al. (2021) developed an uncertainty-based quantitative method to model the uncertainties of renewable power generations using a Beta distribution and model the loads using a typical profile. Bie et al. (2012) developed multi-state models to quantify the uncertainties of different distributed generations. Wu et al. (2014) proposed a stochastic quantitative approach, where the uncertainties of renewable generations were quantified based on the stochastic nature of weather conditions. The uncertainty of power consumption was quantified using a normal distribution.

In these studies, the uncertainties of different renewable generations were usually detailedly quantified and considered. In contrast, the uncertainties of loads (e.g., cooling, lighting, and plug loads) were mostly ignored or considered as a whole. In fact, the building's thermal and other microgrid electrical loads may have different uncertainty characteristics. Ignoring the demand-side uncertainties or quantifying them using a general distribution may cause unreliable assessment results (Li et al., 2019).

### ***2.4.2 Robust optimal design methods concerning the uncertainties***

The optimal design of the microgrids concerning the uncertainties is commonly regarded as “uncertainty-based design” or “robust design optimization” (Li et al.,

2019). Different microgrid robust design methods have been developed in the existing literature concerning different quantitative methods of microgrid uncertainties (Luo et al., 2022; Mendes et al., 2011; Yang et al., 2021; Yin et al., 2022; Zhang et al., 2018). For the investigated uncertainties, the intermittent and fluctuating features of renewable power generations are critical challenges for the system's reliability on the supply side. Zhang et al. (2018) quantified the impacts of PV generation uncertainties on system reliability, where the results show that the proposed optimization method can reduce operational costs and mitigate the risk of a power outage. Yin et al. (2022) conducted a robust optimization to minimize the overall costs of the microgrids where the uncertainties of the power generation from the solar and wind sources are quantified based on historical data. However, these above-mentioned studies mainly considered supply-side uncertainties while ignoring demand-side uncertainties. Besides, exploiting and quantifying demand-side uncertainties have also been considered in the microgrid design, but they still are not in-depth. The load uncertainties regarded as another whole variable are simply estimated according to the historical data or different simple distributions (Arriagada et al., 2015). For instance, Yu et al. (2016) conducted the robust optimization of microgrids to obtain a trade-off between cost saving and reliability enhancement by quantifying the supply-demand uncertainties according to the rough linear estimate of 20-year historical data. To address the impacts of the demand-side uncertainties, the upper and lower boundaries of the loads are calculated based on the historical data and TRNSYS simulation data, which is used in the cost-based microgrid design optimization by Cao et al. (2017). Besides, random distribution (Zhang et al. (2017)) and normal distribution by Sun et al. (2015) and Gupta et al. (2016) are used to quantify the uncertainties of the loads,

which are used in the microgrid optimization to obtain good economics and meet the requirements of reliability simultaneously.

## **2.5 Summary**

This chapter presented a comprehensive review of the existing studies on quantitative assessment and optimal design of the microgrid, as well as uncertainty analysis and its impacts on the microgrid reliability. From the above review, the existing gaps can be summarized as follows:

- As for the microgrid assessment, most existing studies focus on or are limited to assessing the impacts on the system performance using a single indicator. The existing methods consider the performance indicators separately. The interactions (such as correlation, substitutive, complementarity, and preferential dependence) among multiple performance indicators have not been considered. Meanwhile, the intensive computation of simulations in the quantitative assessment is another barrier, while decreasing computation cost has a risk of reducing the accuracy of the assessment results. Thus, a multi-dimensional performance assessment framework with relatively lower computational cost and acceptable accuracy for the microgrids is needed.
- The startup of electrical equipment has a significant impact on microgrid security. However, few previous studies have reported the one-time switching impact of electric induction motors on power grid security and microgrid security, respectively. Increasing the microgrid capacity is the common method to decrease the surge impact on microgrid security, which leads to a huge investment. A quantitative approach to assess microgrid security and the startup performance

quantification of the motors and chillers, including inrush current and startup time, is needed.

- Existing reliability indexes are commonly used in the reliability assessment and optimal design as one of the constraints. They can reflect the magnitude and duration of power inadequacy that may occur but cannot reflect the probability of the power inadequacy when uncertainties are considered. A novel uncertainty-based quantitative approach with a new reliability performance index (i.e., power inadequacy risk) for the reliability assessment of islanded microgrids by considering uncertainties at both supply and demand sides is needed.
- Existing academic studies on optimal microgrid design aim to secure power supply adequacy, while microgrid security is rarely concerned. Setting a safety factor (SaF) and a surge factor (SuF) in the microgrid capacity determination after the microgrid design optimization is the common method to meet the security requirement. However, this measure may result in reduced security/reliability as the impacts of the demand-side systems (e.g., the startup of the large chillers in buildings) on microgrid security are not quantitatively considered. In addition, a higher investment cost is probably required to increase the microgrid capacity to meet the security requirement without making a trade-off between system reliability and overall cost. Therefore, a coordinated optimal design method of islanded microgrids is needed for enhanced security and economics, which coordinates the design optimization of supply and demand systems.
- Robust microgrid optimal designs mostly consider the impacts of the supply-side uncertainties detailedly, while the demand-side uncertainties are ignored or assumed as a simple distribution. This may cause the optimal design is not a global solution. Besides, even though the uncertainties are considered in optimal design,

the power supply adequacy has still a large risk due to no quantified reliability index on the uncertainty-based impact in optimal design. Concerning the uncertainty-based impacts of using power inadequacy risk, a robust optimal design with detailed quantitation of supply-demand uncertainties is needed.

# CHAPTER 3 REFERENCE HOTEL MICROGRID AND HOTEL MICROGRID SIMULATION MODEL

This chapter presents an overview of the reference microgrid and models in this study. Section 3.1 presents the basic information about the reference microgrid. Section 3.2 presents the microgrid models, including the power generation model, the demand-side energy system model, and the battery storage model. Section 3.3 presents the control mechanism of the reference microgrid system. A summary of the reference microgrid and its development of the models are presented in Section 3.4.

## 3.1 Description of the reference hotel microgrid

### 3.1.1 *Basic information about the hotel*

A hotel building microgrid is constructed, which refers to a holiday hotel located on a remote island in Hong Kong, as shown in Figure 3.1. The holiday hotel has fifteen stories, and the total area is about 26,000 m<sup>2</sup>. It has over three hundred rooms, including one large meeting room and eleven multi-function halls. According to the design code (i.e., Hong Kong Code of Practice for Energy Efficiency of Electrical Installations), the commercial electrical load density, including the lighting load density and the equipment load density, is set as 25 W/m<sup>2</sup>. The cooling load density is set as 153 W/m<sup>2</sup>, according to Gang et al. (2015). Note that the islanded mode is adopted solely in this design. The energy system mainly includes wind turbines, PV panels, backup generators, a battery storage system, distributed power end-users, electric chillers, and associated cooling systems.

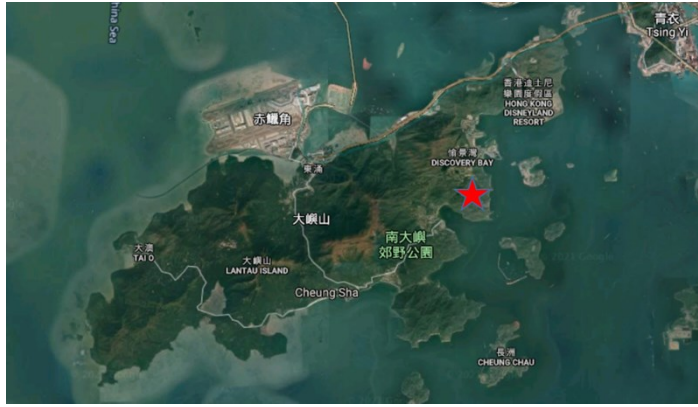


Figure 3.1 Overview of the building microgrid location

In this location, renewable sources have a promising potential to provide the power supply. The annual solar radiation and wind velocity profiles in Hong Kong are shown in Figure 3.2. The highest solar radiation and wind velocity are  $1.1 \text{ kW/m}^2$  and  $15.4 \text{ m/s}$ , respectively. The average solar radiation and the wind velocity are  $0.2 \text{ kW/m}^2$  and  $5.1 \text{ m/s}$ , respectively.

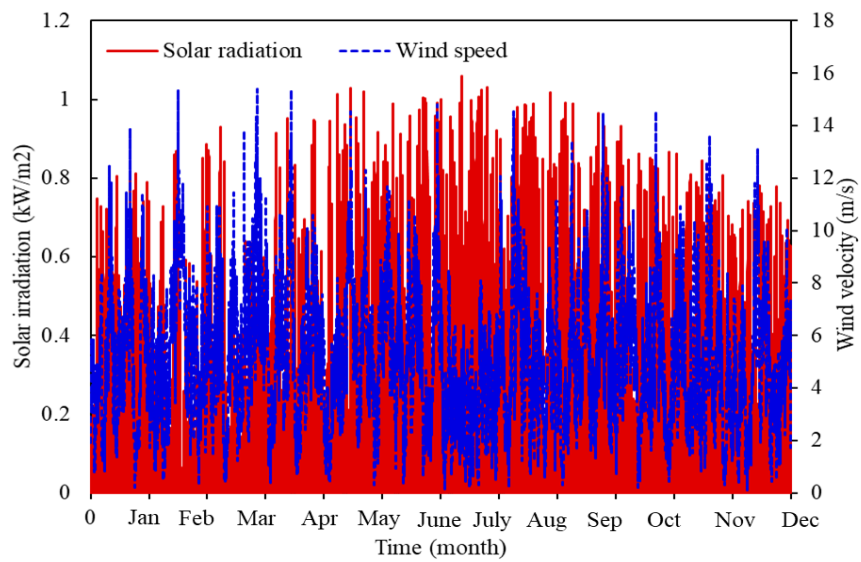


Figure 3.2 Annual solar radiation and wind velocity in this location

### 3.1.2 Configuration of hotel microgrid energy system

The energy system configuration of the hotel microgrid is shown in figure 3.3. The energy systems mainly include wind turbines, PV panels, backup power generators, electric batteries, electric chillers, and other associated cooling system components. The PV panels are installed around the hotel as it has enough space, and the wind turbines are off-shore.

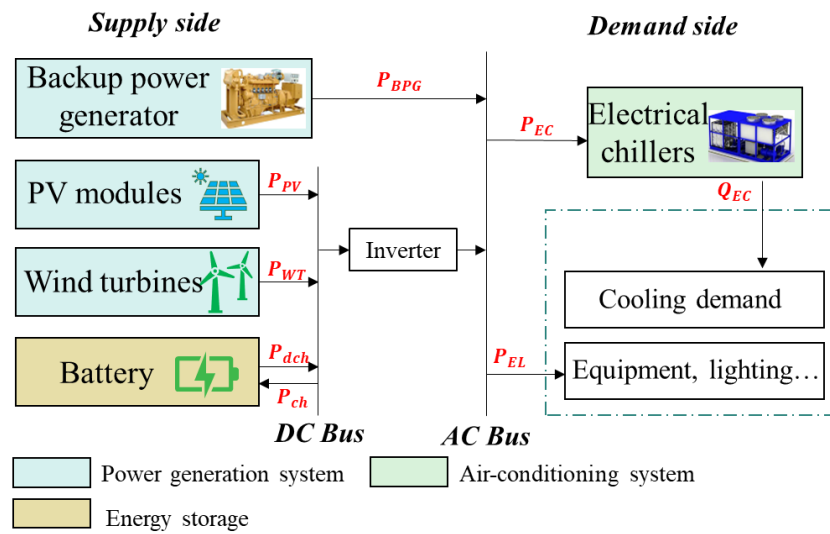


Figure 3.3 Configuration of the hotel microgrid energy systems.

## 3.2 Microgrid simulation model

The detailed microgrid energy system models are introduced, including power generation, demand-side energy system models, and a battery storage model.

### 3.2.1 Power generation models

#### PV model:

The power generation ( $P_{PV}$ ) from PV panels is calculated by Eq. (3.1) and Eq. (3.2) (Daud and Ismail, 2012), where  $Rad$  is the solar irradiance ( $\text{kW}/\text{m}^2$ ).  $A_{pv}$  is the total

area of PV panels ( $m^2$ ).  $T_{pv}$  is the cell temperature of the PV panels ( $^{\circ}C$ ), and  $T_{ref}$  is the reference cell temperature (set to  $25^{\circ}C$  in this study).  $K_{PV}$  (set to  $-3.7 \times 10^{-3}$  in this study) is the temperature coefficient ( $1/K$ ).  $T_{amb}$  is the ambient temperature ( $^{\circ}C$ ).  $\eta_{PV}$  is the overall efficiency of the PV panels.

$$P_{PV} = Rad \times A_{PV} \times (1 + K_{PV}(T_{PV} - T_{ref})) \times \eta_{PV} \quad (3.1)$$

$$T_{PV} = T_{amb} + 0.0256 \times Rad \quad (3.2)$$

### **Wind turbine model:**

The power generation from the wind turbines ( $P_{WT}$ ) can be calculated using Eq. (3.3) and Eq. (3.4) (Lu et al., 2002). When the wind speed ( $v_{wind}$ ) is within the range of 3.65 m/s and 10.4 m/s, Eq. (3.3) is adopted. When  $v_{wind}$  is within the range of 10.4 m/s and 18.0 m/s, Eq. (3.4) is adopted. It should be noted that the power generation from the wind turbine is 0 when  $v_{wind}$  is out of these ranges.

$$P_{WT} = 0.12615 \times v_{wind}^2 - 0.4915 \times v_{wind} - 0.008 \quad (3.3)$$

$$(3.65m/s \leq v_{wind} < 10.4 m/s)$$

$$P_{WT} = -0.078 \times v_{wind}^2 + 1.78144 \times v_{wind} - 0.016 \quad (3.4)$$

$$(10.4m/s \leq v_{wind} \leq 18.0 m/s)$$

### **Backup power generation model:**

As required in government policy, the natural gas generator is adopted as the backup power generator (Fong and Lee, 2015). The electrical output ( $P_{BPG}$ ) of the backup power generator is calculated by Eq. (3.5). It is assumed to be linear to the natural gas consumption ( $Con_{BPG}$ ). The generation efficiency is denoted by  $\eta_{BPG}$ . The backup power generator can be switched on or off at any time for power supply.

$$P_{BPG} = Con_{BPG} \times \eta_{BPG} \quad (3.5)$$

$$0 \leq P_{BPG,t} \leq Cap_{BPG} \quad \forall t \in [1,8760] \quad (3.6)$$

### 3.2.2 Demand-side energy system model

The electrical loads consumed by the end-users are divided into two types of loads, i.e., the electricity consumption of other electrical appliances and the cooling load. Here, the electricity consumption of other electrical appliances is simulated according to the electrical load density and occupant profile. The cooling load is simulated using the cooling load density and weather data. The simulation is achieved using TRNSYS, a commonly-used simulation tool to obtain the load profile.

The chiller systems meet the obtained cooling load from the TRNSYS simulation. The power consumption ( $P_{CL}$ ) of chillers is a function of its cooling load ( $CL$ ) and coefficient of performance ( $COP$ ), as shown in Eq. (3.7). The  $COP$  of the chiller is determined by its rated  $COP$  ( $COP_{rat}$ ) and the relative  $COP$  ( $\alpha_{pl}$ ), as shown in Eq. (3.8). The relative  $COP$  is calculated by the fitting function in Figure 3.4, as shown in Eq. (3.9) proposed by Kang et al. (2017). The rated  $COP$  differs from the size of the chiller, as shown in Eq. (3.10) (Gang et al., 2015). If the load ratio is near 80%, the relative  $COP$  is high. It can be found that the proper size and number of chillers can significantly improve the actual  $COP$  in operation.

$$P_{CL} = CL/COP \quad (3.7)$$

$$COP = \alpha_{pl} \times COP_{rat} \quad (3.8)$$

$$\alpha_{pl} = -0.569 \times (CL/Cap_{chi})^3 - 0.258 \times (CL/Cap_{chi})^2 + 1.52 \times (CL/Cap_{chi}) + 0.321 \quad (3.9)$$

$$COP_{rat} = 2.886 \times 10^{-9} \times (Cap_{chi})^2 + 0.293 \times 10^{-4} \times Cap_{chi} + 4.711 \quad (3.10)$$

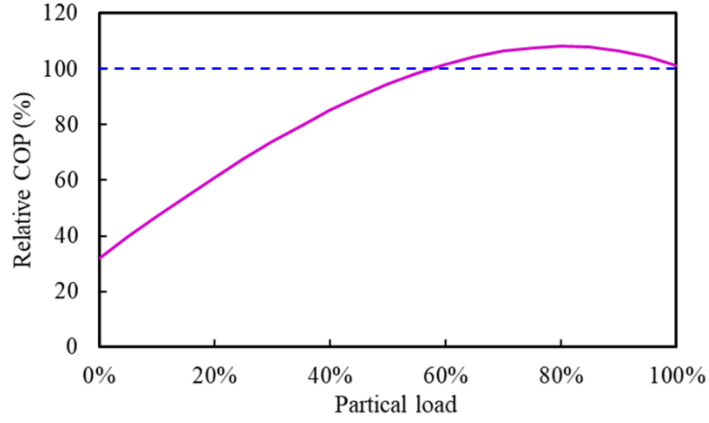


Figure 3.4 Relative COP of chillers at different load ratios

### 3.2.3 Energy storage model

A battery is installed to store the surplus renewable power generation and enhance the reliability of the microgrid system. The maximum and minimum storage limits ( $E_{bat,max}$  and  $E_{bat,min}$ ) are set to prolong the battery life cycle, which is set to 80% and 20% of the battery capacity, respectively, as shown in Eq. (3.11). The maximum hourly power charging rate and maximum hourly power discharging rate are set to 20% and 50% of the battery capacity, respectively, as shown in Eq. (3.12) and Eq. (3.13). The charge efficiency and discharge efficiency are both assumed to be 85% in this study.

$$E_{bat,min} \leq E_{bat} \leq E_{bat,max} \quad (3.11)$$

$$0 \leq P_{ch} \leq P_{ch,max} \quad (3.12)$$

$$0 \leq P_{dch} \leq P_{dch,max} \quad (3.13)$$

### 3.3 Microgrid system control mechanism

Battery storage is widely used to store surplus electricity from renewable power generations and maintain reliable system operation. Setting the charging and discharging limitations and providing a proper control mechanism are effective measures to prolong the battery lifetime. The minimum and maximum limits of the battery storage are set as 20% and 80% of the battery capacity ( $Cap_{bat}$ ), respectively.

To ensure the power supply adequacy and limit the battery charging and discharging in the proper range, the control mechanism of the battery charging/discharging and the backup power generation are illustrated in Figure 3.5. Renewable power generation ( $P_{re}$ ) is utilized to meet the demand ( $P_{de}$ ) including the power consumption ( $P_{EC}$ ) of the electric chillers and individual electrical appliances ( $P_{EA}$ ) as the first choice. Due to the intermittency of renewable energy generation, battery discharging is the second choice to avoid power outages. Once the battery storage ( $E_{bat}$ ) is equal/lower than 20% of its capacity, the battery cannot be further charged to provide power to the system. As the last choice, the backup power generators are turned on to meet the demand. When the power generation from renewable sources is higher than the power demand, the battery acts as a consumer to be charged until the remaining power is up to 80% of its capacity.

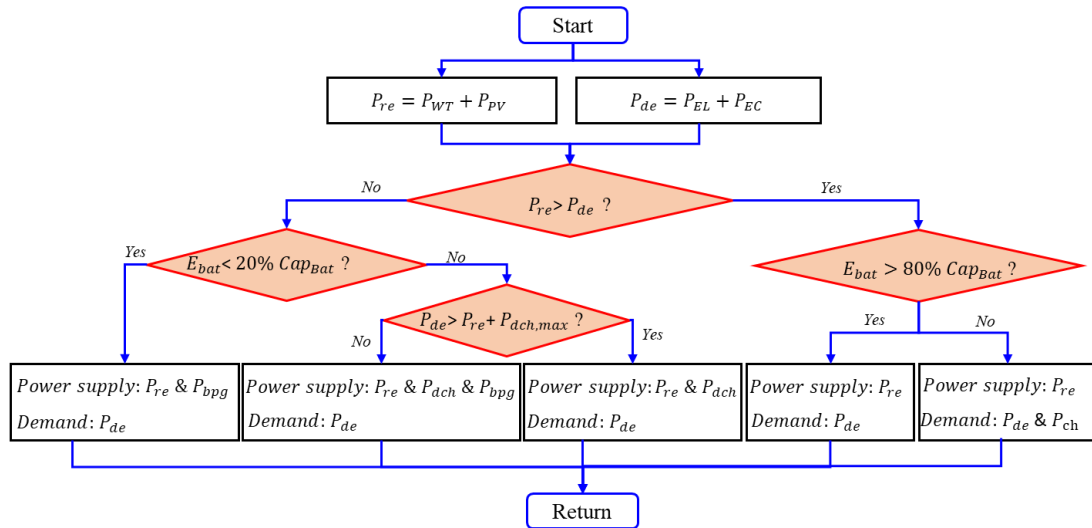


Figure 3.5 Flowchart of the Microgrid system control mechanism

### 3.4 Summary

This chapter presents an overview of the hotel microgrid and the microgrid simulation model used in this study. The hotel microgrid model consists of the power generation models and demand-side model, as well as the battery storage model. An energy system configuration and its control strategy have been proposed.

# **CHAPTER 4 A MULTI-DIMENSIONAL PERFORMANCE ASSESSMENT FRAMEWORK FOR MICROGRIDS CONCERNING RENEWABLE PENETRATION, RELIABILITY, AND ECONOMICS**

This chapter aims to develop a multi-dimensional performance assessment framework for conveniently assessing microgrids concerning their key performance indicators. Section 4.1 introduces the procedure of the assessment approach. Section 4.2 and Section 4.3 presents the validation cases and results, respectively. Section 4.4 presents the performance assessment results and suggestions concerning the impacts of these three indicators, and Section 4.5 summarizes this chapter.

## **4.1 Quantitative assessment framework and procedure**

### ***4.1.1 Outline of the quantitative assessment framework***

Figure 4.1 illustrates the proposed framework of the microgrid assessment and its procedure. This assessment framework involves three steps, as elaborated below:

***Step 1:*** Sampling of the energy portfolios according to the microgrid variables. At this step, the microgrid renewable power generation's types, sites, and capacity ranges are determined. The Latin hypercube sampling (LHS) method is used to generate samples of the microgrid energy portfolios since a smaller sampling size is required (Li and Wang, 2019).

***Step 2:*** Generation of key performance indicators by system simulation. At this step, the presumed occupant profile and load density, together with the presumed samples

of the energy portfolios from the first step and the weather data, are all fed into the microgrid model. As the outputs of the microgrid model, the key indicators of the microgrid performance (economies, renewable energy penetration, microgrid reliability) are obtained.

**Step 3:** Microgrid multi-dimensional performance assessment quantification. At this step, the parameters of the empirical cost model are identified according to the obtained key indicators. Then, the quantitative assessment results can be obtained using the empirical model.

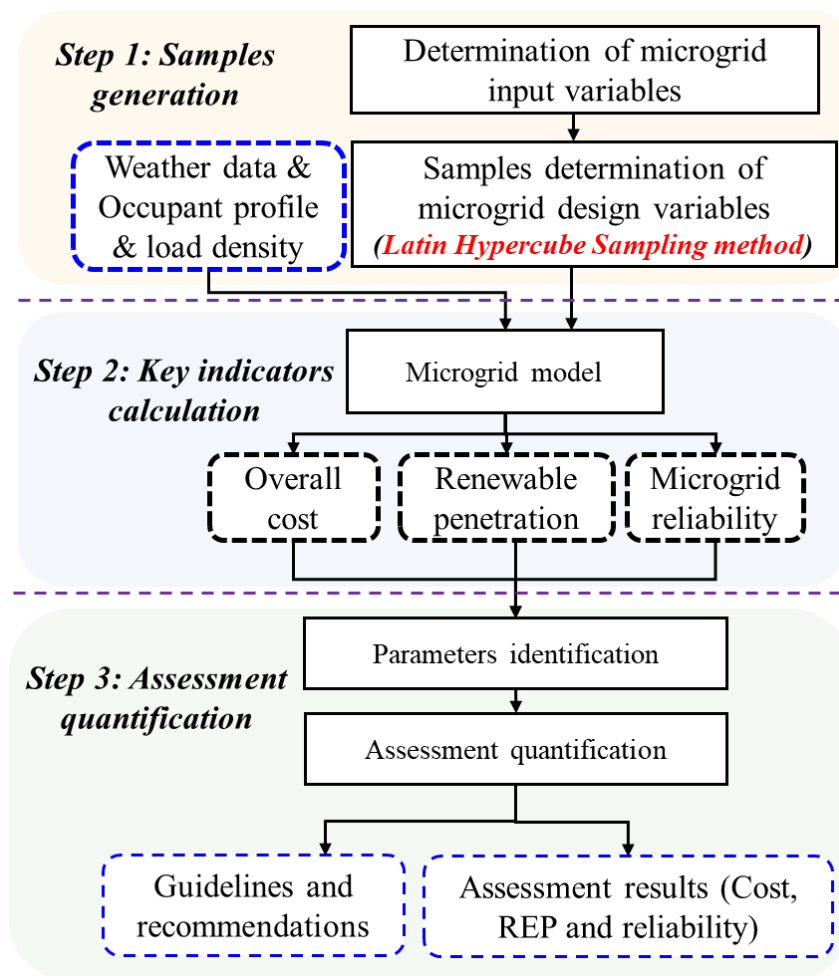


Figure 4.1 The framework of the microgrid quantitative assessment

#### 4.1.2 Quantification of the key microgrid performance indicators

##### Economics:

The economics of the microgrid is quantified as the overall cost. The overall cost ( $C_{ov}$ ) consists of the initial cost ( $C_{ini}$ ) and the operation cost  $C_{opt}$  calculated using Eq. (4.1). The initial cost is the average annual initial cost that the investors have to pay per year as shown in Eq. (4.2). The operation cost is calculated by multiplying the annual primary energy consumption of the backup power generators and the price ( $Pr_{BPG}$ ) of the primary energy as shown in Eq. (4.3), where the  $C_{fac,k}$  is the initial cost of the  $k$ th microgrid facility and the  $Y_k$  is the total years of its life cycle.  $P_{BPG}^t$  is the power generation from the backup power generation at the time  $t$ . The subscript “ $fac$ ” represents the microgrid facility, and the subscript “ $BPG$ ” means a backup power generator.

$$C_{ov} = C_{ini} + C_{opt} \quad (4.1)$$

$$C_{ini} = \sum (C_{fac,k} \times 1/Y_k) \quad (4.2)$$

$$C_{opt} = \left( \sum_{t=1}^{8760} P_{BPG}^t \right) \times Pr_{BPG} \quad (4.3)$$

##### Renewable energy penetration:

As a key performance indicator, the renewable energy penetration ( $REP$ ) is calculated using Eq. (4.4), where  $P_{re}$  is renewable power usage, and  $P_{de}$  is total electrical load. Almost all the power generation is from renewable sources if the ratio is close to one.

$$REP = \sum_{t=1}^{8760} P_{re,t} / \sum_{t=1}^{8760} P_{de,t} \quad (4.4)$$

##### Reliability:

Reliability ( $Re$ ) is another key indicator. It is used to assess the power balance of the microgrid. The reliability depends on the power consumption of the demand-side energy system and the power supply of the hybrid power generation system, as shown in Eq. (4.5).

$$Re = \sum_{t=1}^{t=8760} (P_{dem,t} - P_{sup,t}) / \sum_{t=1}^{t=8760} P_{dem,t}, \quad \forall P_{dem,t} > P_{sup,t} \quad (4.5)$$

#### 4.1.3 The empirical cost model of microgrids

An empirical cost model is developed to quantify the correlation among microgrids' multiple key performance indicators, including renewable energy penetration, reliability, and microgrid economics. The overall cost of a microgrid varies significantly because of the different energy portfolios implemented under given renewable penetration and expected reliability. Thus, the model consists of the upper and lower boundaries, as shown in Eq. (4.6) and Eq. (4.7), respectively. The maximum and minimum overall costs are the upper and lower boundaries of the model, considering the renewable energy penetration ( $X_{pen}$ ) and reliability ( $X_{re}$ ). The developed empirical cost model can directly represent and quantify the correlation among the three mentioned key indicators, i.e., the impacts of the renewable energy penetration and reliability on the system economics, under various energy portfolios implemented.

$$Cost_{max} = f_{max}(X_{pen}, X_{re}) \quad (4.6)$$

$$Cost_{min} = f_{min}(X_{pen}, X_{re}) \quad (4.7)$$

## 4.2 An overview of the validation case

### 4.2.1 Overview of the microgrid system and its model development

An existing vacation hotel microgrid, located in the subtropical area, with fifteen stories, is considered the reference for testing and validating the proposed quantified assessment approach. The details have been described in Section 3.1, and the microgrid model is developed in Section 3.2.

### 4.2.2 Energy system control strategy

To enhance the system reliability and simultaneously limit the battery operation within the safe range, a typical and simple control strategy of the microgrid is implemented in this study. The priority of power supply is renewable power generation, battery, and backup power generation. The detailed control strategies have been presented in Section 3.4.

### 4.2.3 Main microgrid design parameters concerned

Table 4.1 lists the main microgrid design parameters and their ranges, in this case, at the planning stage. The microgrid hybrid power generation system consists of renewable power generators (i.e., wind turbines, PV panels), backup power generators (i.e., natural gas turbines), and a battery storage system.

Table 4.1 Microgrid variables and their range at the planning stage

Category	Microgrid variables	Search range	Unit
Renewable power generation	Wind generator capacity	[0 5000]	kW
	PV areas	[0 10000]	m <sup>2</sup>
Backup power generation	Gas generator capacity	[0 5000]	kW
Energy storage	Battery capacity	[0 1000]	kWh

Table 4.2 presents the basic data of the microgrid hybrid power generation system. They are listed in four categories. Renewable power generation involves PV panels and wind power generators (such as unit price, lifetime, and overall efficiency). The backup power generator adopts the natural gas turbine, so the natural gas price, the generator lifetime, and overall efficiency are the main performance data. The unit price of the gas generator ( $UP_{gas}$ ) is sensitive to the change in size. It is calculated according to the different capacities of the gas generator ( $Cap_{gas}$ ), as shown in Eq. (4.8) based on (Zheng et al., 2016). The third category is battery storage. The last category is the microgrid component cost. The component cost of microgrid capacity is the estimated overall value, where the initial costs of the vital equipment associated with renewable power generation are included, such as the initial cost of the hardware (system controller, inverter, transformer, and power filter), soft cost (e.g., engineering, construction, commissioning, and regulatory costs) and additional electric infrastructure costs (Giraldez, 2018; Khodaei and Shahidehpour, 2012).

$$UP_{gas} = 3711.78 - 280.47 \times \ln(Cap_{gas}) \quad (4.8)$$

Table 4.2 Basic data of microgrid hybrid power generation system\*

Category	Parameter	Value	Unit
Renewable power generation	The unit price of the PV area	576	USD/m <sup>2</sup>
	The overall efficiency of PV	0.2	-
	The lifetime of the PV	20	year
	The unit price of the wind generator	2880	USD/kW
	The lifetime of the wind turbine	20	year
Backup power generation	The lifetime of the gas generator	25	year
	The unit price of natural gas	0.0571	USD/kWh
	Gas generator efficiency	0.32	-
Battery storage	The unit price of the battery	213	USD/m <sup>2</sup>
	The lifetime of the battery	10	year

Renewable power generation capacity	Renewable capacity per unit	1500	USD/kW
	The lifetime of the renewable facilities	20	year

\* *Remark:* the selection of reference data refer to (Li and Wang, 2019; Li, 2000; Lu et al., 2015; Venkateswari and Sreejith, 2019).

### 4.3 Model development, validation, and computation cost assessment

#### 4.3.1 A proposed empirical cost model

##### Empirical cost model development:

As introduced in Section 4.1.3, an empirical cost model is developed and used in the microgrid performance assessment. The final forms of this model are presented in Eq. (4.9) and Eq. (4.10) as the lower and upper boundaries, respectively. The lower and upper boundaries represent the maximum and minimum overall cost concerning the different energy portfolios (different capacities of the battery storage and power generators) implemented. Regression analysis, as a well-known statistical method, is used to determine the coefficients of the upper and lower boundaries concerning indicators, such as reliability ( $Re$ ) and renewable energy penetration ( $Pen$ ).

$$C_{ov,max} = 295922 + 716045 \times Re - 534821 \times Pen + 1519573 \times Re^2 + 681551 \times Pen^2 \quad (4.9)$$

$$C_{ov,min} = 232293 + 528128 \times Re - 587898 \times Pen + 1285746 \times Re^2 + 487306 \times Pen^2 \quad (4.10)$$

The empirical cost model can provide strong support for microgrid performance assessment. Using this cost model, the impacts of renewable energy penetration and reliability on economic performance are quantified. The maximum and minimum costs can be obtained under particular renewable penetration and expected reliability. For instance, if this model requires 30% renewable energy penetration and the

expected reliability is 90% or more, the overall cost saving can be obtained (around 28%).

**Fitness verification concerning different powers of the input variables:**

The regression analysis determines the coefficients of the significant input variables (i.e., reliability and renewable energy penetration). The model fitness verification is evaluated using the R-squared values concerning different powers of the input variables, and the results are shown in figure 4.2. The R-squared ( $R^2$ ) is a statistical measure commonly used to evaluate the proportion of the variance for a dependent variable (Cameron and Windmeijer, 1997). The linear model cannot provide high R-squared values. When the power is 2, the values of the  $R^2$  are 0.93 for the upper boundary and 0.96 for the lower boundary, respectively. It can be observed that the empirical cost model can provide an accurate prediction if the power is two or above.

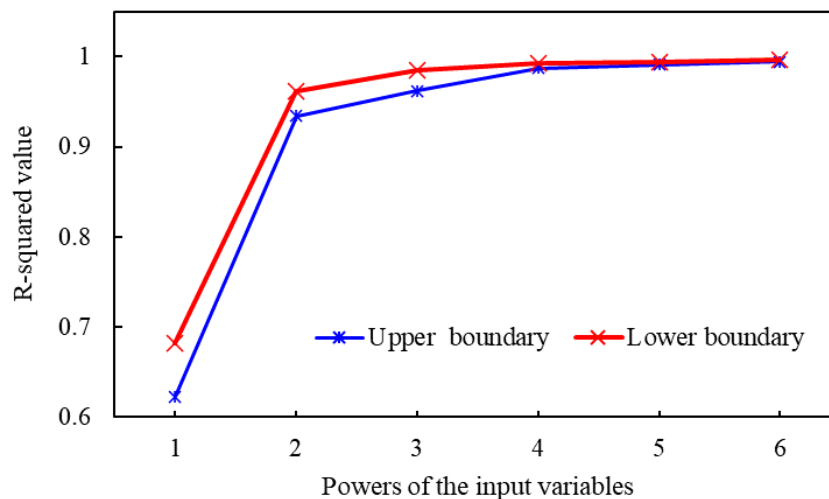


Figure 4.2 R-squared values of empirical cost model concerning different powers of the input variables

**4.3.2 Model accuracy validation and computation cost assessment**

**Reference model**

Using the empirical cost model and the LHS method can simultaneously reduce computation costs and maintain adequate accuracy. The exhaustive searching method is adopted for the reference model to test and validate the model's accuracy and computation cost.

The exhaustive searching method (ESM), also called the complete trial-and-error method or the brute-force method, is commonly used to test all possible samples to achieve the final objective. It is very accurate and robust but also causes huge computation costs. The reference model parameters are identified according to the obtained indicators and the corresponding system performance. For the exhaustive searching method, a total of 1,000,000 samples are generated and tested according to the presumed intervals of the four concerned variables, as shown in Table 4.1.

Table 4.3 Microgrid variables concerned with the reference model development

Variables	Interval	Range	Number of samples	Unit
Area of the PV panels	100	0-10,000	100	m <sup>2</sup>
Capacity of the wind turbine	100	0-5,000	50	kW
Capacity of the backup generator	100	0-2,000	20	kW
Capacity of the battery storage	100	0-1,000	10	kWh

### **Model accuracy validation**

The model accuracy ( $MA$ ) of the empirical cost model is quantified according to the relative error of the model, as shown in Eq. (4.11). The relative error of the model ( $E_R$ ) is calculated as shown in Eq. (4.12) by using a reference model, where  $T$  is the total number of steps.  $\Delta V_{upper,t}$  is the upper boundary difference between the empirical cost model and reference model, as shown in Eq. (4.13), and  $\Delta V_{lower,t}$  is the lower boundary difference between the empirical cost model and reference model, as shown in Eq.

(4.14) at the step  $t$ . If the model accuracy is close to one, the model accuracy is high or is close to its best possible.

$$MA = (1 - E_R) \times 100\% \quad (4.11)$$

$$E_R = \frac{1}{T} \times \sum_{t=1}^T (\Delta V_{upper,t}/V_{ref,t}^{upper}) + \frac{1}{T} \times \sum_{t=1}^T (\Delta V_{lower,t}/V_{ref,t}^{lower}) \quad (4.12)$$

$$\Delta V_{upper,t} = abs(V_{LHS,t}^{upper} - V_{ref,t}^{upper}) \quad (4.13)$$

$$\Delta V_{lower,t} = abs(V_{LHS,t}^{lower} - V_{ref,t}^{lower}) \quad (4.14)$$

### **Computation cost assessment**

Since this work aims to provide a practical assessment approach in engineering, model computation cost in this assessment is important to be quantified. If the model has a relative-lower computation cost, it can widely be accepted by the engineering. Computation time is a vital indicator to assess the model computation cost. The computation work is performed on the same computer to precisely obtain the difference between the computation costs using the reference model and the empirical cost model. The major specifications of the computer are shown in Table 4.4.

Table 4.4 The detailed specifications of the adopted computer

Items	Major computer specifications
System version	Windows 10
Processor	Intel(R) Core (TM) i7-8700 CPU @ 3.20 GHz
Installer memory (RAM)	32.0 GB (31.8 GB usable)
System type	64-bit Operating system, x64-based processor

### ***4.3.3 Results of the model accuracy validation and computation cost assessment***

To directly reflect the impact of the sampling size on the model performance (i.e., accuracy and computation cost), five empirical cost models concerning different

numbers of samples are developed. The number of samples is determined according to the number of input variables and a multiple of ten. The resulting model accuracy and computation time are shown in Table 4.5. A comparison of the accuracy and computation load using these models is also shown in figure 4.3. It can be seen that, with the number of samples increasing, the model accuracy increases while the computation cost saving decreases. The trade-off is at the intersection of these two lines. At this point, the model accuracy and the computation cost saving are both relatively high (up to 80%). Thus, the recommended sampling size is 193,500. It means that about 20% of exhaustive searching samples are the proper sampling size needed and used for developing the empirical cost model. With this sampling size, relatively high model accuracy and low computation cost can be achieved at the same time.

Table 4.5 Accuracy and computation cost of empirical cost models

Model	Sampling size	Accuracy	Computation time
Empirical cost model 1	$4 \times 10^1$	3.00%	2.0 s
Empirical cost model 2	$4 \times 10^2$	10.22%	19.5 s
Empirical cost model 3	$4 \times 10^3$	41.59%	3.3 min
Empirical cost model 4	$4 \times 10^4$	64.46%	30.8 min
Empirical cost model 5	$4 \times 10^5$	89.45%	5.0 hr

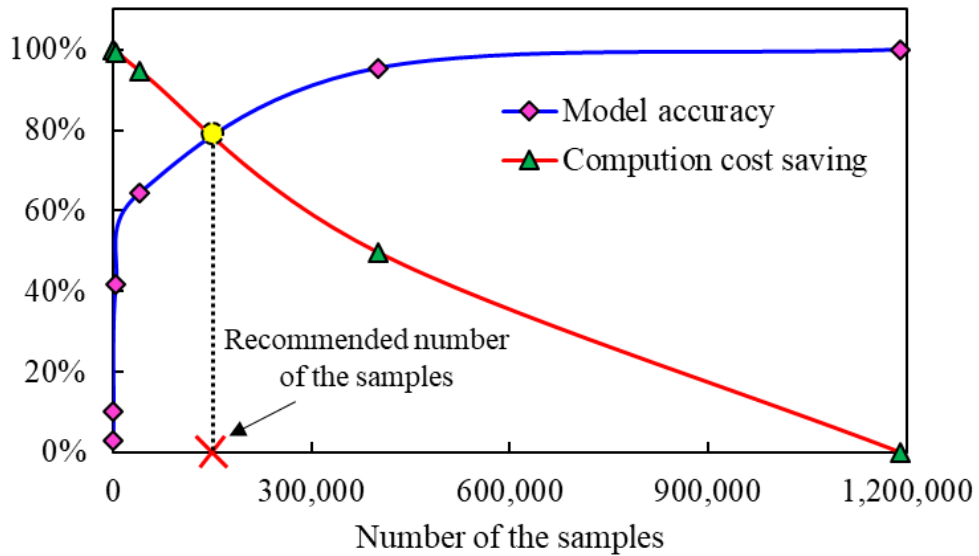


Figure 4.3 A comparison between accuracy and computation cost of the empirical cost models

#### 4.4 Microgrid performance assessment results and analysis

##### 4.4.1 Overall correlations among REP, reliability, and overall cost of microgrid adopting different energy portfolios

The correlations of the three performance indicators (renewable energy penetration, reliability, and economics) are presented in a 3-D graph (Figure 4.4 (a)). Under given renewable penetration and expected reliability, the maximum and minimum overall costs are obtained according to the upper and lower boundaries of the proposed empirical cost model. The lighter colour represents the higher overall cost, while the darker colour represents the lower overall cost. The overall cost is high if high reliability is required. If the reliability and renewable energy penetration are nearly 100%, the overall costs in the upper and lower boundaries are calculated as  $2.0 \times 10^6$  USD and  $2.7 \times 10^6$ , respectively.

Figure 4.4 (b) shows the difference (i.e., overall cost saving) between the upper and lower boundaries, considering the different ratios of reliability and renewable energy penetration. If reliability and renewable energy penetration are required at nearly 100%, the overall cost savings exceed  $7.5 \times 10^5$  USD. It shows that the cost-saving potential (i.e., 37.5%) of microgrid system optimization is high when both high reliability and renewable energy penetration are required.

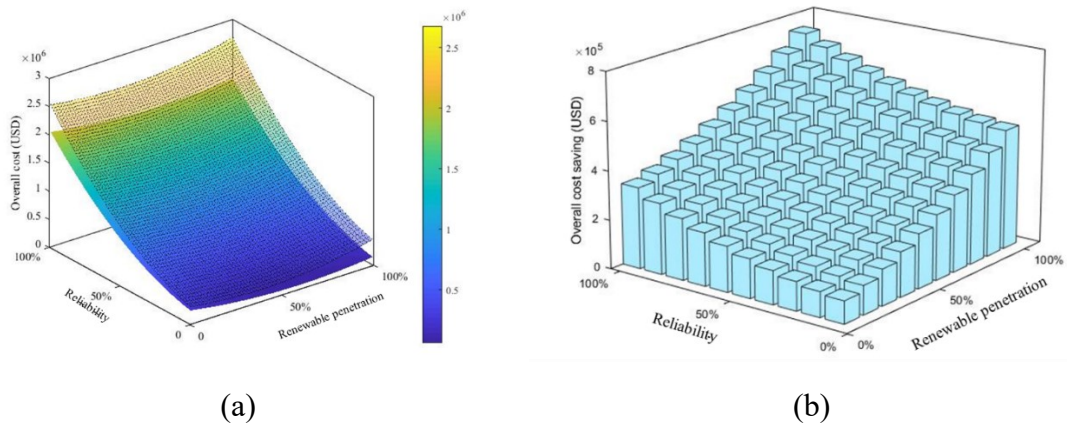


Figure 4.4 Correlation among three microgrid performance indicators

#### 4.4.2 Renewable energy penetration vs. economics

Figure 4.5 shows the correlations between renewable energy penetration and economics under different microgrid energy portfolios. The upper and lower boundaries are obtained according to the empirical cost model. The difference between the minimum and maximum overall costs increases with the increase of renewable energy penetration under the expected reliability. In other words, the microgrid has a large cost-saving potential when the renewable energy penetration is high. It is worth noticing that the lower boundary can provide a valuable guideline of the best economic performance for the decision-makers at the microgrid planning stage. Almost all the lower boundaries associated with different reliabilities have a similar trend. Under the expected reliability, the overall cost decreases obviously with the increase of the

renewable penetration at the range between 0% and 60.3%. If the renewable penetration is over 60.3%, the overall cost gradually increases with the renewable penetration (between 60.3% and 100%). Under relatively high expected reliability (over 80%), compared to the 0% and 100% renewable penetration, the maximum cost savings of the proper renewable energy penetration cost are about 12% and 6%, respectively. Thus, 60.3% of renewable energy penetration is the best choice to achieve good economics for the microgrid power generation system.

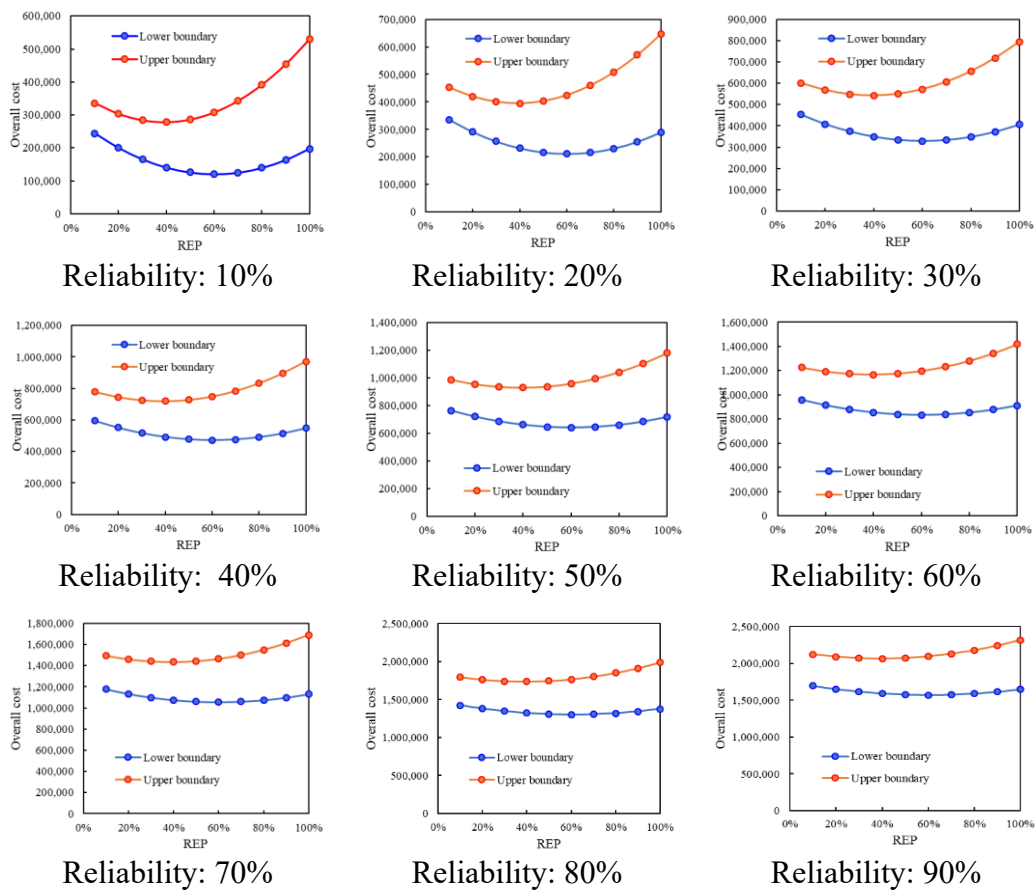
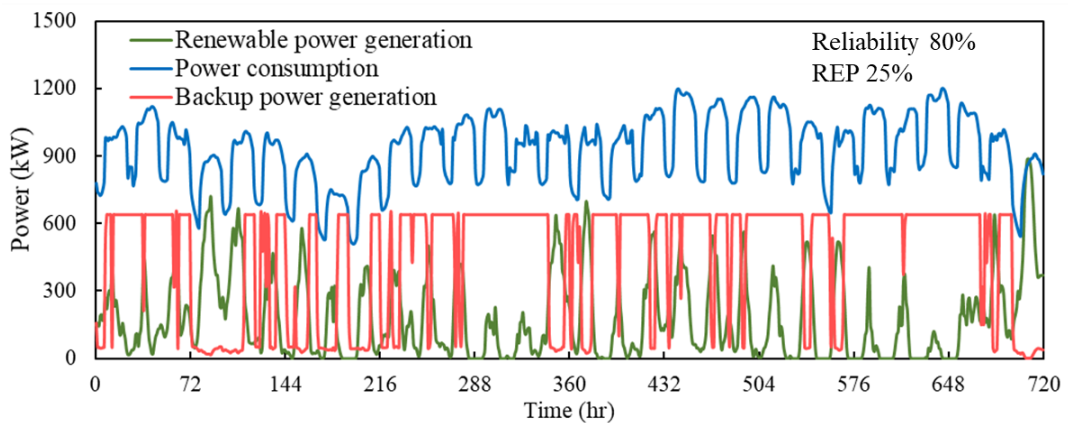


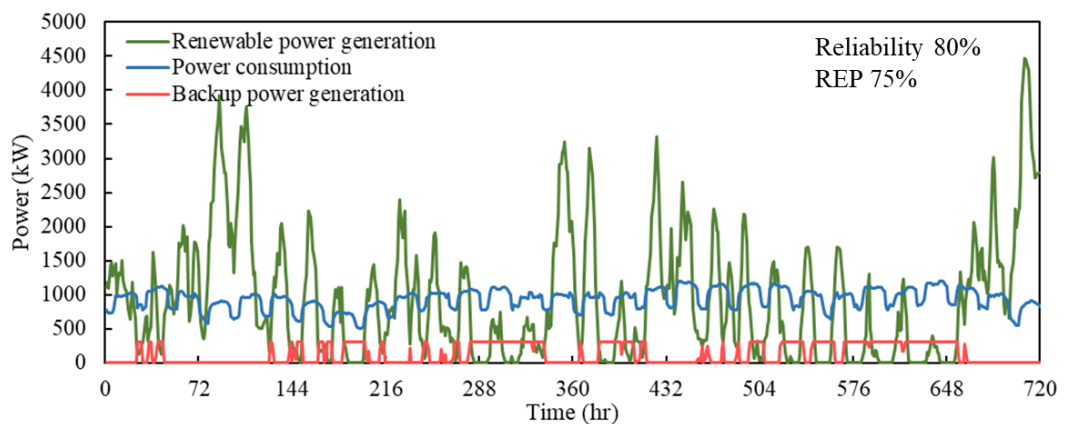
Figure 4.5 The correlations between REP and economics of the different microgrid energy portfolios under different reliabilities

To directly depict the impact of renewable energy penetration on the microgrid system performance during the operation, Figure 4.6 shows the microgrid systems' monthly power and load profiles with two different ratios of renewable energy penetration.

Almost the same overall cost and reliability are considered in the two scenarios. Under the low renewable energy penetration of 25% (first scenario), the backup power generators are switched on nearly all the time. The system's reliability mainly depends on backup power generation, while the intermittent nature of renewable power generation has a relatively low impact on reliability. Under high renewable penetration of 75% (Scenario 2), renewable power generation significantly impacts the system's reliability. Due to the fluctuation and intermittent nature of renewable power generation, renewable power generation sometimes varies from zero to over six times the power consumption. Such a huge fluctuation in renewable power generation is also a big challenge for the wear and tear of the major electrical facilities, such as inverters and transformers.



(a) Scenario 1



(b) Scenario 2

Figure 4.6 Monthly microgrid power and load profiles under two renewable energy penetration scenarios

#### 4.4.3 Reliability vs. economics

Figure 4.7 shows the correlations between reliability and economics under the different microgrid energy portfolios. The upper and lower boundaries represent the maximum and minimum overall costs. It can be seen that the overall cost increases with the increase of the expected reliability in general. The overall cost will increase by over six times if the expected reliability increases from 10% to 100%. It means that the overall cost will be increased significantly if high reliability is expected. Solely optimizing the energy portfolios cannot effectively limit the overall cost. Some other technologies, such as the engagement of demand response and system flexibility, should have promising potential to enhance reliability while limiting the overall cost at the same time.

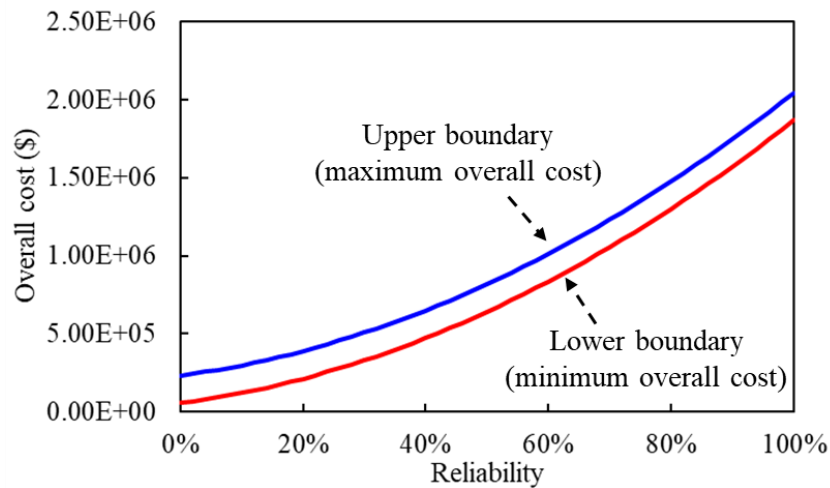
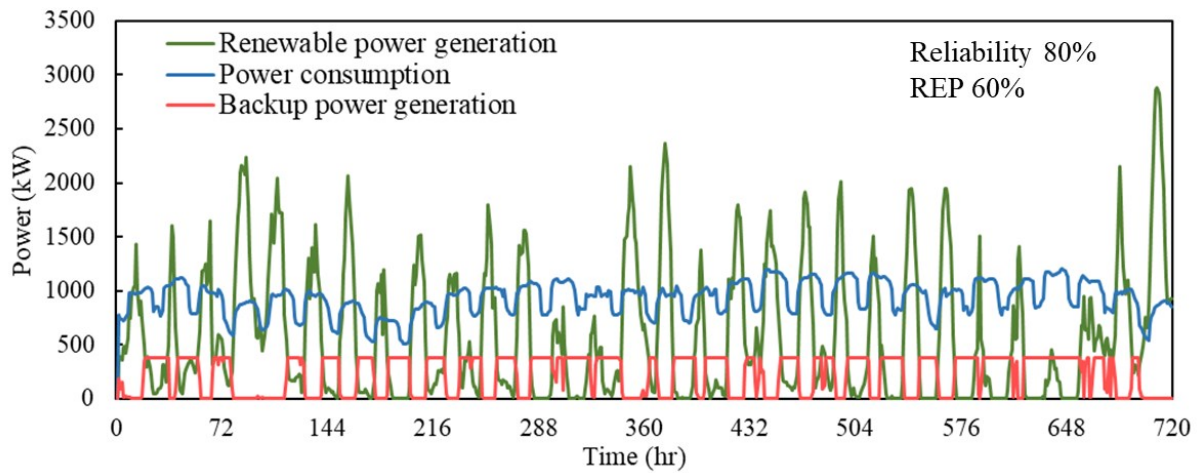


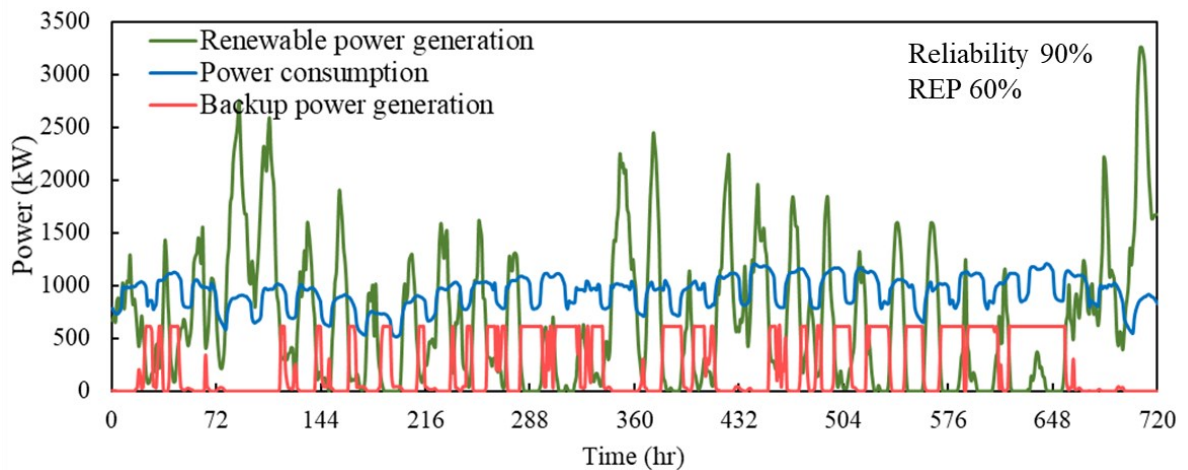
Figure 4.7 Quantification results of the reliability and the economics

Figure 4.8 shows the microgrid systems' monthly power and load profiles with two different reliability requirements (i.e., 80% and 90%). 60% of the renewable energy penetration is selected in these two scenarios. Under the reliability requirements of 80%

(the third scenario), the smaller capacities of the power generators are selected (i.e., maximum power generation: 2,850 kW). The larger capacities of the power generators (maximum power generation: 3,350 kW) are selected to meet the higher reliability requirements of 90% (the fourth scenario). Concerning economics, it can be seen that overall cost can increase by over 12% to enhance the reliability from 80% to 90%, i.e., from Scenario 3 to Scenario 4.



(a) Scenario 3



(b) Scenario 4

Figure 4.8 Monthly microgrid power and load profiles under two reliability requirements

## **4.5 Summary**

This chapter proposes a multi-dimensional performance assessment framework for microgrids at the planning stage. This framework can effectively assess the multi-dimensional performance of the microgrid, considering three key performance indicators, including economics, renewable energy penetration, and reliability. The proposed assessment approach is tested and verified on an islanded microgrid located on an island in the subtropical region.

# **CHAPTER 5 A QUANTITATIVE APPROACH AND SIMPLIFIED GENERIC TRANSIENT MOTOR STARTUP POWER MODELS FOR MICROGRIDS SECURITY ASSESSMENT**

This chapter presents a quantitative approach to assess the security of microgrids' dynamic load of power consumers. Section 5.1 introduces the procedure and methods of the security assessment approach. Section 5.2 develops two simplified generic transient models to quantify chiller motor startup performance, including inrush current and startup time. Section 5.3 presents the results of the performance assessment, and Section 5.4 provide a summary of this chapter.

## **5.1 Procedure and method of quantitative security assessment**

### ***5.1.1 Outline of security assessments quantification procedure and method***

Previously, the developed reliability performance indicators in the reliability assessment are used to assess the power supply adequacy performance. Due to lacking security performance indicators, security assessment is rarely considered and studied. To bridge this gap, Figure 5.1 depicts the procedure of the microgrid security assessments and its two major outputs, microgrid blackout risk, and system wear potential. To quantify the microgrid blackout risk, the annual inrush load-embedded dynamic load of the microgrid (defined as the “total transient load” in this study) is the combination of the “instantaneous load” from the electrical equipment and the “inrush load” from the startup of electrical equipment. Its load profile is estimated by

adding its inrush current during chiller startup on its annual dynamic electrical load profile.

To quantify the microgrid blackout risk, the annual dynamic electrical load profile is generated in the first step using the microgrid model based on the power load profiles of the cooling systems and other electrical appliances. The power load profile of the cooling systems is obtained using the cooling load profile estimated based on annual weather data, internal load, and occupant profile. In the second step, the inrush current is estimated using an inrush current model according to chiller specifications. In the third step, according to the presumed chiller capacity and the estimated cooling load profile, the chillers' startup (and stop) profile is determined through chiller startup evaluation. In the fourth step, by using the annual inrush load-embedded dynamic load profile of the microgrid generated by combining the inrush current, chiller startup profile, and annual dynamic electrical load profile, the overloaded transient load, is estimated. At last, the microgrid blackout risk is obtained using the total overloaded transient load and the presumed failure probability function of the microgrid.

To quantify the system wear potential, the inrush current and startup time of chillers are first calculated using the developed inrush current and startup time models, respectively. Then, inrush current shock is estimated using inrush current and startup time. The system wear potential is at last quantified based on the estimated overloaded transient load of the microgrid and its inrush current shock. The microgrid blackout risk and system wear potential can provide quantitative indexes to assess microgrid security.

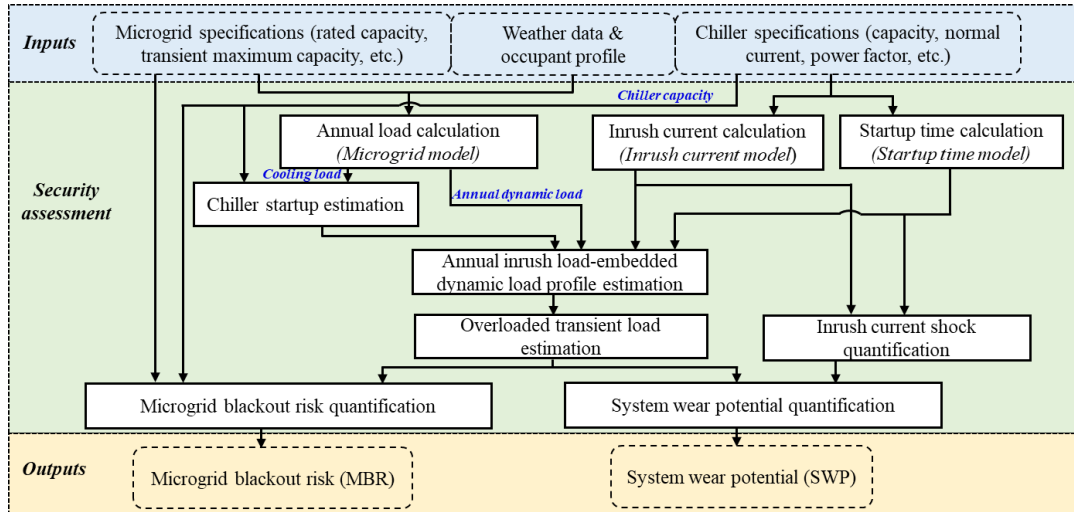


Figure 5.1 Outline of the proposed security assessment

### 5.1.2 Determination of microgrid transient load capacity

The annual inrush load-embedded dynamic load profile of a microgrid is a dominating factor in system security. The operation of a microgrid can be classified into two operation states, the normal operation state, and the overload operation state, as shown in Figure 5.2. In this study, the operation state of a microgrid at a particular time is determined by its total transient load. When the total transient load of the microgrid is below its rated capacity, the grid operates at a normal operation state. At this state, the failure probability of the microgrid is ignorable. When the total transient load of the microgrid is below its rated capacity, it operates at a normal operation state. At this state, the failure probability of the microgrid is ignorable. When the total transient load is above its rated capacity, the grid operates at the overload operation state, which is regarded as an overloaded case. When the total transient load is between the rated capacity and the transient load capacity, the failure probability is moderate, and the microgrid is considered to operate at the moderate-risk region. When the total transient load is above the transient load capacity, the failure probability is high, and the microgrid is considered to operate at the high-risk region.

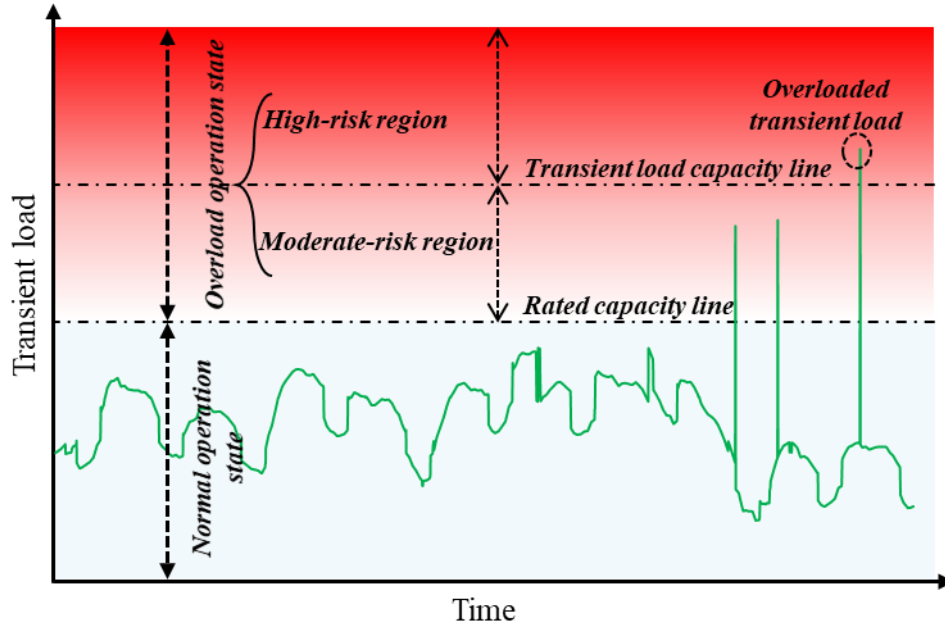


Figure 5.2 Schematic representation of the microgrid operation states

Transient load capacities between 110% and 263% have been tested (Choi et al., 2018). 150% of rated capacity was recommended as the transient load capacity of a microgrid in that study. Another study (Endo et al., 20007) recommended 140% of the rated capacity as the transient load capacity of a power grid, where the transformer properties were the main concern. In this study, the transient load capacity is set to 140% of the rated capacity.

### 5.1.3 Introduction of equivalent overloaded load

The intensity of the overloaded transient current is normally used to detect and evaluate the system state according to the presumed threshold of the overloaded load limit. The voltage and power factor are assumed to be constant in this study. The overloaded transient load is usually used in system state evaluation without considering the duration, as the duration of peak current is not easy to be quantified. However, both the duration and the intensity of the overloaded transient load significantly impact system security. For instance, a 200 kW overloaded transient load

with 0.1s and a 200 kW overloaded transient load with 0.5s pose the same threat to the system security if the duration is not considered. Therefore, in this study, an equivalent overloaded load is introduced to reflect both the intensity and duration of an overloaded current/load, following the common practice of using load or current. The equivalent overloaded load ( $L_{equ}$ ) is defined as the equivalent load of the same overloaded energy over the “reference duration” in Eq. (5.1), where  $L_{ove}$  is the overloaded current or load and  $\Delta T$  is the reference duration. In this study, the reference duration is 0.2 seconds, as inrush current typically lasts about ten cycles (Cui et al., 2005).

$$L_{equ} = \frac{\int L_{ove}(t)dt}{\Delta t} \quad (5.1)$$

#### **5.1.4 Formulation of the quantitative approach**

##### **Estimation of the chiller startup profile**

The commonly used sequence control scheme, conventional total-cooling-load-based chiller startup, is adopted to estimate the chiller startup profile. According to (Zhuang et al., 2020), Eq. (5.2) describes the selection of the number of operating chillers at a particular cooling load of a chiller plant in a microgrid or a building, where  $N^t$  is the number of the chiller startup, and  $CL_t$  is the microgrid cooling load at the time  $t$ .  $Cap_{chi}$  is the chiller capacity in operation.

$$N^t = \text{ceil}\left(\frac{CL_t}{Cap_{chi}}\right) \quad (5.2)$$

##### **Formulation of failure probability distribution and assessment of blackout risk**

A microgrid has different failure probabilities under different instantaneous loads. To perform a quantitative blackout risk assessment, the annual inrush load-embedded

dynamic load profile and failure probability distribution under different simultaneous loads are needed. Thus, the accumulated annual number of microgrid blackouts ( $R_{acom}$ ) and the annual average failure probability ( $R_{av}$ ) of overloaded cases can be calculated by using Eq. (5.3) and Eq. (5.4), respectively. Where, the number of overloaded cases is  $N_{ove}$ , and  $FP$  is the failure probability.

$$R_{acom} = \sum FP \times N_{ove} \quad (5.3)$$

$$R_{av} = \frac{R_{acom}}{N_{ove}} \quad (5.4)$$

The failure probability  $FP$  is defined as shown in Eq. (5.5), which is obtained by multiplying the occurrence probability  $Oc(Fa)$  and the severity probability  $Se(Fa)$  (Li et al., 2015). The occurrence probability  $Oc(Fa)$  and the severity probability  $Se(Fa)$  can be calculated by the failure mode and effects analysis (FMEA). Where, a 10-point FMEA scale is used according to the review of Liu et al. (2013). In the literature, several models were proposed to describe the failure probability distributions (Henneaux, 2015). The failure probability distributions were assumed to follow a linear function in (Chen et al., 2005; Zima and Andersson, 2005). An exponential function (Nedic, 2003) and cumulative distribution function (CDF) (Bhatt et al., 2009; Lee, 2008) were also proposed.

$$FP = Oc(Fa) \times Se(Fa) \quad (5.5)$$

In fact, a large amount of site or experimental data regarding microgrid failure cases is needed to determine the exact failure probability distribution statistically, but it is hardly available. A linear relation is not reasonable. For instance, if the magnitude of the overload is reduced by half, the failure probability of the microgrid would be reduced by more than half of its previous risk. A power function for the failure

probability is proposed by simplifying the above exponential function and the cumulative distribution function, and  $j$  is set to two in this study, as shown in Figure 5.3 and Eq. (5.6). The failure probability distributions are adopted according to the different operation states in this study. The failure probability is set to zero when the instantaneous load is below the rated capacity. When the instantaneous load is between the rated capacity and the transient load capacity, the failure probability is set to functions of the instantaneous load, as shown in Eq. (5.6). When the instantaneous load is above the transient load capacity, the failure probability is set to one.

$$FP = \begin{cases} 0 & (0\% \leq PL < 100\%) \\ a \times PL^j & (100\% \leq PL < 140\%) \\ 1 & (140\% \leq PL) \end{cases} \quad (5.6)$$

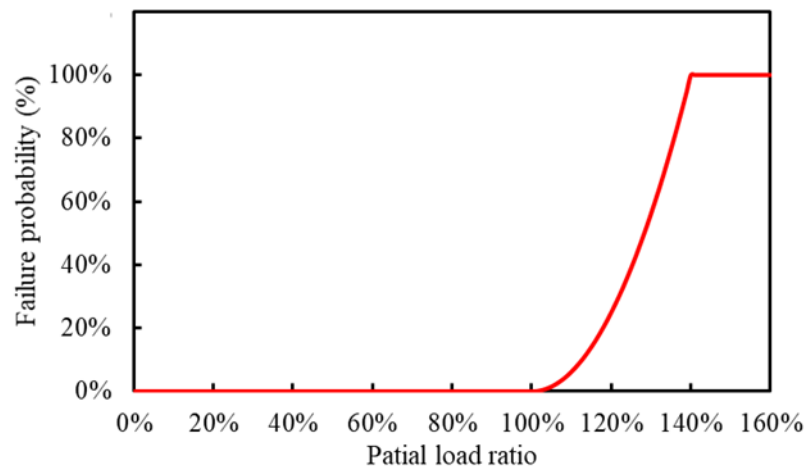


Figure 5.3 Functions of the failure probabilities in different partial load ratios

### **Estimation of inrush current shock and system wear potential**

The startup of any electromagnetic facility causes an inrush current, which naturally leads to an inrush current shock to the microgrid concerned. However, this only leads to an effective inrush current shock when it pushes the total transient load of the microgrid above the rated capacity. It is proposed to quantify the strength of an inrush current shock as the total transient load over the rated capacity (i.e., the part of load

over the rated capacity) accumulated over time, as shown by Eq. (5.7). The accumulation of total overloaded cases, shown in Eq. (5.8), is used to quantify the system wear potential over the entire operation period of concern, where  $n$  is the number of overloaded cases during the operation period of concern.

$$\text{Inrush current shock (ICS)} = \int L_{ins}(t)dt \quad (5.7)$$

$$\text{System wear potential (SWP)} = \sum_{i=1}^n ICS \quad (5.8)$$

## 5.2 Development and validation of transient startup power models for chillers/motors

### 5.2.1 Basic assumption and features of models and the model development procedure

Figure 5.4 shows a typical inrush current waveform and the simplified waveform assumed in this study. The real inrush current waveform is shown in Figure 5.4 (a) and the basic assumption of inrush current calculation is shown in Figure 5.4 (b). As shown in Figure 5.4 (a), the inrush current reaches its peak at the beginning, and then it gradually decreases until it stabilizes at the steady-state current, typically within one second. The peak current is defined as the inrush current value, and the duration is defined as the startup time. To simplify the waveform representation of inrush current in the modeling process, a triangle waveform is assumed, as shown in Figure 5.4 (b), where the current reaches its peak at the start and then decreases following a linear function.

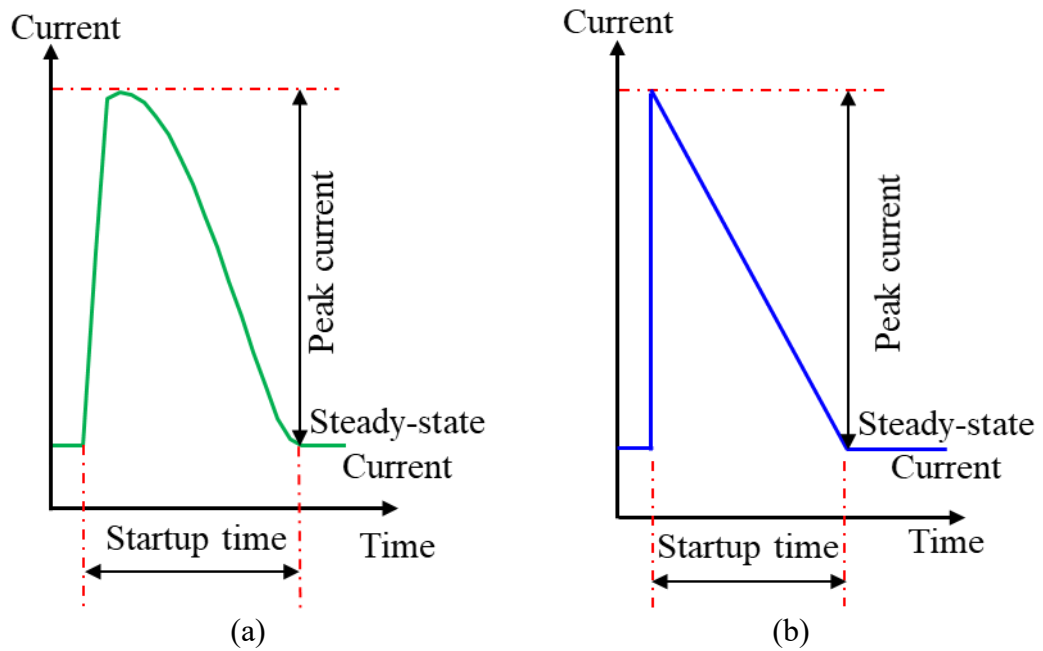


Figure 5.4 Schematic representation of inrush current waveform and basic assumption of inrush current calculation

The features and benefits of the transient startup power models for chillers/motors developed in this study are summarized as follows. They are generic and simplified empirical models. The models can directly calculate inrush current and the startup time for different chillers and motors using a common-used starting mode (i.e., directly starting). Meanwhile, unlike the physical models, these simplified empirical models have much lower computational costs. In general, models with fixed coefficients benefit from the high accuracy in the training domain but suffer from poor accuracy in wide applications. To overcome this limitation, data from three large manufacturers (Siemens, Asea Brown Boveri, and Leroy-Somer) are used in the model development and validation, increasing their accuracy and robustness. Similar models of chillers/motors using other starting modes can be developed using the same approach based on the startup performance data of motors of corresponding starting modes (e.g., star-delta starting or soft starting).

Figure 5.5 shows the procedure for model development. Firstly, the motor or chiller specifications of a particular manufacturer (i.e., Siemens) are inputted into the detailed physical motor model (i.e., existing components in Matlab-Simulink). This model is a classical physical model, which is proven to be accurate and reliable when predicting the transient behavior of motors during startup (Ansari and Deshpande, 2010). The startup performance is then simulated using the motor model. The simulation results using the motor or chiller specifications are then analyzed to identify coefficients of the pre-selected empirical models (i.e., polynomial functions). Only the significant input variables remain as the inputs of the empirical models to keep the models simple. The Residual and R-squared values are analyzed to evaluate the model deviation. Model fitness verification is conducted to ensure prediction accuracy. Finally, the simplified generic empirical models are validated using the startup performance data of the other two motor manufacturers (i.e., Asea Brown Boveri and Leroy-Somer).

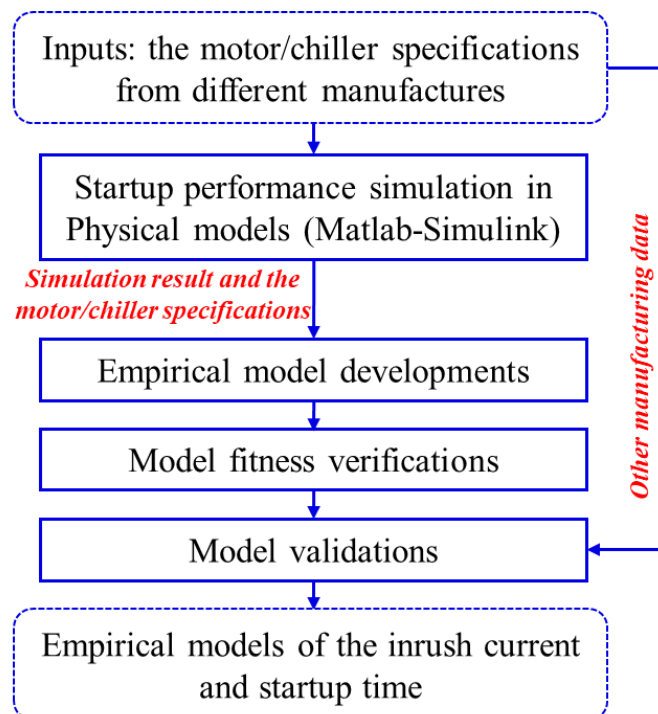


Figure 5.5 Procedure of the model development

### 5.2.2 Identification of input variables of significance and model inputs

At the preliminary stage of model development, all eight motor/chiller specifications are selected and tested as the input variables of the motor/chiller models. As the objective of the model development is to obtain simplified generic models of accepted accuracy, simple functions were tested. It was found that first-order proportional functions of individual input variables combined with the first-order proportional functions of the combinations of these input variables (i.e.,  $X_i \times X_j$ ) satisfy accuracy expectations. Table 5.1 shows the list of motor specifications and input variables of models. Two major steps are involved in model development, including identifying the input variables (i.e., the terms) of significance using the ANOVA (a statistical approach) method and determining the model coefficients using regression analysis.

Table 5.1 List of motor specifications and model inputs

Specification/input variable	Unit	Symbol
Motor capacity	kW	A
Nominal electrical current	A	B
Maximum electrical current	A	C
Nominal Torque	Nm	D
Maximum Torque	Nm	E
Speed difference	rpm	F
Initial partial load	%	G
Power factor	%	H

### 5.2.3 Inrush current model and startup time model

The transient startup power models for chillers/motors to be developed include an inrush current model and a startup time model. The final forms of the simplified generic inrush current model and the startup time model developed are presented as shown in Eq. (5.9) and Eq. (5.10), respectively. The input variables included in the

models are those of significance identified among the input variables (including the combinations of any two variables), according to the P-value using the ANOVA method. Inrush current and the startup time are represented as the first-order proportional functions of individual input variables together with the first-order proportional functions of the combinations of input variables, which are identified to be significant. Regression analysis, as a well-known statistical method, is used to determine the coefficients of the models using the motor startup performance data. The coefficients and parameters of the inrush current and startup time models are presented in Table 5.2 and 5.3, respectively.

$$I_{current} = [\partial_1 \partial_2 \partial_3 \partial_4] \times [V_1^{current} V_2^{current} V_3^{current} V_4^{current}]^T + \partial \quad (5.9)$$

$$T_{startup} = [\partial_1 \partial_2 \partial_3 \dots \partial_{11}] \times [V_1^{time} V_2^{time} \dots V_{11}^{time}]^T + \partial \quad (5.10)$$

Table 5.2 Detailed information of the inrush current model

Coefficients				
$\partial_1$	$\partial_2$	$\partial_3$	$\partial_4$	$\partial$
31.25	-12.98	0.67	-705	579
Parameters				
$V_1^{current}$	$V_2^{current}$	$V_3^{current}$	$V_4^{current}$	-
<i>A</i>	<i>B</i>	<i>C</i>	<i>H</i>	-

Table 5.3 Detailed information on the startup time model

Coefficients					
$\partial_1$	$\partial_2$	$\partial_3$	$\partial_4$	$\partial_5$	$\partial_6$
$2.152 \times 10^{-1}$	-6.8	-4.48	$-2.8 \times 10^{-5}$	$-4.41 \times 10^{-2}$	8
$\partial_1$	$\partial_2$	$\partial_3$	$\partial_4$	$\partial_5$	$\partial$
$1 \times 10^{-6}$	$-1.265 \times 10^{-1}$	$2.58 \times 10^{-2}$	$1 \times 10^{-7}$	$-1 \times 10^{-7}$	4.35
Parameters					
$V_1^{time}$	$V_2^{time}$	$V_3^{time}$	$V_4^{time}$	$V_5^{time}$	$V_6^{time}$
<i>A</i>	<i>G</i>	<i>H</i>	<i>A</i> × <i>B</i>	<i>A</i> × <i>G</i>	<i>G</i> × <i>H</i>
$V_7^{time}$	$V_8^{time}$	$V_9^{time}$	$V_{10}^{time}$	$V_{11}^{time}$	

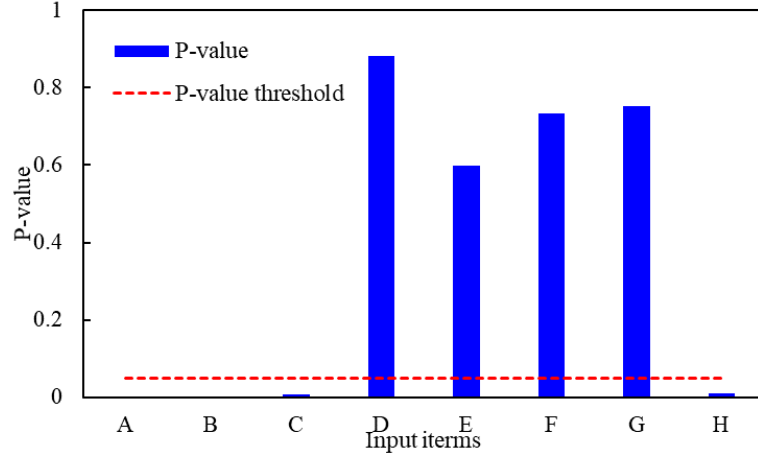
#### ***5.2.4 Identification of inputs for inrush current and startup time models***

Two model formats are considered for both inrush current and startup time models. One (namely “linear model”) includes the first-order items of the individual input variables only, and the other (namely “nonlinear model”) involves both the first-order items of the individual input variables and the combinations of any two input variables. Between these two models, the linear model, which is simpler and has satisfactory accuracy, is eventually selected for use in this study.

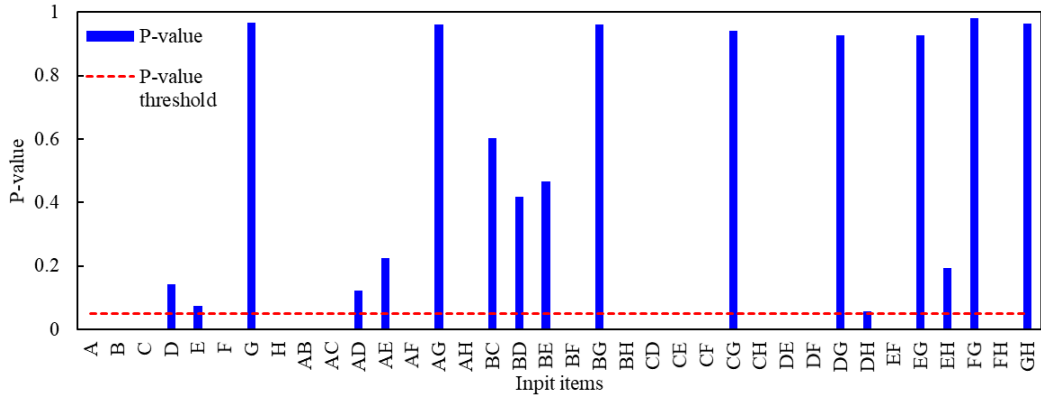
The P-value is used to determine input variables' impact on model outputs, thereby identifying the most significant inputs. Commonly, the P-value threshold is set to 0.05, and input variables with a P-value above the threshold are removed.

#### ***Inrush current models***

According to the P-value, the significant input variables and their combinations, i.e., those having significant impacts on the inrush current, can be determined. Figure 5.6 (a) and Figure 5.6 (b) show the individual input variables and the combinations of the input variables, respectively. Eventually, Eq. (5.11) and Eq. (5.12) are the final formats of the linear model and nonlinear inrush current models, where the significant items, i.e., those having P-values below the threshold (0.05), are identified and used as the inputs of both inrush current models, respectively.



(a) P-value of the linear model



(b) P-value of the nonlinear model

Figure 5.6 Identification of inrush current model inputs of significance

$$I_{peak,lin} = [\partial_1 \partial_2 \partial_3 \partial_4] \times [V_1^{peak,lin} V_2^{peak,lin} V_3^{peak,lin} V_4^{peak,lin}]^T + \partial \quad (5.11)$$

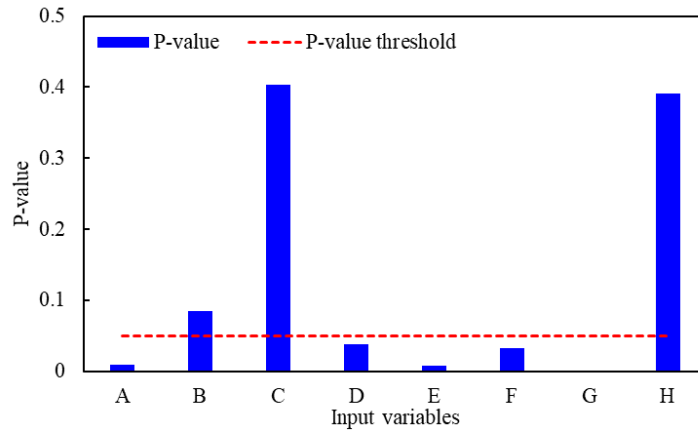
$$I_{peak,nonlin} = [\partial_1 \partial_2 \dots \partial_{19}] \times [V_1^{peak,nonlin} V_2^{peak,nonlin} \dots V_{19}^{peak,nonlin}]^T + \partial \quad (5.12)$$

### **Startup time models**

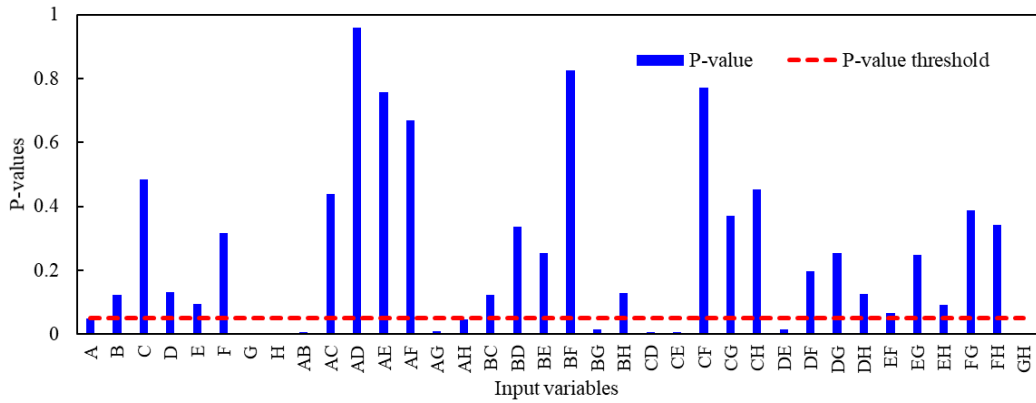
Using the P-value, the significant input variables (i.e., the terms) of startup time are identified, as shown in Figure 5.7 (a) for the linear model and Figure 5.7 (b) for the nonlinear model, respectively. The final forms of these two models, including the remaining inputs, are shown in Eq. (5.13) and Eq. (5.14), respectively.

$$T_{start,lin} = [\partial_1 \partial_2 \partial_3 \partial_4] \times [V_1^{start,lin} V_2^{start,lin} V_3^{start,lin} V_4^{start,lin}]^T + \partial \quad (5.13)$$

$$T_{start,nonlin} = [\partial_1 \partial_2 \dots \partial_{11}] \times [V_1^{start,nonlin} V_2^{start,nonlin} \dots V_{11}^{start,nonlin}]^T + \partial \quad (5.14)$$



(a) P-value of the linear model



(b) P-value of the nonlinear model

Figure 5.7 Identification of startup time model inputs of significance

### 5.2.5 Identification of model coefficients and fitness verification

The coefficients of the significant input variables (i.e., the terms) are determined based on regression analysis. R-squared ( $R^2$ ), as a statistical measure, refers to the proportion of the variance for a dependent variable, which is explained by independent variables in a regression model (Cameron and Windmeijer, 1997). The model fitness evaluation is conducted according to the values of the  $R^2$ . If the  $R^2$  of the model is one, the model prediction is perfectly accurate. Thirty-six motors of different specifications, each with

three different initial partial loads, are considered. A total of 108 samples are involved in the model development and training.

### Inrush current models

Residuals can be represented by the actual residual and standardized residual, respectively. The former represents the deviation between the outputs of the proposed model and the actual performance data. Figure 5.8 (a) shows the actual deviations of linear and nonlinear inrush current models in all working conditions with available performance data. Figure 5.8 (b) shows the box charts of the standardized residuals for these two models. Most standardized residuals are within  $[-1, 1]$ , while the range of  $[-2, 2]$  remains acceptable.

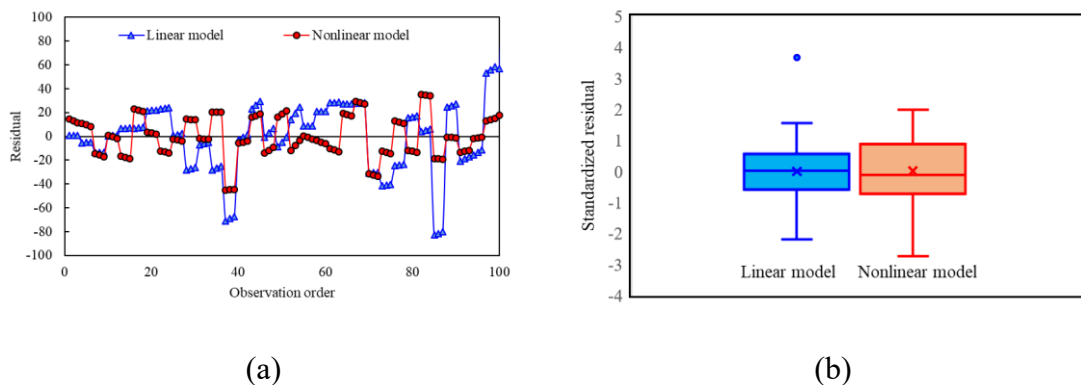


Figure 5.8 Actual residuals (a) and standardized residuals (b) of linear and nonlinear inrush current models

Figure 5.9 shows the fitness of these two models over the working conditions concerned. Both linear and nonlinear models can accurately predict the motor inrush current and have similar accuracy. As the linear model is much simpler, it is selected and recommended for predicting motor inrush current.

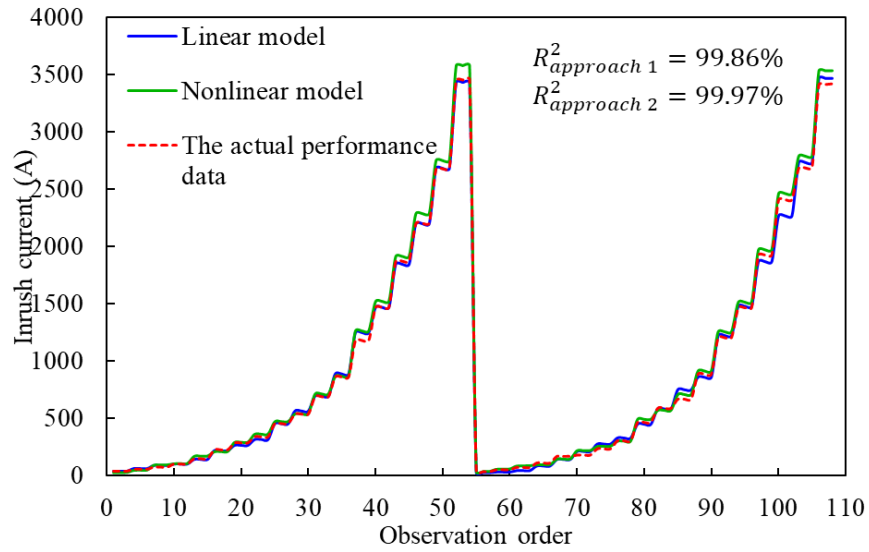


Figure 5.9 Fitness verification of the two inrush current models

### Startup time models

Actual and standardized residuals of the linear and nonlinear startup time models in all working conditions with available performance data are shown in Figure 5.10 (a) and Figure 5.10 (b), respectively. The residual of the linear startup time model is higher than that of the nonlinear model. The box charts in Figure 5.10 (b) show their standardized residuals, where most standardized residuals are within  $[-1, 1]$  as well.

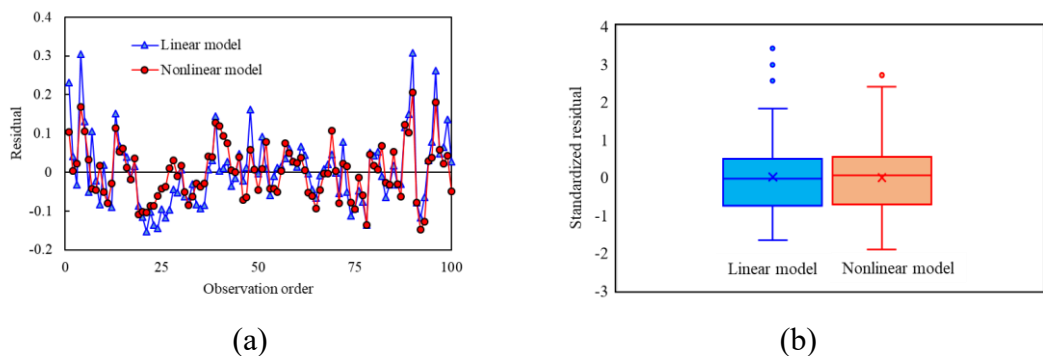


Figure 5.10 Actual residual and standardized residual for the startup time model

Figure 5.11 shows the fitness of these two startup time models over the working conditions concerned. The nonlinear model predicts startup time with satisfactory accuracy ( $R^2=80.24\%$ ), while the linear model has an  $R^2$  of 71.78% below the normal

threshold for satisfactory accuracy ( $R^2=80\%$ ). Thus, this study selects the nonlinear startup time model for startup time prediction.

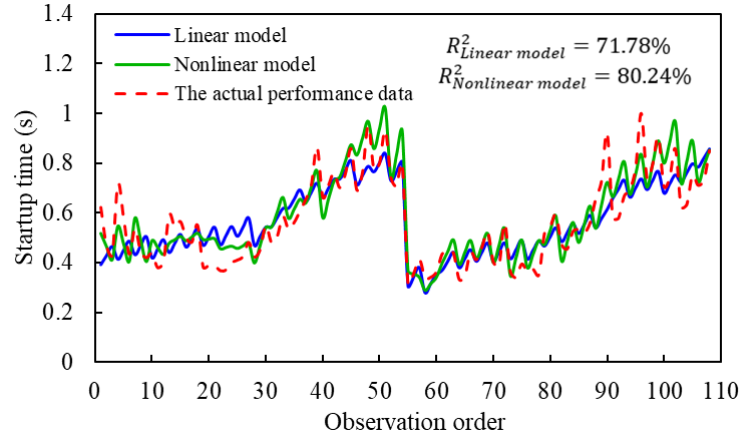


Figure 5.11 Fitness verification of the startup time model

### 5.2.6 Model validation

As mentioned in Section 5.2.1, the performance data of the motors from the other two major manufacturers (Leroy-Somer and Asea Brown Boveri) are used to validate the models. The validation is conducted using two criteria, Normalized Mean Bias Error (NMBE), shown in Eq. (5.15), and Coefficient of Variance of the Root Mean Square Error (CVRMSE), shown in Eq. (5.16). These criteria are both widely used in model validation.

$$NMBE(\%) = \frac{\sum_{t=1}^N (d_t - s_t)}{\bar{m} \times (N - p)} \times 100 \quad (5.151)$$

$$CVRMSE(\%) = \frac{\sqrt{\sum_{t=1}^N \frac{(d_t - s_t)^2}{(N - p)}}}{\bar{m}} \times 100 \quad (5.16)$$

where,  $d_t$  and  $s_t$  are the values from actual performance data and model predictions, respectively.  $N$  is the number of total data points.  $\bar{m}$  is the average value of the actual performance data.  $p$  is the number of the adjustable model parameters.

Table 5.4 presents the model validation results of the inrush current and startup models. The motor specifications are referred to the published information/data from the three manufacturers (Leroy-Somer, 2013; ABB, 2020; Siemens, 2021). There are 108 data sets, i.e., 36 motors of different specifications, each having three initial partial loads. Therefore, a total of 324 (108×3) samples are used in the model validations. Most of the NMBE values are lower than 10%, and the CVRMSE values are lower than 20%, indicating that the accuracy of the models is acceptable.

Table 5.4 Model validation results

Manufacturer	Inrush current model		Startup time model	
	NMBE(%)	CVRMSE(%)	NMBE(%)	CVRMSE(%)
Leroy-Somer	7.63	5.12	8.70	19.61
Asea Brown Boveri (ABB)	-11.65	6.34	-7.51	14.11
Siemens	-3.47	5.3	3.60	17.80

### 5.3 Security assessment and assessment results

#### 5.3.1 Overview of the microgrid assessed and estimation of annual inrush load-embedded dynamic load profile

The microgrid used in this chapter serves a holiday hotel on a remote island in Hong Kong. Hong Kong is located in the subtropical region with a long hot and humid summer. The chiller plant consumes a large portion of the electricity for cooling and dehumidification. The rated capacity of the microgrid is 2,000 kW, and the transient maximum overloaded capacity is 2,800 kW using 140% of the rated capacity, as mentioned in Section 5.1.2. The basic information about the hotel has been introduced in Section 3.1, and the detailed microgrid model is introduced in Section 3.2. To simplify the calculation, the coefficient of performance (COP) of the chillers is assumed to be four as a constant. Based on the developed TRNSYS model, the annual

dynamic cooling load and annual dynamic electrical load profile are simulated and obtained, as shown in Figures 5.12 (a) and 5.12 (b), respectively. The typical annual Hong Kong weather data is used in this simulation.

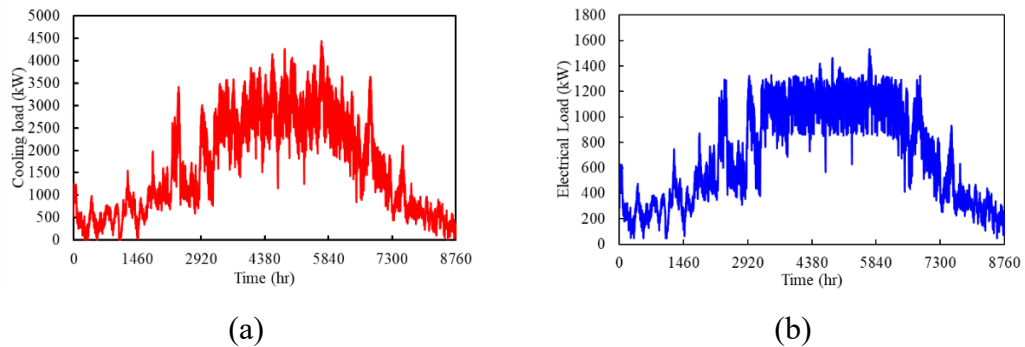


Figure 5.12 The profile of the annual dynamic cooling load (a) and dynamic electrical load (b) in the hotel microgrid

The total capacity of chillers is determined based on the maximum annual cooling load multiplied by a factor of 1.2. To study the impacts of chiller size on the inrush current, the sizes of chillers selected range from 80 kW to 3,000 kW, including 37 scenarios in total, in the study. This is equivalent to a 20 kW to 750 kW motor as well as a ratio of microgrid capacity from 1% to 37%. The detailed test results of three typical scenarios involving very small chillers (15 chillers of 400 kW, 14 duty and one standby), medium chillers (six chillers of 1,200 kW, five duty and one stand-by), and very large chillers (three chillers of 3,000 kW, two duty and one stand-by) respectively were presented. A high number (i.e., 15) of chillers is set by considering the scenario when multiple buildings with a high aggregated number of chillers are involved in a microgrid. In this scenario, the building considered in the assessment can be regarded as a “virtual building” with aggregated loads from multiple buildings.

The microgrid model consists of the supply-side system model and the demand-side system model. The demand-side system model is developed using TRNSYS according to the presumed specifications of the demand side. The supply-side system model is

virtual, which is developed by assuming the power supply and demand are balanced. Inrush current in the microgrid system is further predicted by estimating the annual chiller operating sequence profile. When an additional chiller starts in operation, an inrush current occurs. This inrush current is added to the dynamic electrical load of the microgrid to form the inrush load-embedded dynamic load profile. Figure 5.13 shows the inrush load-embedded dynamic load profiles of three typical scenarios in a month. Only the profiles during a month are presented to make them clear to readers. When using very small chillers, the total transient load of the chiller startup has a negligible impact on system security. In fact, the chillers, with very frequent startups (more than 80 activations per month), may pose a higher risk to damage the chillers and reduce the life of chillers. In the second typical scenario, the total transient load increased greatly during the chiller startup. It occasionally even exceeded the rated capacity of the microgrid (the green line in figure 5.13) but remained lower than the transient load capacity of the microgrid. The microgrid risked blackout due to the high inrush current but said the risk was not high. In the third typical scenario, despite a low frequency of chiller plant startup, the risk of system blackout was almost 100%. The very large chillers are hard to operate efficiently, as the cooling load ratio was very low, and chillers operated at low COP most of the time. Although the low frequency of startup reduced the inrush current frequency, the instantaneous load due to the huge inrush current was much higher than the microgrid transient load capacity and thus posed a big threat to the microgrid security. Therefore, the chillers selected should not be too large. To obtain a reasonable arrangement for chiller size, a detailed analysis of the impact of chiller size on microgrid security is further conducted in the following sections.

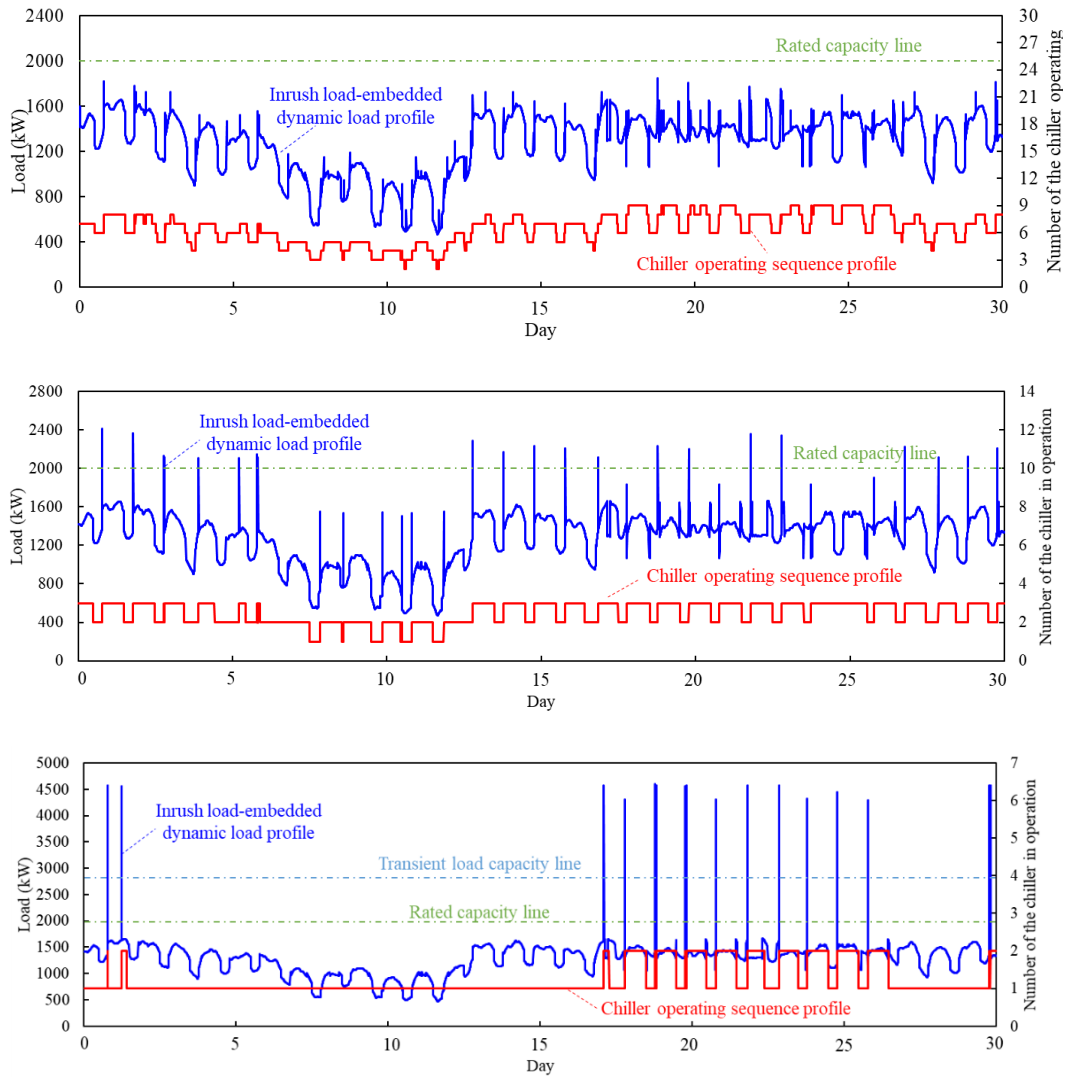


Figure 5.13 Three scenarios of the monthly number of the chillers in operation and their inrush load-embedded dynamic load profiles of the microgrid employing three different sizes of chillers

### 5.3.2 Results of risk-based microgrid capacity quantification and analysis

Risk-based microgrid capacity quantification is accomplished by determining the cumulative number of microgrid blackouts and the average microgrid blackout risk across all overloaded cases over a year. The cumulative number of microgrid blackouts is the accumulation of the failure probabilities of all overloaded cases in a year. The average microgrid blackout risk is the average risk of all overloaded cases, which is the accumulation of the failure probabilities divided by the total number of overloaded

cases over a year. The first indicator reflects the comprehensive risk of blackouts through the estimated frequency per year. The second indicates the average probability of individual overloaded cases.

Figure 5.14 shows the quantification results among the different motor capacity ratios. When the ratio is lower than 8%, the cumulative times of microgrid blackouts and the average microgrid blackout risk of overloaded cases are zero over one year. In other words, if the presumed microgrid rated capacity is 2,000 kW, the chiller motor capacity should be no more than 160 kW for the hotel microgrid to keep the blackout risk at a negligible value considering the inrush current due to motor startup. The presumed rated capacity is obtained according to the peak electrical load from the dynamic electrical load profile in this study. In normal design practice, the rated capacity is determined based on the peak electrical load multiplied by a safety factor of 1.2 and a surge factor of 1.5 (1.8 in total) or more. If the ratio is lower than 8%, the instantaneous load involving inrush current from the chiller startup has no effective impact on microgrid system security. The motor capacity ratio is typically less than 0.083 for using the chillers of medium size, a normal chiller size for a hotel of such scale, if microgrid capacity is multiplied by a safety factor and a surge factor. In this case, inrush current from motor startup would not lead to significant microgrid blackout risk.

In addition, the cumulative number of blackouts changed from increase to decrease after the capacity as individual chiller motor size reached 580 kW, or over 29% of microgrid capacity, as shown in the red dash box of the top figure. However, it does not mean that the security of the microgrid system increases. The cumulative number of microgrid blackouts fell due to the limited total number of chiller startups in the test cases. Compared with the scenarios using small chillers, the number of operating

chillers in the system using large chillers is not sensitive to changes in cooling load in operation. Looking at the average microgrid blackout risk of individual overloaded cases, as shown in the bottom figure, the average risk of the microgrid blackout almost reaches 100% in the cases when the ratio of motor capacity exceeds 29% of microgrid capacity.

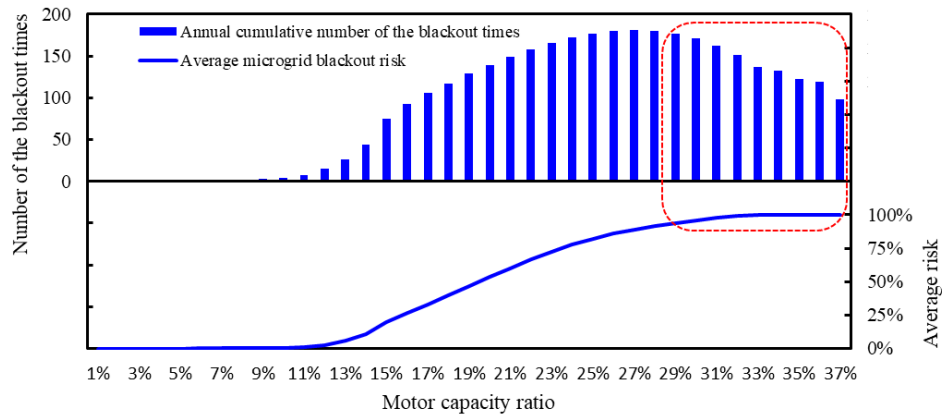


Figure 5.14 The microgrid blackout risk quantification in the overloaded cases among the different motor capacity ratios

### 5.3.3 Results of microgrid system wear potential quantification and analysis

The system wear potential is quantified by the total inrush current shock of the overloaded cases using the annual inrush load-embedded dynamic load profile of the microgrid. The high system wear potential means that the system has high maintenance costs. In cases using small chillers/motors, the startup frequency of the chillers is high, while the inrush current per individual startup is small. In contrast, in cases using large chillers/motors, the startup frequency of the large chillers is low, while the inrush current of an individual startup is large.

Figure 5.15 shows the system wear potential using different sizes of chillers. The system wear potential increased with the increase of the motor capacity ratio. Overloaded cases were rare when the motor capacity ratio was low (especially below 8%). The system wear potential due to inrush current shock was negligible. As the

ratio increased, system wear potential rose sharply. Limiting the motor capacity ratio to 8% (so that the motor capacity is =160 kW) is recommended to decrease the impact of the system wear potential on the maintenance cost.

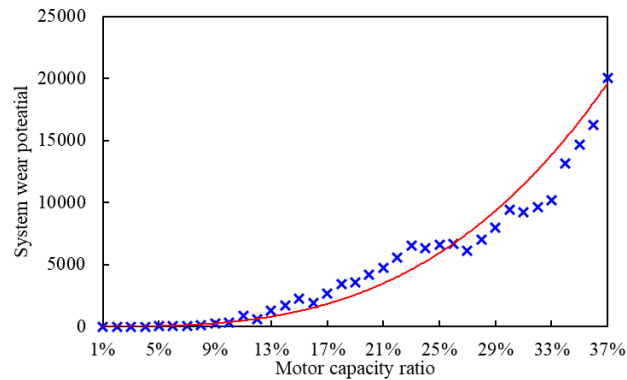


Figure 5.15 System wear potential quantification among the different motor capacity ratios

## 5.4 Summary

This chapter proposes a quantitative approach for microgrid security assessment at the design stage by considering dynamic loads of power consumers (e.g., chiller). Two simplified generic transient models are developed based on the ANOVA method to quantify the dynamic startup performance of chiller motors. The microgrid blackout risk and the system wear potential are the two major outputs of the assessment. The quantitative approach and simplified generic transient startup power models are tested on a hotel microgrid on a remote island. It is found that the approach and models can effectively assess both microgrid blackout risk and system wear potential due to inrush current.

# **CHAPTER 6 COORDINATED OPTIMAL DESIGN OF ISLANDED MICROGRIDS FOR ENHANCED RELIABILITY AND ECONOMICS BASED ON QUANTITATIVE SECURITY ASSESSMENT**

This chapter presents the procedure and methods of the proposed coordinated design optimization method for microgrids, simultaneously considering the parameters on the supply and demand sides. Section 6.1 presents the procedure and methods of the proposed coordinated design optimization method for microgrids. Section 6.2 presents the basic information of the design variables, and Section 6.3 presents the results of the optimization case studies and performance analysis. In the end, Section 6.4 provide a summary of this chapter.

## **6.1 Procedure of the developed coordinated optimal design**

### ***6.1.1 Procedure and its major steps***

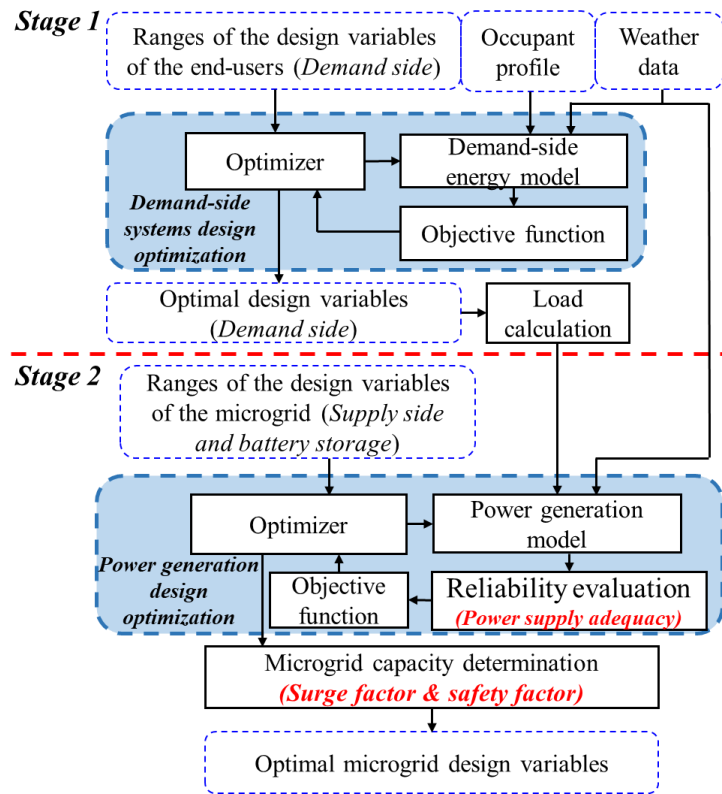
Since the background of microgrid designers is in electrical engineering mostly, the load calculation of the microgrid is assumed with peak value, or the designs of electricity facilities on the demand side are optimized by the designers in the building energy engineering field. Thus, existing microgrid optimal design methods (namely, conventional optimal design method in the rest of this paper) are typically separated into two stages, illustrated in Figure 6.1 (a) to easily understand the optimal design method. In Stage 1, the design variables of the systems on the demand sides are optimized within their searching ranges to make a trade-off between energy use efficiency and cost. The electrical demands of the microgrid, including the cooling

load from HVAC system and the electricity consumption of other electrical appliances, are then calculated according to the optimized results. In Stage 2, the power generation and battery storage design variables are optimized within their search ranges based on the demand-side loads and the weather condition. The reliability index is one of the optimization constraints to secure power supply adequacy. After the supply-demand system design optimization, the microgrid capacity is determined based on the peak power consumption of the optimized supply-demand systems by using presumed safety and surge factors to design the main electrical facilities (e.g., inverters, rectifiers, and electrical cables) in the microgrid. The surge factor is adopted to enhance the ability to withstand disruptions (e.g., the start-up inrush current) from main electromagnetic facilities at the demand side and thus to meet the security requirement.

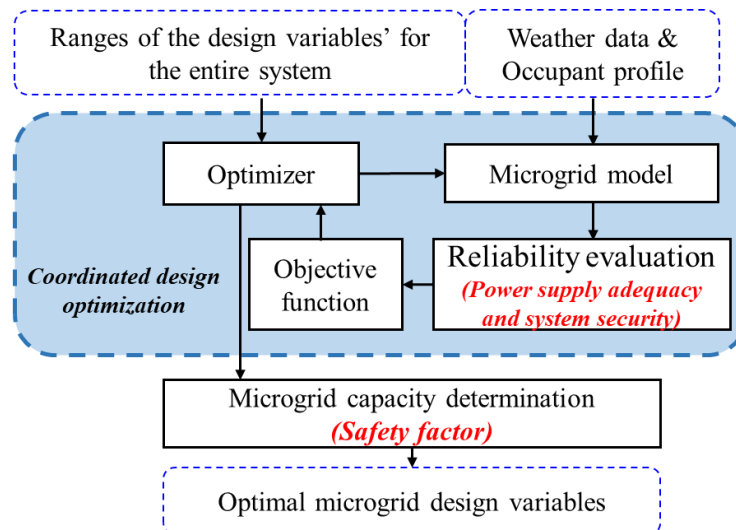
The coordinated optimal design method is developed for supply and demand systems in the microgrid based on the weather data and occupant profile, as shown in figure 6.1 (b). The impacts of the startup of the designed main electromagnetic facilities at the demand side on the microgrid security are assessed quantitatively and considered as the optimization constraints and power supply adequacy. The optimal design solution of microgrid energy systems can then be obtained by making a trade-off between system reliability and overall cost. After the supply-demand system optimization of the microgrid, the microgrid capacity is determined based on the peak power consumption of the optimized supply-demand systems by solely using a safety factor to design the main electrical facilities in the microgrid.

Compared with the conventional design method, the advances/benefits of the proposed coordinated optimal design method include: (i). the impacts of demand-side system design on the system security are quantitatively assessed and considered in the design optimization of microgrid systems instead of using a simple surge factor; (ii). a trade-

off between system cost and microgrid reliability (particularly microgrid security) can be achieved instead of enlarging the microgrid capacity roughly by using a surge factor to meet the microgrid security requirement.



(a) Conventional optimal design method



(b) Coordinated optimal design method

Figure 6.1 Procedure of the conventional optimal design method and the proposed coordinated optimal design method for power generation and demand-side systems of microgrids

### 6.1.2 Optimization objectives for optimal microgrid design

The optimal function  $F$  of the microgrid design is formulated as Eq. (6.1), which includes two sub-objective functions formulated as Eq. (6.2) for cost and Eq. (6.3) for carbon emission.

$$\text{Overall objective function: } F_{ove} = (F_{cos}, F_{emi}) \quad (6.1)$$

$$\text{Sub-objective function 1: } F_{cos}(X_{dem}, X_{sup}) \quad (6.2)$$

$$\text{Sub-objective function 2: } F_{emi}(X_{dem}, X_{sup}) \quad (6.3)$$

$$\text{Subject to: } X_{dem,min} \leq X_{dem} \leq X_{dem,max}$$

$$X_{sup,min} \leq X_{sup} \leq X_{sup,max}$$

where  $X$  is the vector of the design variables, the subscript “*cos*” refers to the overall cost, and the subscript “*emi*” refers to carbon emission. The subscript “*dem*” refers to demand-side power consumers, while the subscript “*sup*” refers to suppliers. The microgrid design variables are optimized concerning their own searching ranges.

The overall objective of the microgrid design optimization is to minimize the microgrid's overall cost ( $C_{ov}$ ). Optimization can be conducted in weather conditions over a particular period, such as a typical year to effectively quantify the overall cost. As shown in Eq. (6.4), the overall cost (i.e., annual cost) of the entire system is a sum of the microgrid costs, is further divided into the average annual initial cost ( $C_{ini}$ ) of the microgrid facilities, the annual operation cost ( $C_{opt}$ ) of the backup power generation and carbon emission cost ( $C_{emi}$ ). The initial cost of the microgrid facility is calculated by multiplying the design size and number by the unit price of the facility.

Considering the unit price of the microgrid facility may fluctuate greatly in the future, a simple calculation considering the impacts of the lifetime on the initial cost is considered while the discount factor is not considered in this design. The lifetime of the facility and the initial cost are used in the calculation of the average annual initial cost that the investors have to pay per year, as shown in Eq. (6.5). For instance, if the life cycle of one wind generator is assumed at 15 years, where the average annual initial cost is one-fifteenth of the initial cost if the interests of the investments are ignored. The annual operational cost is the primary energy cost obtained by the power generation from the backup generators, as shown in Eq. (6.6).

$$F_{ove} = C_{ove} = C_{ini} + C_{opt} + \quad (6.4)$$

$$C_{ini} = \sum (C_{fac,k} \times 1/Y_k) \quad (6.5)$$

$$C_{opt} = \left( \sum_{t=1}^{8760} P_{BPG}^t \right) \times GP_{BPG} \quad (6.6)$$

where the  $C_{fac,k}$  is the initial cost of the  $k$ th microgrid facility and the  $Y_k$  is the total number of years for the life cycle of the  $k$ th microgrid facility. The subscript “*fac*” refers to the microgrid facility. The subscript “*BPG*” refers to backup power generators.  $P_{BPG}^t$  is the power consumption of the backup generators and  $GP_{BPG}$  is the unit price of natural gas.

Besides, the carbon emission cost is the carbon emission tax (or equivalent cost) that the investors have to pay for the carbon emission due to the combustion from backup power generators, as shown in Eq. (6.7). Where,  $T_{emi}$  is the carbon emission tax and  $cef_{BPG}$  is the carbon emission factor of backup generator combustion.

$$C_{emi} = \left( \sum_{t=1}^{8760} P_{BPG}^t \right) \times T_{emi} \times cef_{BPG} \quad (6.7)$$

### 6.1.3 Constraints for microgrid system design

Microgrid reliability measures the system's overall ability to meet the demand during the operation. Hence, the constraints include both power supply adequacy and security.

#### Power supply adequacy

To ensure the power supply adequacy during the operation, the equivalent loss factor (ELF) as an index is adopted, as shown in Eq. (6.8) proposed by Allan (2013) and Baghaee et al. (2016), where  $t$  represents the time step, which is involved in the system reliability evaluation. The capital 'T' is the number of the total steps.  $E(t)$  is the energy not supplied at time step  $t$ . According to the definition, the number and the magnitude of outages are embodied in this equation. Two levels have been commonly adopted by Garciaa and Weisser (2006): ELF below 0.01 and ELF below 0.0001. The former is mostly adopted in some rural areas, while the latter is mostly adopted in developed countries/regions. Hence, the middle value (0.001) in between is adopted in the study.

$$ELF = 1/T \sum_{t=1}^T E(t)/P_{dem,t} < 0.001 \quad (6.8)$$

#### Microgrid security

The surge factor ( $SuF$ ) and safety factor ( $SaF$ ) are normally adopted in microgrid capacity determination to limit the load fluctuation within a safe range. Setting  $SuF$  as the aside margin aims to handle the inrush current due to the startup of the electromagnetic facilities (e.g., chillers), while  $SaF$  is set to consider the peak load. According to Xu et al. (2016) and Isatezde et al. (2018), the  $SuF$  and  $SaF$  are recommended as 2 and 1.1, respectively. The microgrid capacity ( $Cap_{mic}$ ) is

determined according to these two factors and peak load ( $P_{peak}$ ), as shown the Eq. (6.9).

$$Cap_{mic} \geq P_{peak} \times (SaF + SuF) \quad (6.9)$$

The conventional optimal method focuses on providing a reliable capacity in operation without considering the contribution of the demand-side systems for the microgrid security of the entire system. On the contrary, the surge impact is quantified and evaluated in the proposed coordinated optimal design method. 140% of the rated microgrid capacity as the transient load capacity is assumed as Endo et al. (2007) recommended. In this study, the “transient load” refers to the combination of the load from the demand-side energy system and the load due to the inrush load startup of electromagnetic facilities. The “inrush load” is obtained according to the inrush current from the electromagnetic facility startup. The transient load ratio is the transient load to the microgrid capacity. The microgrid system blackout will occur if the transient load ratio exceeds 140% of the rated capacity. If the transient load ratio is between 100% and 140%, the risk of the microgrid blackout is negligible. However, within the range (from 100% to 140%) of the transient load ratio, the risk of system wear and tear ( $R_{WAT}$ ) exists as shown in Eq. (6.10). Where,  $N_{over}$  is the occurrence number of the transient load ratio between 100% and 140% and  $N_{total}$  is the number of the electromagnetic facility startup. To avoid the microgrid blackout and decrease the risk of system wear and tear effectively, the ratio of the largest electromagnetic facility capacity ( $EF_{siz}$ ) to the microgrid capacity ( $Cap_{mic}$ ) has to be set below 8%, according to the study in Section 5. Besides, the  $SaF$  is also set to consider the peak load. In summary, the limits for the surge and safety impact are set as the constraints in coordinated optimal design, as shown in Eq. (6.11). and Eq. (6.12).

$$R_{WAT} = N_{ove}/N_{tot} \quad (6.10)$$

$$EF_{siz}/Cap_{mic} \leq 8\% \quad (6.11)$$

$$Cap_{mic} \geq P_{peak} \times SaF \quad (6.12)$$

## 6.2 Overview of the design case study and the microgrid system models

### 6.2.1 Description of the microgrid and its control strategies

The introduced holiday hotel, as shown in Section 3.1, is selected in the case study. Besides, the following typical control strategies are implemented in the case study. The priority (high to low) of power supply is renewable power generators, power charging from the battery storage, and backup power generators.

### 6.2.2 Basic information on the design variables and their search ranges

Table 6.1 shows the design variables and their search ranges in this case study. Seven key variables of four main categories are involved. In the first category, two common renewable energy resources (i.e., solar radiation and wind energy) are adopted as renewable power generation, while natural gas is chosen as the backup source considering the Hong Kong government policy. Using a battery as an energy storage facility is another essential solution for addressing renewable power generations of intermittent nature. On the demand side, the power consumption from the electrical chillers contributes a large percentage of the building power consumption in tropical and subtropical regions. Meanwhile, the frequent start/stop of chillers significantly impacts the microgrid's security. Thus, the size and number of the electrical chillers are selected as the key design parameters to be optimized on the demand side. To

consider the security of the entire microgrid system in the optimization, the microgrid capacity is also selected as another key design parameter to be optimized.

Table 6.1 Design parameters to be optimized and their search ranges

Category	Design parameter	Search range	Unit
Power generation system	Wind generator capacity	[0, 1000]	kW
	PV areas	[0, 15000]	m <sup>2</sup>
	Gas generator capacity	[0, 6000]	kW
Energy storage	Battery capacity	[15, 2000]	kWh
Demand-side systems	Chiller size	[500, 3000]	kW
	Chiller number	[2, 5]	N/A
Microgrid system	Microgrid capacity	[0, ∞]	kW

In microgrid design optimization, the genetic algorithm (GA), one typical heuristic algorithm in a toolbox of Matlab, is adopted as the optimization algorithm, which can effectively solve the optimization problem. The basic performance and cost data of the main microgrid facilities used in this study are listed in Table 6.2. Besides the unit prices of the major facilities, microgrid component costs are introduced to consider the initial cost associated with the microgrid capacity, which is assumed to be proportional to the microgrid capacity. The microgrid component cost consists of the hardware cost of the system controller and its soft cost (e.g., engineering, construction, commissioning, and regulatory costs) as well as the additional electric infrastructure costs (Miner et al., 2018; Khodaei and Shahidehpour, 2012).

Table 6.2 Basic performance and cost data of the main microgrid facilities\*

Parameter	Value	Unit
PV area per unit	229.72	USD/m <sup>2</sup>
Battery storage per unit	213	USD/m <sup>2</sup>
Wind generator per unit	288	USD/kW
Microgrid component costs per unit	1500	USD/kW
The unit price of natural gas	0.1075	USD/kWh
Gas generator efficiency	0.32	N/A
The overall efficiency of PV	0.2	N/A
Charge efficiency of the battery	0.85	N/A
Discharge efficiency of the battery	0.85	N/A
Maximum battery charging capacity	0.8	N/A
Minimum battery discharging capacity	0.2	N/A
The lifetime of the gas generator	25	Year
The lifetime of the chiller	15	Year
The lifetime of the PV	20	Year
The lifetime of the wind turbine	20	Year
The lifetime of the battery	10	Year
The lifetime of the Microgrid facilities	20	Year
Carbon emission tax	0.132	USD/kg
Carbon emission factor	0.055	Kg/kWh

\* *Remark:* the references of the selected data are referring to (Flores and Brouwer, 2018; Kang and Wang, 2018; Kang et al., 2017; Li, 2000; Li and Wang, 2019; Lu et al., 2015; Lu et al., 2015)

In addition, the unit price of the gas generator ( $UP_{gas}$ ) is sensitive to the change of size, which is quantified by referring to (Zheng et al., 2016), as shown in Eq. (6.13). The unit price of the chillers ( $UP_{chi}$ ) is also sensitive to the change in size. Figure 6.2 shows the unit price of the chiller at different sizes according to the practical market. The unit price (per kW) decreases with the increase in chiller size. It can be found that selecting one large-size chiller, compared to several small-size chillers, can decrease the initial cost of the chiller plant. The regression relationship, as shown in Eq. (6.14), is adopted

in this optimal microgrid design, where the  $Cap_{gas}$  is the gas generator capacity and  $Cap_{chi}$  is the chiller size.

$$UP_{gas} = 3711.78 - 280.47 \times \ln(Cap_{gas}) \quad (6.13)$$

$$UP_{chi} = -26.31 \times \ln(Cap_{chi}) + 348.01 \quad (6.14)$$

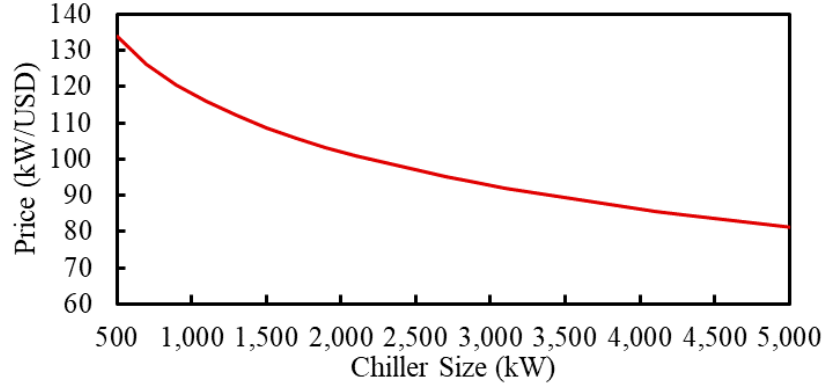


Figure 6.2 The unit price of the chiller under different sizes

### 6.3 Results of optimization case studies and performance analysis

The optimizations of the microgrid design are performed based on the reference holiday hotel using the proposed objective functions as defined in Section 6.1.2. The microgrid performance, including energy efficiency, renewable energy penetration, reliability, and economics, are comprehensively evaluated and compared in this section to identify the proper optimization method of the microgrid design.

#### 6.3.1 Overview of the optimization cases

##### Conventional optimization case

The conventional optimal design consists of two stages (i.e., demand and supply-side optimal designs). During the optimization process, the demand-side systems are concerned with the trade-off between high energy efficiency and low cost. The supply-side systems (e.g., power generators and battery storage) are concerned with a trade-off between the high penetration of renewable power generation and low cost.

Meanwhile, the entire system's reliability is the overall concern, which is addressed by setting the constraint of the power supply adequacy according to the reliability index. The microgrid capacity based on SuF and SaF is determined to meet microgrid security requirements.

### **Coordinated optimization case**

Coordinated optimal design is proposed as a novel microgrid optimal design method. This method considers the major facilities of the entire microgrid system together. The same reliability index is also adopted to ensure power supply adequacy. Considering the microgrid security, a safety factor is adopted to meet the peak load while the surge threat is quantified and prevented in the coordinated design.

#### **6.3.2 Results of microgrid design optimization**

The objective of a typical conventional optimization method is to achieve the highest energy efficiency and reduce the cost, while the objective of the coordinated optimal method is to achieve the global optimal solution of the entire microgrid system. Table 6.3 shows the optimal design solutions of these two optimal design methods. Comparing the outputs of these two optimizations, the optimal capacities of power generation and battery are similar. The chiller size and microgrid capacity are significantly different. The capacity of chillers selected by coordinated optimization is 836 kW, which is 38% of that (i.e., 2,195 kW) selected by conventional optimization. The microgrid capacity selected by coordinated optimization is 4,175 kW, 62% of that (i.e., 6,657 kW) selected by conventional optimization. The larger microgrid capacity can mitigate the surge impact on microgrid security and meet the microgrid security requirement. The quantified surge threat is involved in the optimization using the

coordinated optimization method. Thus, the small chiller and the small microgrid capacity are selected.

Table 6.3 Optimal design solutions given by the two optimal design methods

Case Name	Wind generator (kW)	PV areas (m <sup>2</sup> )	Gas generator (kW)	Battery (kWh)	Chiller (kW)	Microgrid capacity (kW)
Conventional optimization case	760	11218	4893	1620	2195×2	6657
Coordinated optimization case	742	11505	5161	1605	836×5	4175

### 6.3.3 Performance analysis and comparison

#### Economic performance

Figure 6.3 shows the cost results and the comparison ratios between the coordinated and conventional optimization cases. The cost results are presented as bar charts of the primary y-axis in this figure. The comparison ratios are shown in star points of the secondary y-axis. If the cost-saving ratio is positive, the overall cost in the coordinated optimization case is larger than the overall cost in the conventional optimization case. For instance, the initial cost ratio of the chiller is 11%, which means that the coordinated optimization case should spend much more (11% of the initial cost) on the chillers compared to the conventional optimization case.

The costs of most facilities are almost the same, such as PV panels, wind turbines, and the battery. The cost-saving ratio of the initial cost associated with the microgrid capacity is -59%, which means the initial cost associated with the microgrid capacity in the conventional optimization case is much higher than that in the coordinated optimization case. The microgrid capacity is determined to ensure the microgrid system security, while it is ignored in conventional optimization. In the coordinated

optimization, the small chillers are selected to effectively decrease the initial cost associated with the microgrid capacity and decrease the surge impact of the chiller startup on the microgrid security. Although the cost-saving ratio of the initial cost for the small chiller is 11%, the microgrid security is enhanced obviously, and the cost-saving ratio of the initial cost associated with the microgrid capacity decreases significantly. The small chiller has a low-rated COP, which causes COP to be relatively low, especially during the high cooling load period compared to the large chiller that was selected by the conventional optimization. This also causes the conventional optimization case to perform better in some items, such as CO<sub>2</sub> penalty and operation cost. Coordinated optimization aims to provide the global optimal solution for the overall cost. Therefore, considering the economic performance of the entire microgrid system, the coordinated optimization case has better performance with an overall cost saving of 5%.

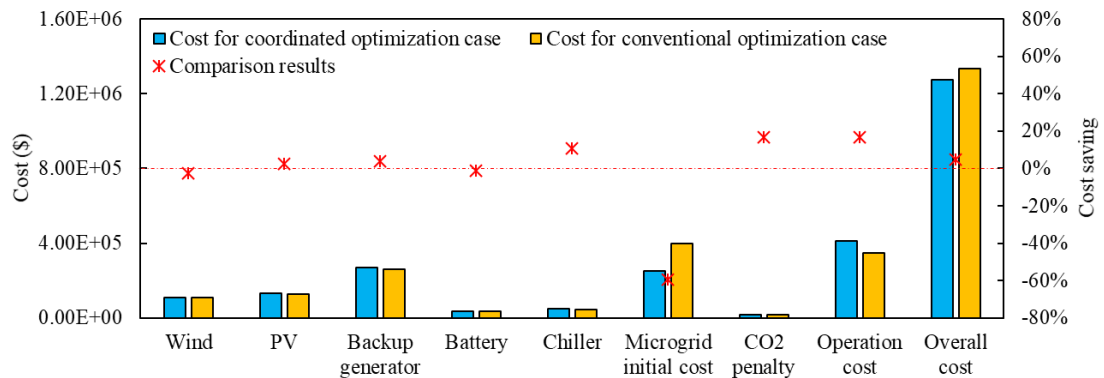


Figure 6.3 Cost of the optimal microgrid system designs given by the coordinated and the conventional optimization

### **Reliability performance**

Since the power supply adequacy is set as the constraint in both optimizations, the power supply adequacy requirement can be met in both optimization cases. In this section, the main concern and comparison are focused on microgrid security in two

optimization cases. Figure 6.4 (a) shows the transient load ratios when a chiller starts. In the conventional optimization case, the largest transient load ratio during the chiller startup is up to 114% of the microgrid capacity. According to the presumed transient limit of the microgrid capacity (i.e., 140%), it can meet the system security requirement but still causes a 3% risk of system wear and tear (defined in Section 2.3.2). In the coordinated optimization case, the largest transient load ratio is lower than 100% of the microgrid capacity. Therefore, the microgrid can meet the system security requirement and effectively avoid the risk of system wear and tear. Figure 6.4 (b) shows the number of chiller startup times over a year in these two optimization cases. The number of chiller startup times in the coordinated optimization case is over three times that in the conventional optimization case. The smaller chillers selected in the coordinated optimization are more sensitive to the change in the cooling load. Considering that the most transient load ratios are between 30% and 50% of the microgrid capacity in the coordinated optimization case, the impact of the chiller startup on microgrid security is ineffective and can be neglected.

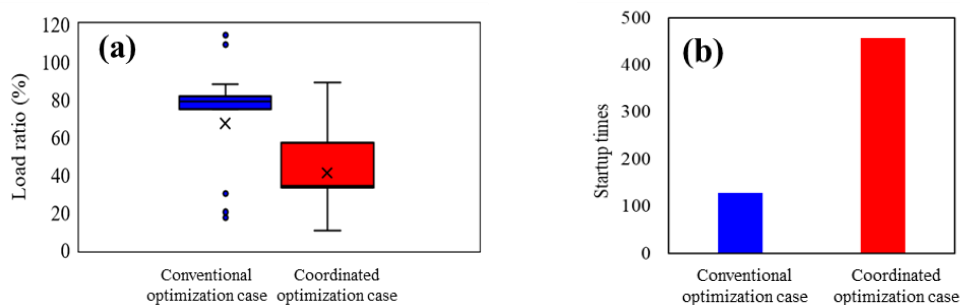


Figure 6.4 Transient load ratios during the chiller startup and the number of the chiller startup times in these two design cases

**Energy use efficiency**

The COP, as an indicator of energy use efficiency, is used to analyze and evaluate system efficiency. The comparison results of the annual COP profiles are presented in Figure 6.5. A larger chiller has a high-rated COP, while a cooling plant of several small chillers can adapt to operate at a higher COP when the cooling load is significantly lower than its design value. The larger chillers are selected by conventional optimization. In this case, higher COP can be achieved during high cooling load (between March and September). The smaller chillers are selected by coordinated optimization. In this case, the average COP (4.03) is 4.9% lower than the average COP (4.23) of the conventional optimization case.

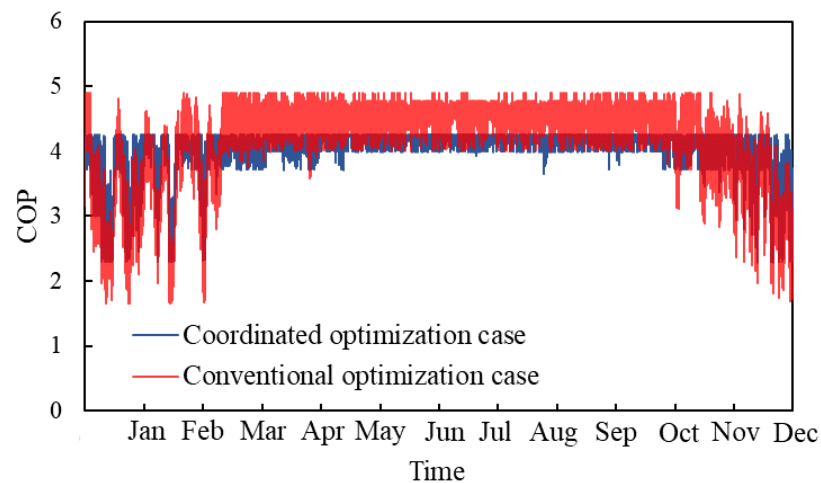


Figure 6.5 Annual COP profiles of the optimized chillers given by the coordinated and the conventional optimization

### **Renewable energy penetration**

Renewable energy penetration (REP) is the vital evaluation indicator to quantify the power generation ratio from renewable resources to the total electrical load served. Higher REP means that the system can achieve lower carbon emissions. For instance, the REP is equal to one if all the electrical loads are satisfied by renewable power generation.

The comparison results of the renewable energy penetration in both cases are shown in Table 6.4. The REP ratios in the coordinated and the conventional optimization cases are 85.9% and 88.1%, respectively. Both optimization cases have good performance concerning renewable energy utilization. The REP ratios of both cases are over 85% of the total power generation. The REP of the coordinated optimization case is 2.2% lower than that of the conventional optimization case since more backup power generation is required in the coordinated optimization to address the lower energy use efficiency and thus ensure power supply adequacy.

Besides, it can be observed that over 10% of power generation still comes from the backup power generators for the islanded microgrid. It shows that utilizing renewable sources alone cannot achieve the microgrid's reliability (power supply adequacy) due to site constraints. The zero-carbon emission objective, therefore, cannot be achieved in these cases.

Table 6.4 Renewable energy penetration in the optimized microgrid systems given by the coordinated and the conventional optimization

	Renewable energy penetration
Coordinated optimization case	85.9%
Conventional optimization case	88.1%

## 6.4 Summary

This chapter develops a novel coordinated optimal microgrid design method for enhanced reliability and economics. The power supply adequacy and system security are both quantitatively assessed and considered optimization constraints. The proposed optimal design method is tested and validated using a hotel microgrid on a remote island in Hong Kong and compared with the typical conventional optimal

design method in terms of reliability, economics, renewable energy penetration, and energy use efficiency.

# **CHAPTER 7 A QUANTITATIVE RELIABILITY ASSESSMENT AND RISK QUANTIFICATION METHOD FOR MICROGRIDS CONSIDERING SUPPLY AND DEMAND UNCERTAINTIES**

This chapter presents a quantitative reliability assessment and risk quantification method for microgrids considering supply and demand uncertainties. The procedure of the quantitative approach for microgrid reliability assessment and the risk quantification method are presented in Section 7.1. Section 7.2 presents the basic information of the tested cases and quantifications of the uncertainties on the supply and demand sides. Section 7.3 presents the tested results of the reliability assessment and Section 6.4 summarizes this chapter.

## **7.1 An uncertainty-based quantitative approach for microgrid reliability assessment**

### ***7.1.1 Outline of the proposed reliability assessment approach***

Figure 7.1 shows the detailed procedure of the proposed uncertainty-based reliability assessment approach. It involves three major steps as follows:

- *In the first step*, the major uncertain parameters are identified concerning the power generation on the supply side and the power consumption on the demand side. Then, the uncertainties of these parameters are quantified using proper probability density distributions. According to the distributions of the parameters,

different scenarios are generated using the Latin hypercube sampling (LHS) approach.

- *In the second step*, the uncertainty-based supply-demand profiles are obtained via dynamic simulation under the generated scenarios using the microgrid models based on the microgrid specifications (e.g., system component capacity and efficiency). The uncertainty-based supply-demand profiles are hourly profiles of dynamic available generation capacity and power consumption under different scenarios considering uncertainties. The available generation capacity refers to the total power generation of the microgrid system, including renewable power generation, backup power generation, and battery discharge. The power consumption includes the power consumption required by supplying the cooling and other electrical loads (e.g., lighting and plug loads).
- *In the last step*, uncertainty-based risk quantification is performed to quantify the power inadequacy risk based on the obtained uncertainty-based supply-demand profiles. The microgrid reliability performance is assessed using the power inadequacy risk and the commonly-used indexes. Finally, the microgrid reliability performance is output, which can be used for microgrid planning and design.

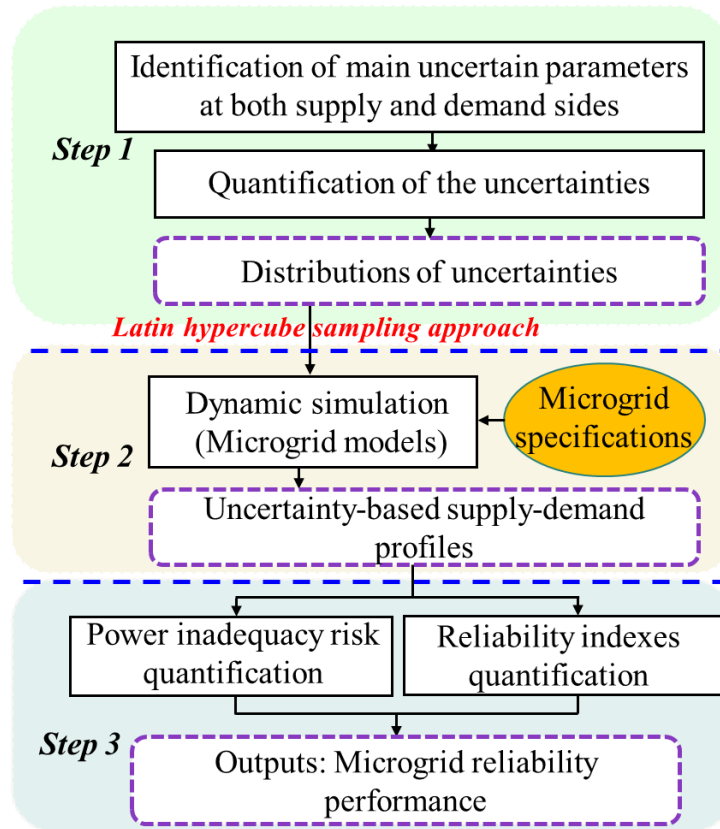


Figure 7.1 Procedure of the proposed uncertainty-based reliability assessment approach

Compared with the conventional (deterministic) reliability assessment approach, the proposed uncertainty-based reliability assessment considers the impacts of uncertainties in a quantitative approach, which can mitigate underestimation or overestimation of actual microgrid reliability performance. Compared with the existing stochastic reliability assessment approach, the proposed approach detailedly quantifies the uncertainties of both power generation and consumption. It assesses power inadequacy risk under uncertainties, enabling a more reliable assessment and risk-conscious microgrid planning/design.

### 7.1.2 Quantification of uncertainties in power generation and consumption

The uncertainties in power generation and consumption are quantified using a bottom-up approach by sampling according to the probability distributions of the main

uncertain parameters, as illustrated by Eqs. (7.1-7.4). The Latin hypercube sampling (LHS) method is adopted as it requires a smaller size of samples compared with the commonly-used Monte Carlo sampling method. The samples  $X$  for the uncertain parameters/inputs  $x_1, x_2, x_3 \dots, x_n$  (such as the outdoor temperature and solar radiation) are generated (Eq. (7.2)) using the LHS method by fitting their distributions  $G$  (Eq. (7.3)). By importing these samples into the calculation in Eq. (7.1), the distributions  $Y$  of the outputs (i.e., renewable power generation and power consumption) can be calculated as shown in Eq. (7.4).

$$(y_1, y_2 \dots, y_m)^T = f(x_1, x_2, \dots, x_n) \quad (7.1)$$

$$X = [X_1, X_2, \dots, X_n] \quad (7.2)$$

$$X_i \sim G_i \quad (7.3)$$

$$Y = (Y_1, Y_2, \dots, Y_m)^T = f(X_1, X_2, \dots, X_n) \quad (7.4)$$

Uncertainty sources and parameters of renewable power generation and power consumption mainly include:

- Uncertainty sources and parameters of renewable power generation: Conventionally, renewable power generation is predicted under the typical meteorological year (TMY) weather condition for microgrid reliability assessment. However, the actual weather conditions (e.g., solar radiation, wind speed, and outdoor temperature) vary in operation. In this study, the uncertainties in the outdoor temperature, solar radiation, and wind speed are quantified and considered in the prediction of renewable power generation.
- Uncertainty sources and parameters of power consumption: The microgrid power consumption in a subtropical region mainly consists of building cooling and other electrical loads (i.e., lighting and plug loads). The uncertainty sources and

characteristics of different loads are different. The main uncertainty source of cooling load includes the outdoor weather parameters and the internal loads (e.g., occupant density and lighting density), while the uncertainty sources of other electrical loads mainly include occupant behavior. In this study, the uncertainties of cooling and other electrical loads are quantified separately using general distributions according to their uncertainty characteristics to simplify the calculation.

### ***7.1.3 Uncertainty-based power inadequacy risk quantification for microgrid reliability assessment***

#### **Concept of uncertainty-based power inadequacy risk quantification**

Conventional reliability assessment of microgrids generally identifies power inadequacy based on fixed and deterministic supply-demand profiles estimated under typical weather conditions (i.e., TMY weather). If the power consumption of the microgrid is higher than the available generation capacity, as highlighted in the red circle in figure 7.2 (a), it will be considered power inadequacy, and the probability of power inadequacy is assumed to be 100%. Otherwise, no power inadequacy occurs, and the probability of power inadequacy is assumed to be 0%. However, due to uncertainties, the available generation capacity and power consumption are probably different from those estimated under typical weather conditions. The probability of power inadequacy at a certain time step may be overestimated and/or underestimated.

The proposed uncertainty-based method identifies power supply inadequacy and quantifies power inadequacy risk considering power generation and consumption uncertainties. The power inadequacy risk means the probability of power supply inadequacy during a certain period. As shown in figure 7.2 (b), the supply-demand

profiles given by the proposed method are no longer deterministic profiles with fixed values during a certain period. Instead, the estimated available generation capacity and power consumption during a certain period have different possible values with different occurrence probabilities. In this way, the power supply inadequacy can be identified if the value of power consumption is higher than that of available generation capacity, like the conventional method, and the power inadequacy risk can be further quantified by considering the occurrence probabilities of the corresponding available generation capacity and power consumption values.

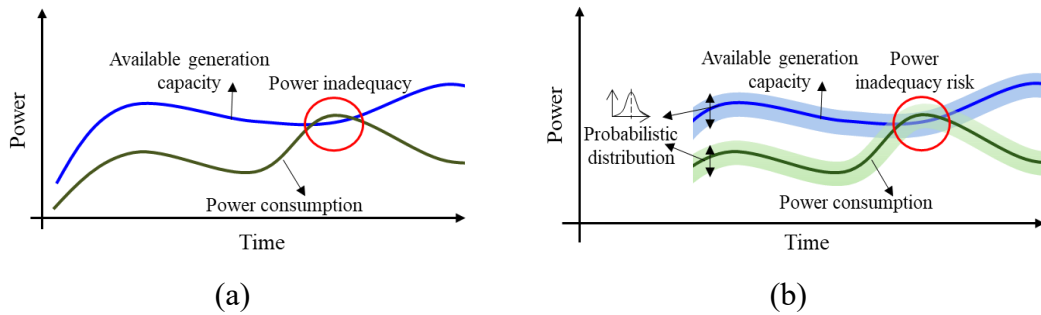


Figure 7.2 Schematic microgrid supply-demand profiles in the conventional reliability assessment (a) and uncertainty-based reliability assessment (b)

### **Uncertainty-based power inadequacy risk quantification method**

An index ( $R_{pi}$ ) for quantifying the power inadequacy risk is proposed in this study, which is calculated using Eqs. (7.5-7.6), where  $pi_{t,s}$  is an index that denotes if power inadequacy occurs at time step  $t$  for the sample  $s$  from the generated uncertainty-based supply-demand profiles. A value of 0 means power inadequacy does not occur, while a value of 1 means power inadequacy occurs.  $Prb_{sup,t,s}$  and  $Prb_{dem,t,s}$  are the occurrence probabilities of the power generation ( $P_{sup}$ ) and consumption ( $P_{dem}$ ) values for sample  $s$  at time  $t$ , respectively.  $S$  is the total number of samples generated from the supply-demand profiles at time  $t$ . The average power inadequacy risk ( $R_{pi,ave}$ ) that can reflect the power inadequacy risk during a certain period can be calculated using Eq. (7.7),

where  $H$  denotes the number of time steps over the period concerned. This study assesses the average power inadequacy risks at different time scales, including hourly, monthly, and 24-h. The average hourly and monthly risks are quantified using Eq. (7.7). Each value of 24-h power inadequacy risk is calculated using Eq. (7.8) by averaging the hourly power inadequacy risk at the same hour over all the days in the year, where  $d$  is a certain day in a year, and  $D$  is the total days over a year.

$$R_{pi,t} = \sum_{s=1}^S pi_{t,s} * Prb_{sup,t,s} * Prb_{dem,t,s} \times 100\% \quad (7.5)$$

$$pi_{t,s} = \begin{cases} 0, & \text{if } P_{sup,t,s} \geq P_{dem,t,s} \\ 1, & \text{if } P_{sup,t,s} < P_{dem,t,s} \end{cases} \quad (7.6)$$

$$R_{pi,ave} = (1/H) \times \sum_{t=1}^H R_{pi,t} \quad (7.7)$$

$$\begin{aligned} & [R_{pi,1}, R_{pi,2}, \dots, R_{pi,24}] = \\ & (1/D) \times \left( \sum_{d=1}^{D=365} R_{pi,1,d}, \sum_{d=1}^{D=365} R_{pi,2,d}, \dots, \sum_{d=1}^{D=365} R_{pi,24,d} \right) \end{aligned} \quad (7.8)$$

#### 7.1.4 Reliability performance assessment using the commonly-used indexes

In addition to the power inadequacy risk quantification, the proposed assessment approach measures the reliability performance using existing commonly-used performance indexes to provide a comprehensive assessment. This study adopts four main common indexes: Loss of Load Expected, Expected Energy not Supplied, Loss of Power Supply Probability, and Equivalent Loss Factor (Baghaee et al., 2016).

- **Loss of Load Expected (LOLE)** represents the load loss duration, which is calculated using Eq. (7.9), where  $E[LOL(t)]$  represents the expected (mathematical) amount of loss of load at the time step  $t$ .

- **Expected Energy not Supplied (EENS)** is also called Loss of Energy Expected (LOEE). It represents the expected amount of energy not served to the end-users (Al-Shaalan, 2012). It can be calculated by Eq. (7.10). The  $LOE(t)$  is the energy loss at time step  $t$ , calculated in Eq. (7.11).
- **Loss of Power Supply Probability (LPSP)** refers to the ratio of the power not supplied to the total power that the power generation system can produce. It can be calculated by Eq. (7.12).
- **Equivalent Loss Factor (ELF)** is the commonly-used index in reliability assessment because it considers both the number and magnitude of the power outage, as shown in Eq. 7.13 (Garcia and Weisser, 2006).

$$LOLE = \sum_{t=1}^H E[LOL(t)] \quad (6.9)$$

$$EENS = LOEE = E[LOE(t)] \quad (6.10)$$

$$LOE(t) = \sum_{t=1}^H (P_{dem,t} - P_{sup,t}) \times \Delta t \quad \forall P_{dem,t} \geq P_{sup,t} \quad (6.11)$$

$$LPSP = LOEE / \sum_{t=1}^H (P_{dem,t} \times \Delta t) \quad (6.12)$$

$$ELF = (1/H) \times \sum_{t=1}^H \frac{P_{dem,t} - P_{sup,t}}{P_{dem,t}} \quad \forall P_{dem,t} \geq P_{sup,t} \quad (6.13)$$

## 7.2 Basic information and its distributions of the main uncertain parameters concerned for the test case

### 7.2.1 Basic information for the test case

The energy systems mainly include wind turbines, PV panels, backup power generators, electric batteries, electric chillers, and other associated cooling system

components. The PV panels are installed around the hotel as it has enough space, and the wind turbines are off-shore. The sizes of the microgrid system components are listed in Table 7.1. In addition, it is noted that the model of the hotel microgrid and its control mechanism, as introduced in Section 3, are used in the chapter.

Table 7.1 Sizes of the hotel microgrid system components

Total capacity of wind turbines	Total area of PV panels	Total capacity of backup power generators	Capacity of battery	Capacity and number of electric chillers
750 kW	11500 m <sup>2</sup>	4800 kW	1600 kWh	5×850 kW

### 7.2.2 *Distributions of the main uncertain parameters concerned*

The main uncertain parameters concerned in the quantification of power generation and consumption uncertainties include the outdoor temperature, solar radiation, wind speed, cooling load, and electrical load. Their distributions are listed in Table 7.2. The uncertainties of the weather parameters (i.e., the outdoor temperature, solar radiation, and wind speed) are quantified using normal distributions. The weather parameter setting in the TMY data is used as the mean value of the distribution, while its standard deviation is set according to the previous study (Gang et al., 2016). The uncertainty in the cooling load is also quantified using a normal distribution. The mean of the distribution is set to the cooling load estimated using the TMY data, while the standard deviation is set to 0.3, according to a previous study (Gang et al., 2015). The uncertainty in electrical load is quantified by assigning an uncertain factor, which follows a triangular distribution, to the typical electric load predicted using TMY data.

Table 7.2 Main uncertain parameters and their distributions concerned

Parameter	Distribution	Value
Solar radiation	Normal distribution	$u$ : TMY; $\sigma$ : 0.2
Outdoor temperature	Normal distribution	$u$ : TMY; $\sigma$ : 1
Wind speed	Normal distribution	$u$ : TMY; $\sigma$ : 0.1
Cooling load	Normal distribution	$u$ : TMY; $\sigma$ : 0.3
Electrical load	Relative triangular distribution	Triangular (0.3, 1.2, 0.9)

*Note: relative triangular distribution means the parameter distribution is obtained by multiplying the typical value by a certain factor following a triangular distribution.*

### 7.3 Test results and reliability performance analysis

The reliability performance of the test microgrid is assessed using the proposed uncertainty-based assessment approach considering uncertainties. Another reliability performance assessment is performed using the conventional approach without considering uncertainties, which is used as a reference case to demonstrate the advances of the proposed approach. These two reliability assessments adopt the same parameter settings of microgrid energy systems.

#### 7.3.1 Distributions of power generation and consumption under uncertainties

##### Distribution of power generation

The probability density distribution and the cumulative density function (CDF) of hourly renewable power generation of the test microgrid are shown in figure 7.3. It can be seen that the hourly renewable power generation varies within a large range between 0 kW and 3,800 kW under uncertainties. The hourly renewable power generation with the highest frequency is around 800 kW. The estimated maximum hourly renewable power generation of the reference case without considering uncertainties is 2,400 kW, which locates at the point where the CDF reaches 0.95. This means that the hourly renewable power generation can be underestimated with a

probability of 5% in the conventional assessment, which treats renewable generation as a deterministic parameter. Therefore, it is necessary to consider the impacts of uncertainties in predicting renewable power generation for reliability assessment to avoid underestimating reliability performance.

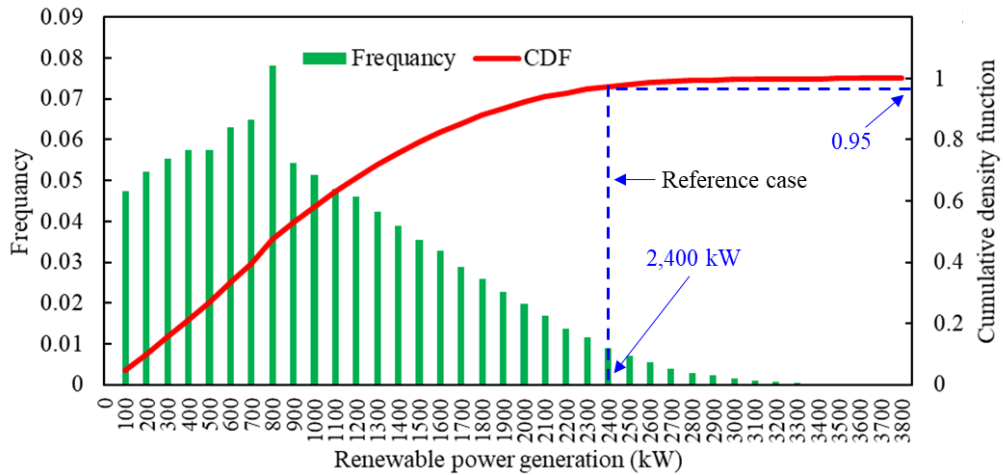


Figure 7.3 Distribution of hourly renewable power generation and its cumulative density function

### **Distribution of power consumption**

Figure 7.4 shows the distribution of the hourly microgrid load and its cumulative density function. It can be seen that the hourly microgrid load varies between 100 kW and 2,000 kW under uncertainties. It has a high probability of falling between 300 kW and 600 kW. The maximum hourly microgrid load (i.e., 1,550 kW) of the reference case locates at around 96% of the CDF, which means the hourly microgrid load can be underestimated with a probability of 4% in the conventional assessment, which treats the load as a deterministic parameter. Therefore, it is also necessary to consider the impacts of uncertainties in predicting microgrid load in the microgrid reliability assessment to avoid overestimating reliability performance.

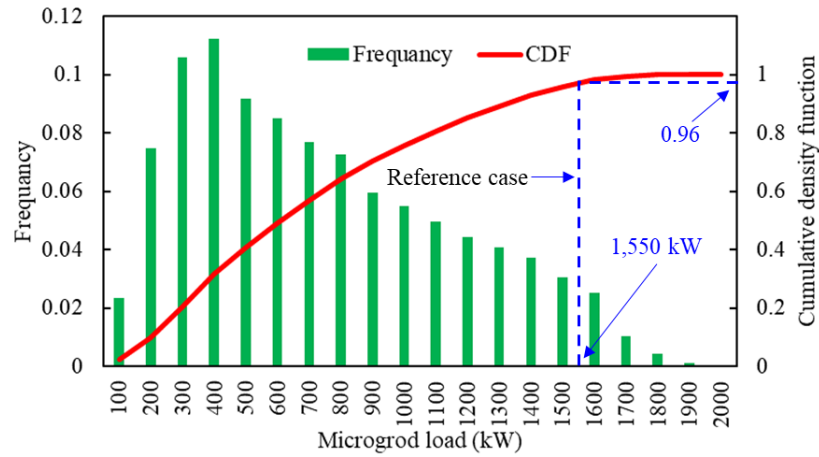


Figure 7.4 Distribution of the hourly microgrid load and its cumulative density function

**Hourly minimum and maximum power generation and consumption under uncertainties**

The hourly minimum and maximum available generation capacity and power consumption under uncertainties are also analyzed and shown in Figure 7.5, as they are necessary to identify the power inadequacy. As seen from Figure 7.5, the power consumption exceeds the available power generation at many time steps, particularly in the summer season when the impacts of uncertainties are taken into account. But the unsatisfied load is much less observed in the hourly available generation capacity and microgrid load profiles provided by the conventional approach without considering uncertainties, as shown in Figure 7.6. This means it is probable to underestimate the power inadequacy risk and overestimate the reliability performance when uncertainties are not involved.

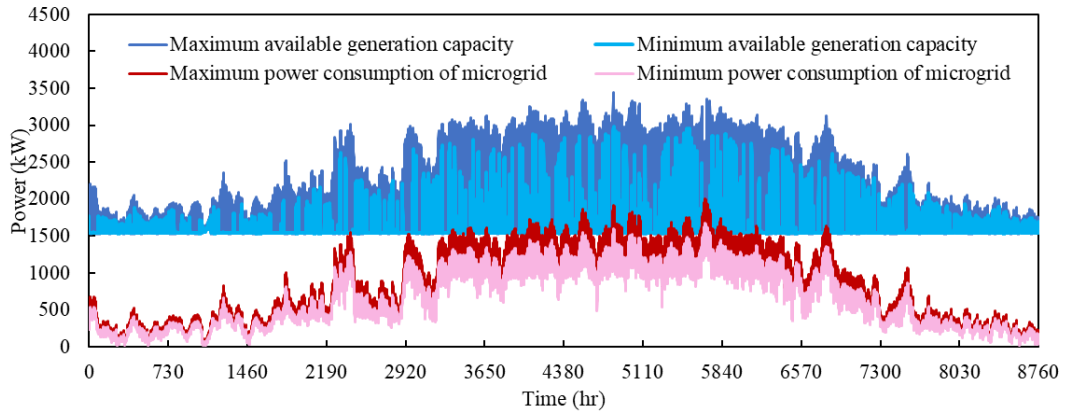


Figure 7.5 Hourly minimum and maximum available generation capacity and power consumption generated using the proposed approach

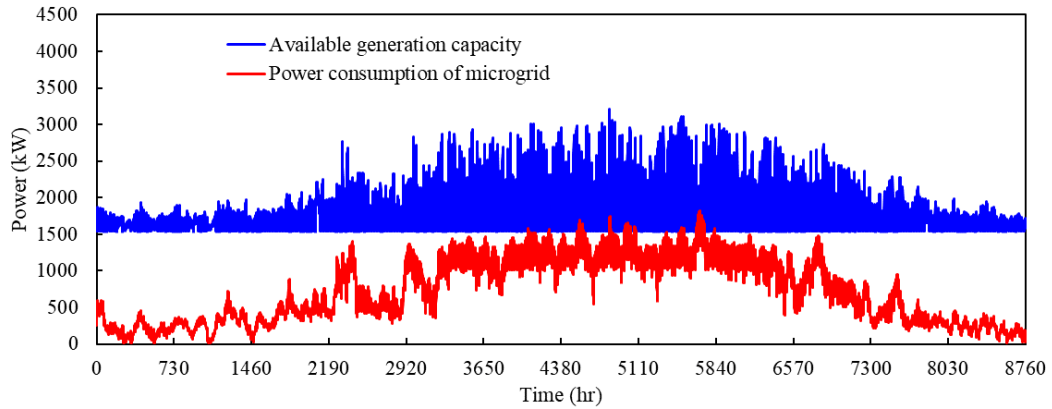


Figure 7.6 Hourly available generation capacity and power consumption generated using the conventional approach

### 7.3.2 Results of power inadequacy risk quantification

The power inadequacy risk is quantified in terms of three different time scales in this study, including hourly, monthly, and 24-h, to investigate how the risk varies over a year, months, and a day. The detailed results are introduced and analyzed as follows.

#### Distribution of outage power

The outage power at the time steps when power inadequacy occurs is calculated according to the supply-demand profiles given by the proposed and conventional methods. The distribution and the cumulative density function of the outage power are

shown in Figure 7.7. It can be seen that the outage power varies between 30 kW and 420 kW under uncertainties, and the frequency gradually decreases with the increase of the outage power. The highest power outage frequency is 0.23 when the outage power is 30 kW. The maximum outage power (i.e., 285 kW) of the reference case is also presented in the figure and highlighted with blue dotted lines, which locates at 92% of the CDF. So it has a probability of 8% that the maximum outage power would be underestimated in the conventional reliability assessment without considering uncertainties.

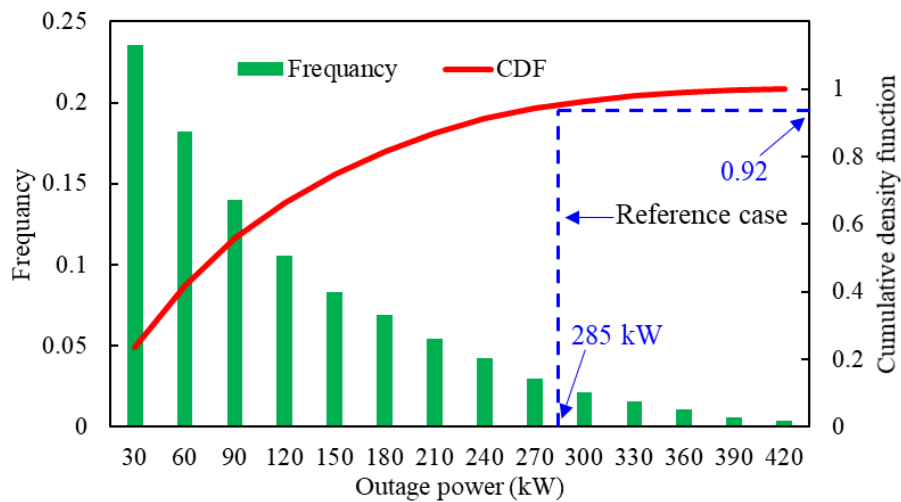


Figure 7.7 Distribution of outage power and its cumulative density function

### Average hourly power inadequacy risk

Figure 7.8 shows the average hourly power inadequacy risk of the hotel microgrid under uncertainties. It can be seen that the power inadequacy risk is zero in the winter and in most time of the spring and autumn because the hourly minimum available power generation exceeds the hourly maximum power consumption during these periods, as seen in Figure 7.5. At several time steps of the spring and autumn seasons, the hourly power inadequacy risk can reach 1.3% and 18.2%, respectively. In the

summer, the hourly power inadequacy risk varies significantly, and the highest risk reaches up to 100% at several time steps.

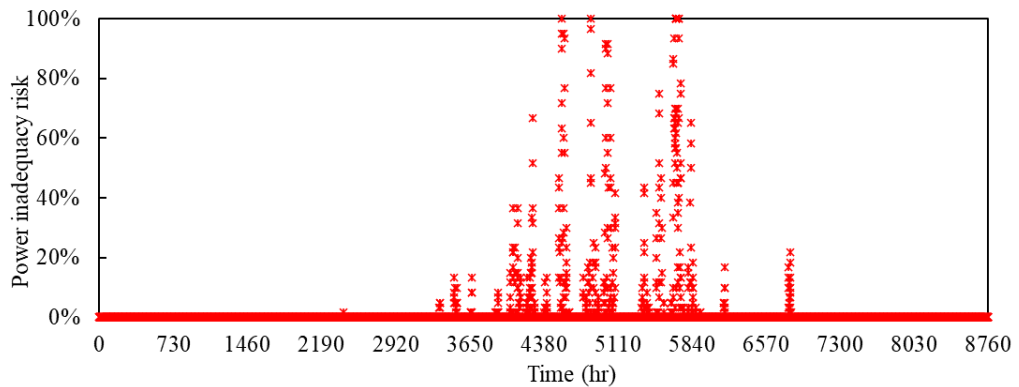


Figure 7.8 Average hourly power inadequacy risk of the test microgrid under uncertainties

**Average monthly power inadequacy risk**

The average monthly power inadequacy risk of the test microgrid under the uncertainties is also quantified and shown in Figure 7.9. The average monthly power inadequacy risk is zero from January to April and November to December. In May, September, and October, the average monthly power inadequacy risk is over zero but very low (i.e., lower than 0.3%). The average monthly power inadequacy risk in June is around 1.5%. From July to August, the average monthly power inadequacy risk is highly increased over 5%. This is because the cooling load is usually very high due to the hot and humid weather in Hong Kong (a typical subtropical region) during this period and power consumption is probably greater than the available generation capacity, as seen in Figure 7.5.

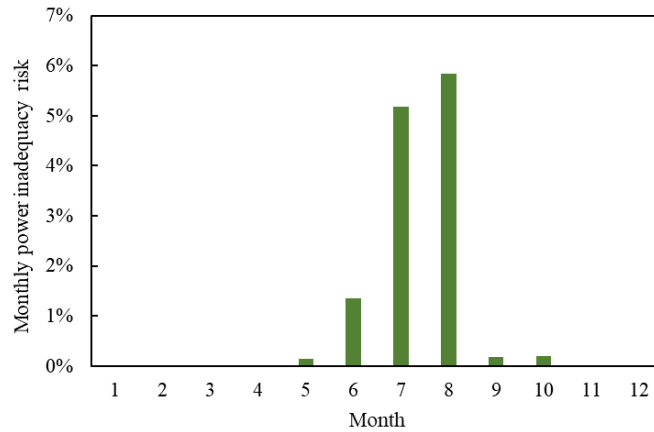


Figure 7.9 Average monthly power inadequacy risk of the test microgrid under uncertainties

### **Average 24-hour power inadequacy risk**

The 24-hour average power inadequacy risk profile is obtained and shown in Figure 7.10 to analyze the average hourly power inadequacy risk over a day. The 24-hour profile can be divided into four main periods according to the variation of the average power inadequacy risk. The variations of the average power inadequacy risk during these four periods are analyzed as follows:

- During Period I, from 0:00 a.m. to 7:00 a.m., the average hourly power inadequacy risk is zero. This is because the power consumption is usually very low due to the cooler outdoor environment and the very limited use of lighting and other equipment, the power consumption can be fully satisfied by the power generation system (e.g., the backup power generator).
- During Period II, from 7:00 a.m. to 10:00 a.m., the average hourly power inadequacy risk gradually increases, but the highest risk is still lower than 1%. This is because the power consumption increases due to the hotter outdoor environment and the increased use of lighting and other equipment, while the increased power consumption may not be satisfied by the backup power generator

and the limited renewable power generation at some time.

- During Period III, from 10:00 a.m. to 5:00 p.m., the average hourly power inadequacy risk gradually decreases and then increases. The hourly risks during Period III are slightly lower than those in Period II. This is because renewable power generation significantly increases during Period III, which can satisfy power consumption most of the time. The increase in the risk appears after 1:00 p.m. due to the decrease in renewable power generation.
- During Period IV from 5:00 p.m. to 12:00 p.m., the average hourly power inadequacy risk significantly increases up to 4.8% at 9:00 p.m. and then largely decreases to 1.9%. The hourly risks are much higher than those during the other three periods, as the power consumption during this period is usually the highest in hotel buildings while the renewable power generation is relatively low. The decrease in hourly risk after 9:00 p.m. is mainly due to the much-reduced use of lighting and other equipment.

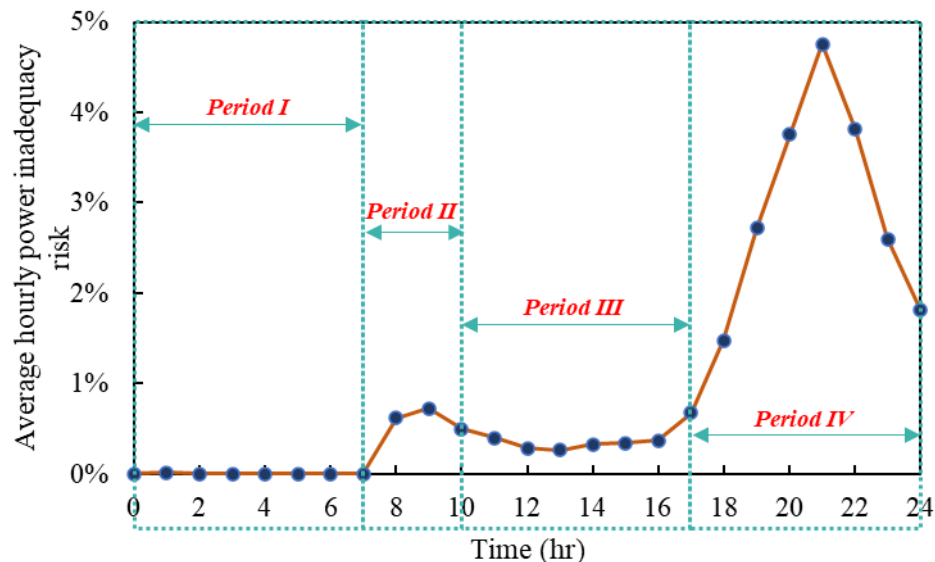


Figure 7.10 24-hour average power inadequacy risk of the test microgrid under uncertainties

### ***7.3.3 Results of reliability performance assessment using commonly-used indexes***

Table 7.3 shows the results of the reliability performance assessment using the four commonly-used indexes introduced in Section 2.4. As seen in Table 7.3, the values of all these indexes given by the proposed uncertainty-based method are much higher than those given by the conventional method without considering uncertainties. The LOLE is 26 hours more, the EENS is 1,403 kWh more, the LPSP is 0.0002 higher, and the ELF is 0.00009 higher. These values are about 15% - 30% higher than the conventional method's. It can be seen that the reliability performance of the microgrid is probably overestimated when the conventional assessment approach is adopted, as the uncertainties of the load and renewable generation are ignored. The overestimated reliability performance result may mislead the designers to make improper decisions at the planning and design stages, resulting in unreliable operation.

Table 7.3 Results of reliability performance assessment using commonly-used indexes

	LOLE (hr)	EENS (kWh)	LPSP	ELF
Uncertainty-based case	111	11,455	0.0017	0.00075
Reference case	85	10,052	0.0015	0.00066

#### ***7.3.4 Impacts of backup power generator capacity on microgrid reliability performance***

As the capacity of the controllable backup power generator has a significant impact on the microgrid reliability performance, the power inadequacy risk and other reliability performance indexes are quantified when different backup power generator capacities are adopted. The ELF is an example of the reliability performance index as it can measure the frequency and magnitude of the power outage. A lower value of ELF means higher microgrid reliability. Figure 7.11 shows the ELF values under different backup power generator capacities when considering uncertainties. It can be seen that the ELF value decreases with the increase of the backup power generator capacity. When the capacity of the backup power generator is over 3,900 kW, the ELF value becomes very low (i.e., lower than 0.008786). As seen from the sub-figure, the backup power generator capacity should be over 3,850 kW and 4,700 kW, respectively, to meet the standards of two different levels (i.e.,  $ELF < 0.01$  and  $ELF < 0.001$ ) required by the standard (Garcia and Weisser, 2006).

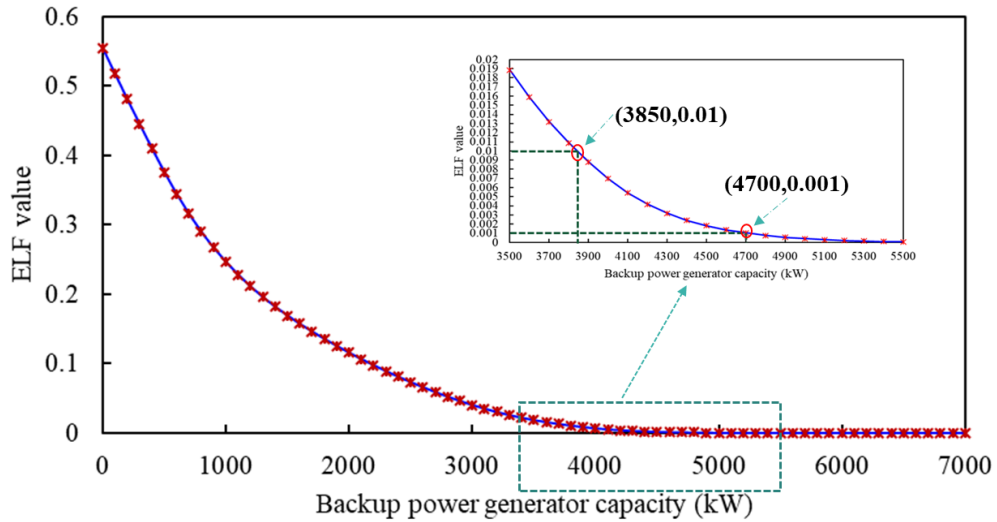


Figure 7.11 ELF values under different backup power generator capacities when uncertainties are considered

Figure 7.12 shows the power inadequacy risks under different backup power generator capacities when uncertainties are considered. It can be seen that the power inadequacy risk decreases with the increase of the backup power generator capacity. When the capacity of the backup power generator is higher than 4,200 kW, the power inadequacy risk is below 5%. Increasing the backup power generation capacity from 3,850 kW to 4,700 kW, which decreases the ELF value from 0.01 to 0.001, can decrease the power inadequacy risk from 9.4% to 0.5%. To eliminate the risk of power inadequacy (i.e., risk = 0), the backup power capacity should be over 6,400 kW.

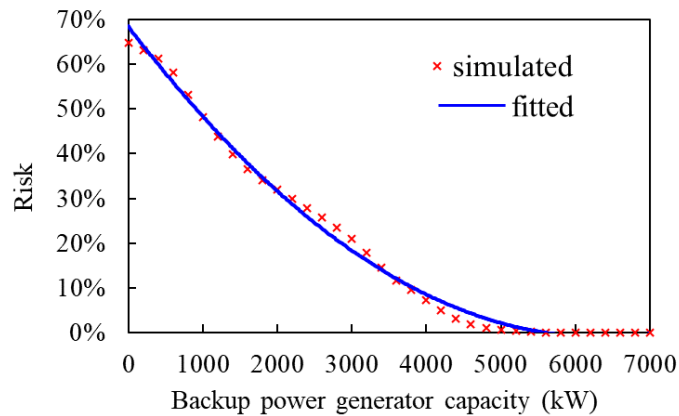


Figure 7.12 Power inadequacy risks under different backup power generator capacities when uncertainties are considered

## 7.4 Summary

This chapter proposes a quantitative reliability assessment and risk quantification method for microgrids by considering power supply and demand uncertainties. A novel index, i.e., power inadequacy risk, is proposed for microgrid reliability assessment under uncertainties. The impacts of the uncertainties in power supply and demand on microgrid reliability are investigated. The uncertainty-based reliability assessment and risk quantification method is tested in an islanded hotel microgrid in Hong Kong via simulation.

# **CHAPTER 8 ROBUST OPTIMAL DESIGN OF MICROGRIDS TO ENHANCE THE RELIABILITY AND ECONOMICS CONSIDERING THE QUANTIFIED POWER INADEQUACY RISK**

This chapter presents the procedure and method of robust design optimization for microgrids considering uncertainties on the supply and demand sides and the impacts of power inadequacy risk on robust design optimization. Section 8.1 presents the major procedure and methods of the proposed robust design optimization method for microgrids. Section 8.2 presents the basic information on the design variables and quantifications of the uncertainties. Section 8.3 presents the results of the optimization case studies and Section 8.4 provide a summary of this chapter.

## **8.1 Procedure and objectives of robust optimal design**

### ***8.1.1 Approach and steps of robust design optimization***

Figure 8.1 shows the outline of the proposed robust optimal design method of the microgrid. It consists of three major steps.

***Step 1:*** The microgrid design variables are identified. Then, the ranges of these microgrid design parameters are determined. The energy efficiency is quantified. For instance, the coefficient of performance (COP) of the building's central cooling systems is quantified using key indicators, e.g., the partial load ratio, relative COP, and rated COP.

**Step 2:** The uncertainties of the parameters on the supply and demand sides are quantified. The distributions of these uncertain parameters are determined concerning their features. Then, the possible uncertain scenarios are determined according to the identified uncertain parameters and their distributions. For instance, on the supply side, the uncertainties of renewable power generation are quantified based on weather factors (e.g., solar radiation, wind speed, etc.). On the demand side, the uncertainties of loads are quantified based on different types of loads (i.e., cooling loads and other electrical loads).

**Step 3:** The design optimization of the microgrid is conducted in the third step. The uncertainty-based supply-demand profile is calculated according to the obtained uncertain scenarios and the generated microgrid design parameters from the optimizer associated with the quantification of the energy efficiency. The quantified power inadequacy risk is added to the final objective function as a cost penalty. The results calculated based on the final objective function are evaluated in the optimizer to determine whether the design parameters are the optimal design option. This process will continue until the design parameters meet the optimal requirements. As for the microgrid design optimization, the typical heuristic optimization algorithm (i.e., genetic algorithm) is selected as the optimization algorithm.

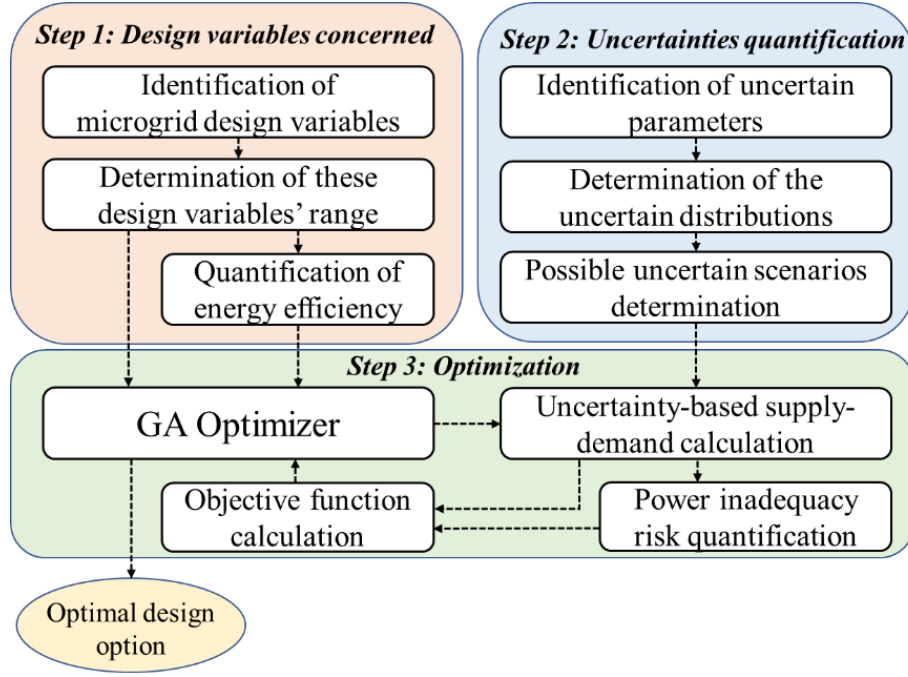


Figure 8.1 Outline of the proposed robust optimal design method of the microgrid

### 8.1.2 Optimization objectives for optimal microgrid design

According to the literature review, the mean of performance indicator (MPI) and standard deviation of performance indicator (SDPI) are commonly adopted as the objective functions in most previous studies of robust optimal design, such as in the aerospace field, structural engineering field, and building engineering field. When adopting them in microgrid design optimization applications, two alternative optimization objective functions concerning these two terms are considered. ‘Objective 1’ focuses on the MPI, and ‘Objective 2’ considers the integration of the MPI and SDPI. These are shown in Eqs. (8.1) and (8.2), where  $\tilde{f}$  is the robust optimization objective and  $x$  represents the vector of design variables. The design inputs concerning their uncertainties are presented as  $p$ .  $\omega$  is the weight ratio and the sum of the  $\omega_1$  and  $\omega_2$  is 1.

$$\text{Objective 1: } \tilde{f}_1 = \mu(x, p) \quad (8.1)$$

$$\text{Objective 2: } \tilde{f}_2 = \omega_1 \times \mu(x, p) + \omega_2 \times \sigma(x, p) \quad (8.2)$$

In this study, the overall objective is the overall annual cost as shown in Eq. (8.3). It is the sum of the annual initial cost ( $C_{ini}$ ), annual operational cost ( $C_{opt}$ ), power inadequacy risk cost ( $C_{pir}$ ), and carbon emission penalty ( $C_{emi}$ ). The initial cost is the sum of the annual initial costs for all the major microgrid facilities. The annual initial cost per microgrid facility is calculated by multiplying the design size and number by the unit price of the facility, as shown in Eq. (8.4). For instance, if the lifespan of one microgrid facility is assumed at 20 years, which means that the average annual initial cost is one-twentieth of the initial cost if the interest of the investment is ignored. The annual operation cost (i.e., the annual primary energy cost) is obtained according to the annual primary energy consumption from the backup generators, as shown in Eq. (8.5).

$$C_{ov} = C_{ini} + C_{opt} + C_{pir} + C_{emi} \quad (8.3)$$

$$C_{ini} = \sum (C_{fac,k} \times 1/Y_k) \quad (8.4)$$

$$C_{opt} = \left( \sum_{t=1}^{8760} P_{BPG}^t \right) \times GP_{BPG} \quad (8.5)$$

The carbon emission is quantified using the carbon emission tax and the total consumption of backup power generators, as shown in Eq. (8.6), where  $T_{emi}$  is the carbon emission tax, and  $F_{BPG}$  is the carbon emission factor of backup generator combustion.

$$C_{emi} = \left( \sum_{t=1}^{8760} P_{BPG}^t \right) \times T_{emi} \times F_{BPG} \quad (8.6)$$

### 8.1.3 Quantification of uncertainties in power generation and consumption

A bottom-up approach is used to quantify the uncertainties of the microgrid. As shown in Eqs. (8.7-8.9), the uncertainties are sampled according to the probability

distributions of the main uncertain parameters by using the Latin hypercube sampling (LHS) method. The Sample  $X$  for the uncertain parameters/inputs  $x_1, x_2, x_3 \dots, x_n$  (such as the outdoor temperature and solar radiation) are generated based on Eq. (8.7) by fitting their distributions  $G$  in Eq. (8.9). In the end, the output distributions  $Y$  (i.e., supply-demand parameters) can be calculated as shown in Eq. (8.10).

$$(y_1, y_2 \dots, y_m)^T = f(x_1, x_2, \dots, x_n) \quad (8.7)$$

$$X = [X_1, X_2, \dots, X_n] \quad (8.8)$$

$$X_i \sim G_i \quad (8.9)$$

$$Y = (Y_1, Y_2, \dots, Y_m)^T = f(X_1, X_2, \dots, X_n) \quad (8.10)$$

#### **8.1.4 Reliability constraints and power inadequacy risk quantification**

##### **Reliability constraints**

Most reliability indexes are introduced in Section 2.2.4, where the ELF is selected as the main reliability constraint for this optimization problem because it contains both the numbers and magnitudes of the outages, as shown in Eq. (8.11), where  $E_{loss}$  is the loss of energy and  $E_{dem}$  is the total energy consumption at time step  $t$ .  $T$  is the number of the total steps ( $T = 8760$  hours).

$$ELF = (1/T) \times \sum_{t=1}^T E_{loss,t}/E_{dem,t} \quad (8.11)$$

##### **Power inadequacy risk cost quantification**

Power inadequacy risk as an index ( $R_{pi}$ ) has been stated by the authors in a previous study, which refers to the “probability of the power supply inadequacy at the time  $t$ .” It is quantified by Eq. (8.12-8.13) **错误!未找到引用源。** . Where,  $Prb_{sup,t,s}$  and  $Prb_{dem,t,s}$  are the probabilities of the power supply ( $P_{sup}$ ) and probabilities of the demand ( $P_{dem}$ ), respectively.  $pi_{t,s}$  is an indicator that denotes whether power

inadequacy exists at time  $t$ . This indicator consists of two values (i.e., 0 and 1). Here, a value of 0 means power inadequacy does not exist, while a value of 1 means power inadequacy exists. The total number of samples generated from the supply-demand profiles is represented as  $S$ .

$$R_{pi,t} = \sum_{s=1}^S p_{i,t,s} * Pr_{b_{sup,t,s}} * Pr_{b_{dem,t,s}} \quad (8.12)$$

$$p_{i,t,s} = \begin{cases} 0, & \text{if } P_{sup,t,s} \geq P_{dem,t,s} \\ 1, & \text{if } P_{sup,t,s} < P_{dem,t,s} \end{cases} \quad (8.13)$$

The power inadequacy risk cost ( $C_{pir}$ ) is one type of penalty cost due to the uncertainty-based power supply inadequacy, calculated in Eq. (8.14), where  $Pr_{ar}$  is the unit price of the penalty.

$$C_{pir} = \sum_{h=1}^{8760} P_{dem,t,s} \times \Delta t \times R_{out,h} \times Pr_{ar} \quad (8.14)$$

## 8.2 Basic information on the microgrid and model development

### 8.2.1 Design variables concerned and basic data of energy system parameters

The basic information about the hotel microgrid is shown in Section 3. The model of the hotel microgrid and its control mechanism, as introduced in Section 3, are also used in this chapter.

As for the design variables, a total of six key microgrid variables are selected to be optimized in this chapter, including wind generator capacity, PV area, backup generator capacity, battery storage, chiller size, and chiller number shown in Table 8.1. The ranges of the wind generator capacity and PV areas are limited, considering the reality. Natural gas is selected as the backup power generation source. Battery storage is another variable in the microgrid design. The last two variables are the demand-side

variables. To effectively consider the energy consumption efficiency in the optimization, the chiller size and its number are considered in this work. The ranges of the chiller size and the number fall within the common ranges.

Table 8.1 Key microgrid design parameters and their searching ranges

Design Parameter	Search Range	Unit
Wind generator capacity	[0, 2000]	kW
PV areas	[0, 15000]	m <sup>2</sup>
Gas generator capacity	[0, 3500]	kW
Battery capacity	[15, 1500]	kWh
Chiller size	[500, 2000]	kW
Chiller number	[2, 5]	N/A

As for the main parameters of the microgrid and its energy system, the natural gas turbine is selected as the backup power generator. Its unit price is calculated according to the change in its capacity, as shown in Eq. (8.15). The unit price of the chillers ( $UP_{chi}$ ) is calculated according to the change in size, as shown in Eq. (8.16), where the  $Cap_{BPG}$  is the gas generator capacity and  $Cap_{chi}$  is the chiller capacity. Moreover, the basic information and cost data of the microgrid and its energy systems are listed in Table 8.2.

$$UP_{gas} = 3711.78 - 280.47 \times \ln(Cap_{BPG}) \quad (8.15)$$

$$UP_{chi} = -26.31 \times \ln(Cap_{chi}) + 348.01 \quad (8.16)$$

Table 8.2 Basic information and cost data of the microgrid and its energy systems \*

Category	Parameter	Specification
Renewable power generation	The unit price of the PV area	230 USD/m <sup>2</sup>
	The overall efficiency of PV	0.2
	The lifetime of the PV	20 years
	The unit price of the wind generator	288 USD/kW
	The lifetime of the wind turbine	20 years
Backup power generation	The lifetime of the gas generator	25 years
	The unit price of natural gas	0.1075 USD/kWh
	Gas generator efficiency	0.32
Battery storage	The unit price of the battery	550 USD/m <sup>2</sup>
	The lifetime of the battery	Ten years

\* *Remark:* the selection of reference data refer to (Li and Wang, 2019; Li, 2000; Lu et al., 2015; Venkateswari and Sreejith, 2019; Flores and Brouwer, 2018)

### 8.2.2 Parameter uncertainty quantifications

As for the parameter uncertainty quantifications, solar temperature, wind speed, and ambient temperature are quantified by using distribution based on (Gang et al., 2015), which are used to quantify the uncertainties of the renewable power generation on the supply side. The uncertainties of the power consumption are quantified for two types of loads (i.e., electricity load and cooling load). Their uncertainties are quantified based on the normal and triangular distributions (Gang et al., 2015; Gang et al., 2016). Table 8.3 shows their mathematical descriptions in the microgrid robust optimal design and base values used in the following case study.

Table 8.3 Parameter uncertainty distributions in the microgrid robust optimal design

Parameter	Distribution	Value
Solar radiation	Normal distribution	$u$ : TMY; $\sigma$ : 0.2
Outdoor temperature	Normal distribution	$u$ : TMY; $\sigma$ : 1
Wind speed	Normal distribution	$u$ : TMY; $\sigma$ : 0.1
Cooling load	Normal distribution	$u$ : TMY; $\sigma$ : 0.3
Electrical load	Relative triangular distribution	Triangular (0.3, 1.2, 0.9)

### 8.3 Results of optimization case studies and performance analysis

#### 8.3.1 Basic information on the proposed cases and their design results

##### Basic information about the proposed cases

To provide a comprehensive comparison and analysis of the microgrid optimal designs, we considered six cases in this study concerning different optimal design methods, as shown in Table 8.4. The first two cases represent the proposed robust design optimization of this work under different objective functions, i.e., MPI and integration of the MPI and SDPI. Besides, four reference cases under four typical existing optimal design methods are set here to provide comparison results regarding economics, reliability, and energy use efficiency.

Reference case R1 and Reference case R2 represent two types of robust microgrid optimal design methods, respectively. The former does not consider the impacts of the power inadequacy risk in the optimization. As for the latter, rated COP instead of the operating COP is used in the optimization. As for Reference case C, the conventional deterministic supply-demand profiles, without considering the uncertainties, are used in the optimization. Reference case D is another typical deterministic microgrid optimal design method. As a conservative method, the peak load instead of the load profile is used in the optimization.

Table 8.4 Basic information of the proposed cases

Case Name	Load	Uncertainty	Power inadequacy risk consideration	Energy use efficiency
Case 1	Load profile	Yes	Yes	Operating COP
Case 2	Load profile	Yes	Yes	Operating COP
Reference case R1	Load profile	Yes	No	Operating COP
Reference case R2	Load profile	Yes	Yes	Rated COP
Reference case C	Load profile	No	No	Operating COP
Reference case D	Peak load	No	No	Operating COP

**Optimization design using ‘Objective 1’ V.S. optimization design using ‘Objective 2’**

Figure 8.2 (a) and (b) show optimization processes for the optimizations with Objective 1 and 2, respectively. Table 8.5 shows the optimal design solutions for these two cases, where they have almost similar optimal design results. This means that the different robust objective functions (i.e., MPI and integration of the MPI and SDPI) have a tiny impact on the microgrid's optimal design results. Almost similar performance can be obtained with different objectives. As a result, Case 1 is solely considered in the following comparison and analysis.

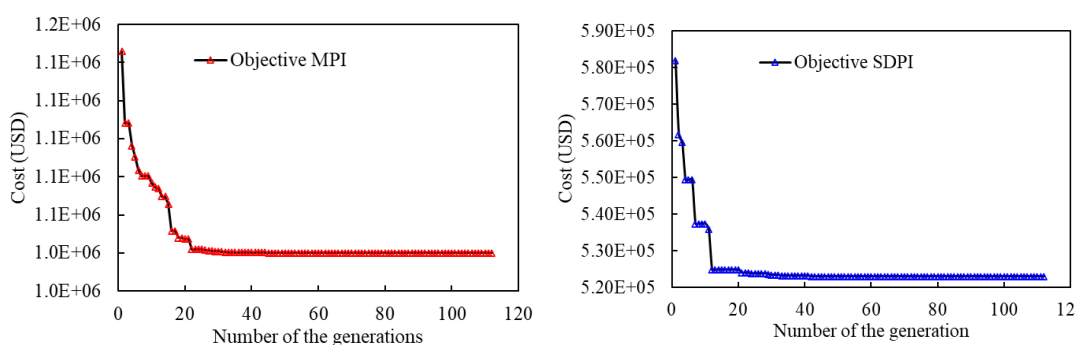


Figure 8.2 The optimization process for the proposed optimization cases

Table 8.5 Optimal design results of the microgrid between Case 1 and Case 2

	Battery (kWh)	PV area (m <sup>2</sup> )	Wind turbine (kW)	Backup generator (kW)	Chiller size (kW)	Chiller number
Case 1	904	10840	1180	5060	1128	4
Case 2	864	10854	1050	5058	1130	4

### Optimization results of these cases

Table 8.6 shows the optimal design results of the microgrid among these cases. With different requirements of the optimal designs, the optimization results of these cases are different. As for the robust optimal design methods, an extra 200 kW backup power generation capacity of Case 1 (i.e., MPI-based case) is required compared to the Reference case R1, which is used to decrease the power inadequacy risk due to the uncertainties. Another large difference is the determination of the chiller size and chiller number. Case 1 prefers to select the smaller size of the chillers considering the operating COP, but Reference case R2 prefers to select the larger size of chillers considering higher rated load COP. Reference case D represents a typical conservative optimization design method. The largest capacities of power generation and battery storage are adopted. Besides, as for Reference case C, the smallest capacities of power generation and battery storage are obtained because the impacts of the uncertainties are not involved in the design optimization.

Table 8.6 Optimal design results of the microgrid among these cases

	Battery (kWh)	PV area (m <sup>2</sup> )	Wind turbine (kW)	Backup generator (kW)	Chiller selection
Case 1	904	10840	1180	5060	1128×3
Reference case R1	984	11070	1222	4660	1130×3
Reference case R2	918	11166	1208	5432	1480×4
Reference case C	808	10034	1076	4562	1130×3
Reference case D	2524	26914	3826	6258	1130×3

### **8.3.2 Comparison and analysis of the economic performance**

Figure 8.2 shows the cost results of different items among different optimization cases. The costs of the backup power generation (including the initial cost of the backup power generator and operation cost) are high. This part of the cost is used to overcome

the intermittent and random features of power generation from renewable sources and secure a reliable power supply for the microgrid. As for Reference case R1, the power inadequacy risk penalty is higher (more than four times compared to Case 1) since the power supply inadequacy risk is not considered in its optimization. The initial cost of the backup power generator and operation cost in Reference case R2 are relatively higher at 5.9% and 1.2%, respectively, compared to Case 1. More power generation from the backup power generators is used to meet the demand, and larger capacities of the backup power generators are needed to meet the reliability requirements since the rated COP instead of the operating COP is considered in this optimization. Two cost results from Reference case C are presented. Reference case C<sub>1</sub> represents the cost results without considering the uncertainty-based scenarios and Reference case C<sub>2</sub> represents the cost results considering the uncertainty-based scenarios. Reference case C has a good performance in power inadequacy risk penalty when the uncertainty-based scenarios are not involved. However, when uncertainty-based scenarios are involved, the cost of power inadequacy risk is very high (around eight times compared to Case 1). It means that the uncertainty-based power supply inadequacy risk is large and has seriously jeopardized the microgrid's reliability. As for Reference case D, the large capacities of the renewable power generator, the backup power generator, and battery storage are selected since the peak load is used in the optimization. It leads to huge costs in power generators and battery storage. More renewable power generation is used to meet the electrical load, which can decrease 29% of the operation cost compared to Case 1. Due to selecting the largest capacities of the power generators, the inadequacy risk cost is zero.

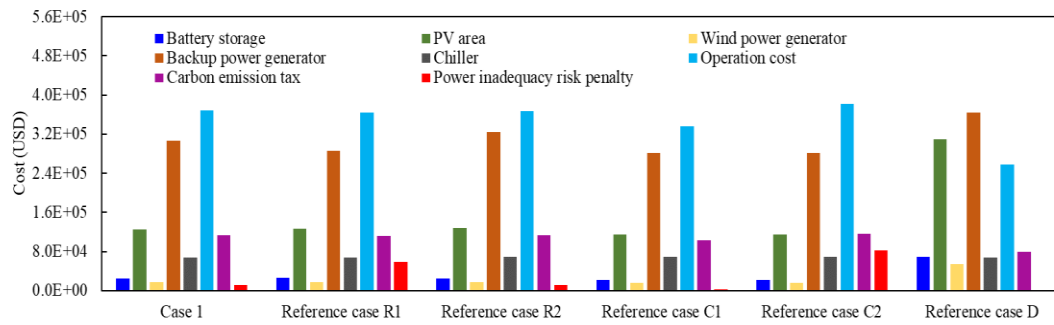


Figure 8.3 Cost results of different items among the different optimization cases

Figure 8.4 shows the overall cost results and the comparison ratios among the different optimization cases. The cost results are presented as bar charts of the primary y-axis in this figure. The comparison ratios are shown in star points of the secondary y-axis. If the comparison ratio is positive, the corresponding case needs to pay more money than Case 1.

The comparison ratios of Reference Case R1 and Reference Case R2 are 2.6% and 2.2%, respectively. Setting the power inadequacy risk penalty in the optimization and using the operating COP instead of the rated COP can effectively decrease the overall cost. Reference case C has a good economic performance (cost-saving achievement at 8.6%) when the uncertain-based scenarios are not involved, as shown in Reference case C1. However, when the uncertainties are considered, the comparison ratio of Reference case C2 (considering uncertain-based scenarios) is 5.1%, which means the overall cost is underestimated at 13.7%. The comparison ratio of the Reference case D is up to 16.5%, which means the microgrid economics are overestimated in this optimization. The reliability of this case can be effectively ensured by using the peak load in the microgrid optimization. However, the extra 16.5% cost means that this optimization design method cannot be considered an economical solution for the microgrid design.

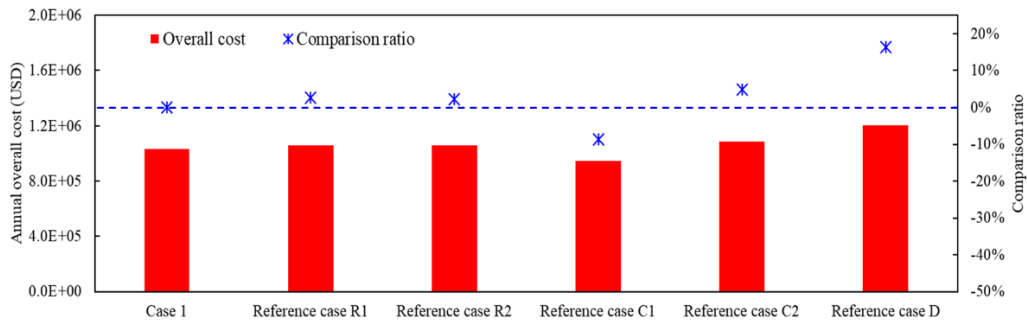


Figure 8.4 Results of the overall cost and the comparison ratios among these optimization cases

### 8.3.3 Comparison and analysis of the reliability performance

#### Reliability performance by using the reliability index

The reliability performance for these optimization cases is obtained, as shown in Table 8.7. The EFL value below  $1.0 \times 10^{-4}$  is set in these cases according to the standard (Garcia and Weisser, 2006). All the cases except Reference C can meet the reliability requirements since it is set as the constraint in those optimizations. Reference case C has two different reliability performance results. When the uncertainties are not considered, the reliability requirement can be met, as shown in the ELF value of Reference case C1. However, the reliability requirement cannot be met when uncertainties are involved, as shown in the ELF value of Reference case C2. This means that using the typical load profile in the optimal design may obtain underestimated results, and the real reliability requirement cannot be met.

Table 8.7 Reliability performance for these optimization cases

Case	ELF value
Case 1	$1.4 \times 10^{-5}$
Reference case R1	$8.6 \times 10^{-5}$
Reference case R2	$5.5 \times 10^{-5}$
Reference case C1	<b><math>1.3 \times 10^{-5}</math></b>
Reference case C2	<b><math>1.8 \times 10^{-4}</math></b>
Reference case D	$1.1 \times 10^{-9}$

**Performance of the power inadequacy risk**

Power inadequacy risk is an indicator to quantify the risk of power inadequacy due to the impacts of uncertainties. The average values of power inadequacy risk among the four cases are presented in Figure 8.5. Case 1 has a very low power inadequacy risk, which means it can effectively avoid the power inadequacy risk and achieve robustness. The largest value is obtained from Reference case C. In this case, both the uncertainties and power inadequacy risk are not considered in the optimization, which causes the power inadequacy risk increases above 220 times, compared to Case 1. Reference case R1 has a relatively lower value of the power inadequacy risk compared to Reference case C since the uncertainties are considered in its optimization. However, power inadequacy risk still increases above 60 times, compared to Case 1. The power inadequacy risk is zero in Reference case D. In this case, since the constant peak load is used in the optimization, the largest capacities of power generation and battery storage are selected. Thus, the power inadequacy risk can be avoided in this case. It proves that the conventional design method may fail to meet the requirement when the requirement on reliability is extremely strict. Even a robust optimal method without considering the power inadequacy risk impacts still poses a large risk of power supply inadequacy.

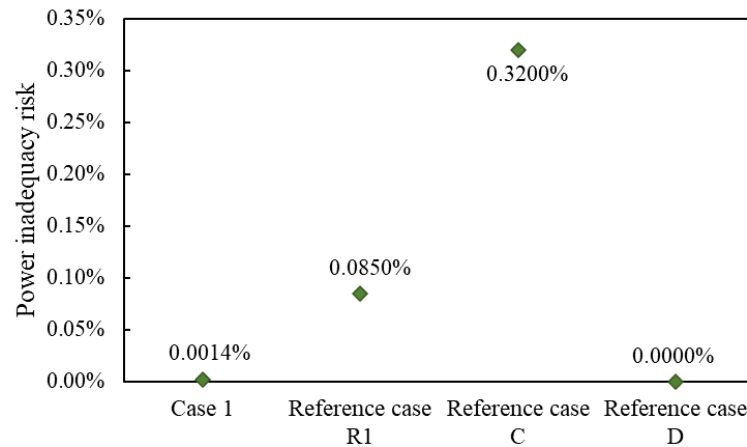


Figure 8.5 Power inadequacy risk performance among four cases

**Quantification of the impacts of the power inadequacy risk on microgrid economics**

The impacts of the power inadequacy risk penalty costs on microgrid economics are quantified, as shown in Figure 8.6 (a). With the unit prices of power inadequacy risk increasing, the power inadequacy risk decreases sharply from 0.1923 USD/kWh (i.e., Hong Kong electricity unit price) to 1.923 USD/kWh. In this study, ten times the electricity unit price (i.e., 1.923 USD/kWh) is selected in the optimization, as shown in Figure 8.6 (red dash line). The power inadequacy risk decreases slowly when the unit price of power inadequacy risk continuously increases from 1.923 USD/kWh to a larger value. Besides, Figure 8.6 (b) shows the changes in the overall cost under different unit prices of the power inadequacy risk. The results show that setting the cost penalty for the power inadequacy risk causes an overall cost increase. If the 1.923 USD/kWh (i.e., ten times the electricity price) is selected as the penalty cost, the power inadequacy risk can decrease above 60 times while the overall cost increases at 3.1%.

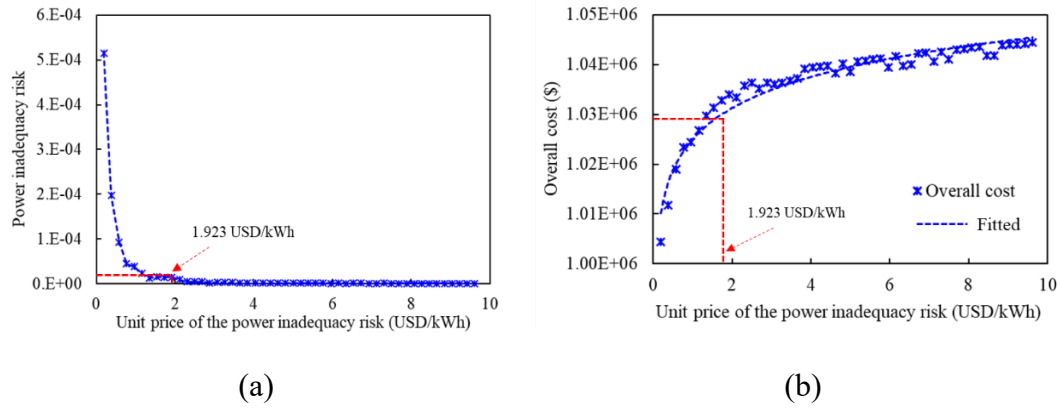


Figure 8.6 Quantification of the impacts of the power inadequacy risk on microgrid economics

### 8.3.4 Energy use efficiency performance comparison and analysis

#### Optimization results of the energy use efficiency

To demonstrate the impacts of the different optimization methods on energy use efficiency performance, this study compares and analyses two cases (i.e., Case 1 and Reference case R2). Here, COP is selected as the indicator to represent energy use efficiency. Table 8.8 shows the results of the COP in these two cases. Case 1 prefers to achieve the high operating COP, while Reference case R2 prefers to achieve the high-rated COP. As a result, the value of the average operation COP in Case 1 is about 3% higher compared to Reference case R2.

Table 8.8 Results of the energy efficiency among the different optimization cases

	Rated COP	Average operating COP
Case 1	4.74	4.68
Reference case R2	4.76	4.54

To directly depict the impact of COP on the microgrid system performance, Figure 8.7 shows the comparison results of the annual COP profiles between Case 1 and Reference case R2 (in the primary y-axis) and the corresponding cooling load profile

(in the secondary y-axis). Four small-size chillers are selected in Case 1, and three large-size chillers are selected in Reference case R2. Higher rated load COP can be achieved during high cooling load (between hour 2950 and hour 7300). When the fluctuation of the cooling load is significant (especially from hour 0 to 2190 and from hour 7300 to hour 8760), the four smaller chillers have a good energy use efficiency.

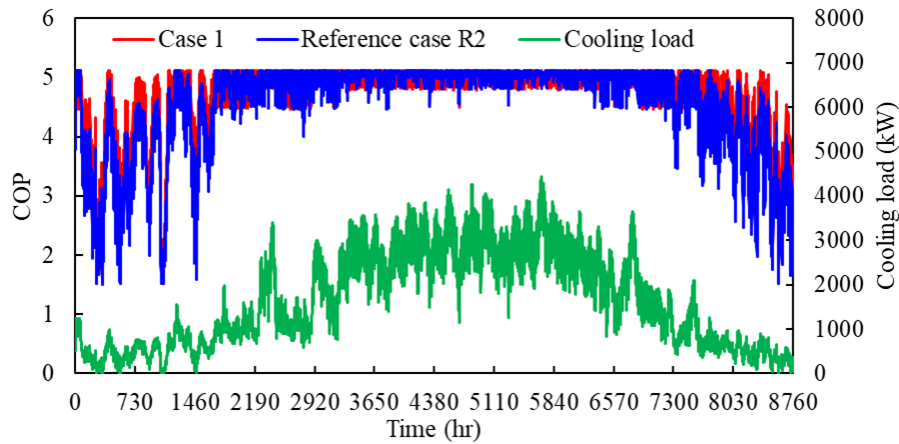


Figure 8.7 Comparison results of the COP profiles between Case 1 and Reference case R2 and the corresponding cooling load profile

**Quantification of the impacts of the power inadequacy risk on microgrid economics**

To directly depict the impact of the COP on microgrid economics, figure 8.8 shows the overall cost results under different average operating COP values. With the COP increasing, the overall cost decreases. When the average operating COP increases from 3 to 4, the overall cost decreases by 51%, but when the average operating COP increases from 5 to 6, the overall cost decreases by 5%. The decrease in the overall cost is not simply proportional to the COP increase. Increasing COP can effectively decrease the overall cost, especially when the COP is very low (i.e., below 4).

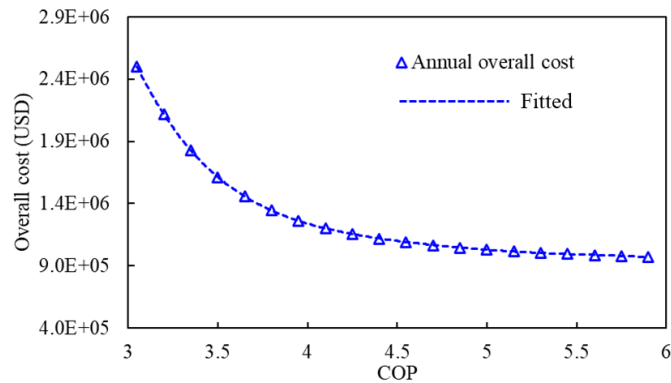


Figure 8.8 Overall cost results under different average operation COP values

## 8.4 Discussion on microgrid optimization developments considering different reliability requirements

错误!未找到引用源。 summarizes the microgrid optimization developments considering different reliability requirements. Three categories are classified to meet the different reliability requirements in microgrid optimization, where the details are stated as follows:

- For the design of the microgrid in the conventional optimization approach, the reliability is set as the constraint in the optimization, as shown in Figure 8.9 (a), where the reliability commonly is quantified by using some indexes (as shown in Table 2.2). The optimal design solution can be easily found, and the computation cost is relatively lower.
- To address the threat due to uncertainties (e.g., solar radiation, wind velocity, cooling load, etc.), we conducted the uncertainty-based optimization (also called robust optimization) by using a stochastic optimization method, as shown in Figure 8.9 (b). Setting the constraints of the reliability in the design optimization is to meet the reliability requirements under the uncertainty-based scenarios.
- To further enhance the reliability, the risk of the power supply inadequacy

considering the supply-demand uncertainties is quantified. This type of robust optimization not only sets reliability constraints in the optimization but also sets the quantified risk as to the penalty cost in the final objective of the optimization, as shown in Figure 8.9 (c). It can effectively provide different optimization results under different reliability requirements by setting power adequacy risk costs for the decision-makers.

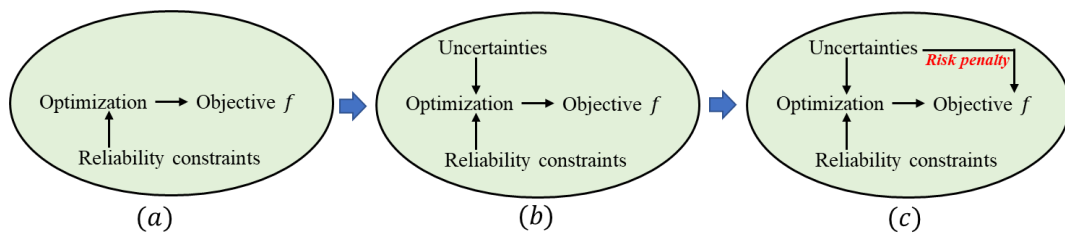


Figure 8.9 Summary of the microgrid optimization developments considering different reliability requirements

## 8.5 Summary

This chapter develops a novel robust optimal design method for islanded microgrids and compares it with several typical microgrid optimal design methods. Two objective functions are tested, and their applicability and difference are analyzed. Energy use efficiency is involved in the optimal microgrid design. The power inadequacy risk is quantified and transferred as the penalty cost. To present the advantages of the proposed robust optimal design method, we tested the robust optimal design solution in a vacation hotel microgrid on an island in Hong Kong and compared it to the design results from several typical optimal design methods via simulations.

## **CHAPTER 9 CONCLUSIONS AND FUTURE WORK**

This chapter consists of three sections. The main contributions of this thesis are summarized in Section 9.1. Section 9.2 presents the conclusions of the studies presented in this thesis. Recommendations for future work are presented in Section 9.3.

### **9.1 Summary of main contributions**

This thesis presents a comprehensive study of the performance assessments and optimal design of microgrids in subtropical regions. Based on characteristics of energy demands and power generation in subtropical regions, the basic hotel microgrid and its main equipment are determined, and the mathematical models for this system are developed. The main contributions can be summarized as follows:

1. A multi-dimensional performance assessment approach of the microgrid is proposed by adopting the empirical cost model using the LHS method, where the impacts of reliability enhancement and renewable energy penetration on system economics are quantified. The correlation among three key indicators (i.e., reliability, renewable energy penetration, and economics) of the microgrid system performance at the planning stage is quantified and analyzed comprehensively. The computation cost of the assessment framework can be significantly reduced while offering acceptable accuracy.
2. This quantitative approach for security assessment is proposed to quantify microgrid blackout risk and system wear potential. The microgrid blackout risk is quantified considering the correlation between the microgrid capacity and chiller motor capacity,

and the inrush current shock also quantifies system wear potential during chiller startup.

3. A coordinated optimal design method of microgrids is proposed for enhanced reliability and economics, which coordinates the design optimization of supply and demand systems. Power supply adequacy and system security are both assessed using a quantitative approach and considered as the optimization constraints in the design.

4. A novel uncertainty-based quantitative approach is developed for the reliability assessment of islanded microgrids by considering uncertainties on both supply and demand sides. A new reliability performance index (i.e., power inadequacy risk) is proposed, and a risk quantification method is developed for the uncertainty-based reliability assessment to measure the probability of power inadequacy under uncertainties. The supply and demand-side uncertainties are both detailedly quantified using a bottom-up approach to improve the prediction accuracy.

5. A novel robust optimal design method of the islanded microgrid is proposed considering the uncertainties simultaneously at both supply and demand sides. A new reliability indicator (i.e., power inadequacy risk) is considered to quantify the risk of power supply inadequacy due to uncertainties and is used in the proposed optimal design to enhance reliability.

## **9.2 Conclusions**

### ***A multi-dimensional performance assessment framework for microgrids concerning renewable penetration, reliability, and economics***

The proposed assessment framework overcomes the limitations of the previous assessment methods, which mainly consider the impact of one performance indicator

on another. Instead, it considers the three key performance indicators considered simultaneously. The insights given by the proposed assessment framework provide essential quantitative correlations of three key performance indicators, as practical guidelines, for making decisions at the planning stage of microgrid systems. These quantitative correlations can also provide valuable guidance for further investigation and optimization at the design and operation stages. Besides, according to the results and experience of the tests, the main findings can be concluded as follows:

- The proposed assessment framework can effectively quantify the correlations among reliability, renewable energy penetration, and economics under different microgrid energy portfolios. For example, the minimum overall cost is  $2 \times 10^6$  USD considering different microgrid energy portfolios if high microgrid reliability (above 90%) and renewable energy penetration (above 90%) are expected.
- The empirical cost model can provide the comprehensive economic performance of the system under different energy portfolios. This model can determine maximum and minimum costs under the different microgrid energy portfolios with expectations on microgrid reliability and renewable energy penetration. The case study results show that the cost-saving potential is significant, and the cost-saving is up to 37.5% if the reliability and renewable energy penetration are met at nearly 100%.
- The empirical cost model developed by the LHS method is assessed and compared with the reference model developed using the conventional exhaustive searching method. The computation cost reduction of the proposed model is about 80%, and the relative error of the proposed model prediction is reduced by 20%.

***A quantitative approach and simplified generic transient motor startup power models for microgrids security assessment***

- Microgrid blackout risk and system wear potential are negligible, with a small motor capacity ratio. With a large motor capacity ratio (i.e., over 29%), inrush current can lead to a very high risk of microgrid blackout.
- A motor capacity ratio of 8% is recommended as a limit for individual motors using direct startup. If the motor capacity ratio is above this limit, inrush current due to motor startup can lead to a significant risk of microgrid blackout. A star-delta starting or soft starting mode for motors is needed to keep microgrid blackout risk low.
- Two simplified generic transient startup power models are developed for motors and chillers based on the ANOVA method to quantify peak inrush current and startup time, respectively. The proposed models have satisfactory accuracy (i.e., an R2 higher than 80%) and are effective for inrush current quantification.
- An inrush load-embedded dynamic load profile is proposed considering both the dynamic electrical load and inrush currents of startup events in a microgrid. This profile not only can be used in microgrid security assessment but can also be used in reliable capacity design/selection at the design stage.
- Different functions of failure probability distributions are compared and evaluated. The proposed power function is more reasonable and closer to reality than the simplified linear function.
- An equivalent overloaded load is introduced according to the reference duration of 0.2 seconds. Considering both the intensity and duration of an overloaded current/load, the equivalent overloaded load can more reliably reflect the overloaded transient load in reality.

- These two major outputs of this work can effectively quantify the system security and wear potential. The vital and valuable quantitative results provide recommendations and guidelines for the decision-makers in optimal microgrid design and chiller size determination.

**Coordinated optimal design of islanded microgrids for enhanced reliability and economics based on quantitative security assessment**

- The coordinated optimal design method of the microgrid can effectively achieve a “global” optimal design solution by considering the power generation and demand-side systems as a whole and quantitatively assessing the impacts of system design on microgrid security in the optimization. As indicated by the test results, the proposed coordinated optimal method offers essential benefits, particularly for the overall performance of the entire microgrid system, although the conventional optimal design method has better performance for some individual indicators (i.e., renewable energy penetration and energy use efficiency).
- The coordinated optimal design method can provide optimal design solutions with enhanced reliability compared with the conventional method. The results show that the dynamic transient load ratio can be effectively limited within 0 to 100% of the microgrid capacity by quantifying the security and considering it as the optimization constraint. Besides, 3% of the system wear and tear potential risk can be avoided effectively.
- The coordinated optimal design method can provide a “global” optimal design solution for the entire microgrid system with reduced overall cost compared with the conventional optimal design method. The case studies show that 5% of the cost

savings can be achieved compared to conventional optimization while providing the same or improved microgrid reliability. It should be noted that the cost saving can be larger if the cost for the main electrical facilities (e.g., inverters, rectifiers, and electrical cables) in the microgrid is also considered.

***A quantitative reliability assessment and risk quantification method for microgrids considering supply and demand uncertainties***

- The proposed reliability assessment approach can provide more robust results by considering the uncertainties at both supply and demand sides compared with the conventional assessment approach. The test results show that it has a probability of 8% that the maximum outage power would be underestimated in the conventional reliability assessment. The values of the reliability performance indexes given by the proposed approach are 15%-30% higher (i.e., lower reliability) than those given by the conventional approach, which avoids the overestimation of microgrid reliability performance.
- The proposed reliability assessment approach can provide a more comprehensive reliability assessment through risk quantification, compared with conventional assessment using commonly-used reliability indexes. In addition to assessing the duration and magnitude of the power inadequacy, the proposed approach can measure the probabilities of power inadequacy under uncertainties at different time scales. The risk quantification results show that the hotel microgrid has the highest average monthly power inadequacy risk (i.e., 5.8%) in August and the highest hourly risk (i.e., 4.8%) at 9:00 p.m. in a day.
- The microgrid reliability is sensitive to the capacity of the backup power generator. The results show that increasing the backup power generation capacity can decrease the power inadequacy risk and improve reliability

performance. But a larger capacity is required to reduce the power inadequacy risk to a very low level than to satisfy the requirements of the commonly-used reliability indexes in standards.

**Robust optimal design of microgrids to enhance the reliability and economics considering the quantified power inadequacy risk**

- The power supply inadequacy risk due to uncertainties is quantified, and the cost of the power inadequacy risk is first introduced as a cost penalty in design optimization. The new measure can effectively decrease 220 times of power inadequacy risk.
- The proposed robust optimal method can achieve cost savings and enhance reliability in providing optimal design solutions for microgrids. 2.2% - 5.1% of the cost-saving can be achieved compared to other optimization cases. Meanwhile, the power inadequacy risk can decrease from 0.32% to 0.0014%.
- Simply using the typical supply-demand profiles cannot provide satisfying microgrid optimal design results. It causes a huge underestimated ratio of the overall cost (i.e., 13.7%) and poses a threat of power supply inadequacy. Besides, as for the conventional deterministic optimal design method, using constant peak load to conduct optimization can effectively enhance reliability, but the overestimated load results lead to a substantial overall cost (i.e., 16.5% of the extra cost) compared to the proposed robust optimal methods.
- The efficient chiller system has a promising potential to decrease the overall cost for the optimal microgrid design, especially when the COP is below 4. The cost saving is not simply proportional to the increased operating COP. The operating COP instead of a constant value (i.e., rated COP) is considered in the proposed

optimization, which can provide significant cost savings for the microgrid optimization design.

### **9.3 Recommendations for future work**

This study has made great efforts to develop quantitative performance assessment and design optimization approaches for microgrids, considering the impacts of uncertainties on reliability. It would be very desirable and valuable to make further efforts on the following aspects for enhancing the reliability and convenience of the methods in practical applications.

1. In this study, the developed performance assessment and optimal design approaches are all tested and verified via the simulations of a hotel microgrid instead of experiments. It is worthwhile to validate further the proposed approaches using experimental data, which requires a large amount of site or experimental data regarding microgrid blackout cases and so significant surveying or data collection is needed in the future.

2. In this study, the main equipment on the supply and demand sides of microgrids is used in microgrid security performance assessment. In practical operation, the operation and power load of microgrids are inherently unstable, which leads to uncertainties inevitably. An assessment method that takes uncertainties into account is more realistic. In the future, the variables' uncertainties, such as the dynamic cooling load, other electrical loads, and failure rates of the equipment in microgrid systems, should be studied and quantified.

3. The proposed security assessment approach can be used under different startup modes, but the transient load model needs to be developed according to the startup

mode adopted. The direct startup mode is adopted for testing the proposed assessment approach in this study because it has the most prominent startup current and may pose the greatest threat to system security. Other startup modes also need to be considered, and the corresponding transient load models should be developed in future studies.

4. In this study, as for the demand-side equipment, the chiller system, as the representative electromagnetic equipment, is solely selected in the microgrid assessments and optimal designs. Other equipment with high power consumption (such as water pumps, elevators, and so on) is not considered, which significantly affects the final choice and is an important factor in practice. This equipment, therefore, needs to be considered in future studies to achieve more comprehensive microgrid performance assessments and optimal design.

5. With the development of demand-side energy systems, new and hot concepts are emerging, including demand response, building flexibility, and machine-learning-based load management. The major demand-side power consumers, especially buildings, are required to provide more support to ensure the system's reliability and mitigate the impacts of the natural and random features of renewable power generations on the stable power supply. This results in the necessity to study the design of the integration of microgrids and those smart building energy system technologies. It is worthwhile to investigate the advantages and potential problems of this integration.

## REFERENCES

- ABB motos Low voltage general performance motors for hazardous area. (2020). Retrieved from <http://12215510215.com/rev-power/INDUSTRIAL-MOTORS/ABB%20M2JA.pdf>
- Adefarati, T., and Bansal, R. C. (2019). Reliability, economic and environmental analysis of a microgrid system in the presence of renewable energy resources. *Applied Energy*, 236, 1089-1114.
- Adefarati, T., Bansal, R. C., and Justo, J. J. (2017). Reliability and economic evaluation of a microgrid power system. *Energy Procedia*, 142, 43-48.
- Aghajani, G. R., Shayanfar, H. A., and Shayeghi, H. (2017). Demand side management in a smart micro-grid in the presence of renewable generation and demand response. *Energy*, 126, 622-637.
- Akhtar, Z., and Saqib, M. A. (2016). Microgrids formed by renewable energy integration into power grids pose electrical protection challenges. *Renewable Energy*, 99, 148-157.
- Akinyele, D. O., and Rayudu, R. K. (2016). Community-based hybrid electricity supply system: A practical and comparative approach. *Applied Energy*, 171, 608-628.
- Al-Shaalan, A. M. (2012). Reliability evaluation in generation expansion planning based on the expected energy not served. *Journal of King Saud University-Engineering Sciences*, 24(1), 11-18.
- Allan, R. N. (2013). *Reliability evaluation of power systems*: Springer Science and Business Media.
- Amir, V., and Azimian, M. (2020). Dynamic Multi-Carrier Microgrid Deployment Under Uncertainty. *Applied Energy*, 260.
- Ansari, A., and Deshpande, D. (2010). Mathematical model of asynchronous machine in MATLAB Simulink.
- Arriagada, E., Lopez, E., López, M., Blasco-Gimenez, R., Roa, C., and Poloujadoff, M. (2015). A probabilistic economic dispatch model and methodology considering renewable energy, demand and generator uncertainties. *Electric Power Systems Research*, 121, 325-332.
- Ayodele, E., Misra, S., Damasevicius, R., and Maskeliunas, R. (2019). Hybrid microgrid for microfinance institutions in rural areas – A field demonstration in West Africa. *Sustainable Energy Technologies and Assessments*, 35, 89-97.
- Babazadeh, H., Gao, W., Wu, Z., and Li, Y. (2013). *Optimal energy management of wind power generation system in islanded microgrid system*.
- Baghaee, H., Mirsalim, M., Gharehpetian, G., and Talebi, H. (2016). Reliability/cost-based multi-objective Pareto optimal design of stand-alone wind/PV/FC generation microgrid system. *Energy*, 115, 1022-1041.

- Baimel, D., Chowdhury, N., Belikov, J., and Levron, Y. (2021). New type of bridge fault current limiter with reduced power losses for transient stability improvement of DFIG wind farm. *Electric Power Systems Research*, 197.
- Balderrama, S., Lombardi, F., Riva, F., Canedo, W., Colombo, E., and Quoilin, S. (2019). A two-stage linear programming optimization framework for isolated hybrid microgrids in a rural context: The case study of the “El Espino” community. *Energy*, 188.
- Barbaro, M., and Castro, R. (2020). Design optimisation for a hybrid renewable microgrid: Application to the case of Faial island, Azores archipelago. *Renewable Energy*, 151, 434-445.
- Bechtler, H., Browne, M. W., Bansal, P. K., and Kecman, V. (2001). New approach to dynamic modelling of vapour-compression liquid chillers: Artificial neural networks. *Applied Thermal Engineering*, 21(9), 941-953.
- Bhatt, N., Sarawgi, S., O'Keefe, R., Duggan, P., Koenig, M., Leschuk, M., . . . Povolotskiy, M. (2009). *Assessing vulnerability to cascading outages*.
- Bie, Z., Zhang, P., Li, G., Hua, B., Meehan, M., and Wang, X. (2012). Reliability evaluation of active distribution systems including microgrids. *IEEE Transactions on Power Systems*, 27(4), 2342-2350.
- Blair, M. J., and Mabee, W. E. (2020). Evaluation of technology, economics and emissions impacts of community-scale bioenergy systems for a forest-based community in Ontario. *Renewable energy*, 151, 715-730.
- Bracco, S., and Delfino, F. (2017). A mathematical model for the dynamic simulation of low size cogeneration gas turbines within smart microgrids. *Energy*, 119, 710-723.
- Cameron, A. C., and Windmeijer, F. A. G. (1997). An R-squared measure of goodness of fit for some common nonlinear regression models. *Journal of Econometrics*, 77(2), 329-342.
- Campanari, S., Valenti, G., Macchi, E., Lozza, G., and Ravidà, N. (2014). Development of a micro-cogeneration laboratory and testing of a natural gas CHP unit based on PEM fuel cells. *Applied Thermal Engineering*, 71(2), 714-720.
- Cao, T., Hwang, Y., and Radermacher, R. (2017). Development of an optimization based design framework for microgrid energy systems. *Energy*, 140, 340-351.
- Cattaneo, A., Madathil, S. C., and Backhaus, S. (2018). Integration of optimal operational dispatch and controller determined dynamics for microgrid survivability. *Applied Energy*, 230, 1685-1696.
- Çetinbaş, İ., Tamyürek, B., and Demirtaş, M. (2021). Sizing optimization and design of an autonomous AC microgrid for commercial loads using Harris Hawks Optimization algorithm. *Energy Conversion and Management*, 245.
- Chen, H., Gao, L., and Zhang, Z. (2021). Multi-objective optimal scheduling of a microgrid with uncertainties of renewable power generation considering user satisfaction. *International Journal of Electrical Power & Energy Systems*, 131, 107142.

- Chen, J., Thorp, J. S., and Dobson, I. (2005). Cascading dynamics and mitigation assessment in power system disturbances via a hidden failure model. *International Journal of Electrical Power and Energy Systems*, 27(4), 318-326.
- Choi, J., Khalsa, A., Klapp, D. A., Illindala, M. S., and Subramaniam, K. (2018). Survivability of Synchronous Generator-Based Distributed Energy Resources for Transient Overload Conditions in a Microgrid. *IEEE Transactions on Industry Applications*, 54(6), 5717-5726.
- Cui, Y., Abdulsalam, S. G., Chen, S., and Xu, W. (2005). A sequential phase energization technique for transformer inrush current reduction - Part I: Simulation and experimental results. *IEEE Transactions on Power Delivery*, 20(2 I), 943-949.
- Daud, A. K., and Ismail, M. S. (2012). Design of isolated hybrid systems minimizing costs and pollutant emissions. *Renewable Energy*, 44, 215-224.
- Ding, X., Sun, W., Harrison, G. P., Lv, X., and Weng, Y. (2020). Multi-objective optimization for an integrated renewable, power-to-gas and solid oxide fuel cell/gas turbine hybrid system in microgrid. *Energy*, 213.
- DOE, (2017), Microgrid. Retrieved from: <https://energy.gov/oe>
- Domenech, B., Ferrer-Martí, L., and Pastor, R. (2015). Including management and security of supply constraints for designing stand-alone electrification systems in developing countries. *Renewable energy*, 80, 359-369.
- EEA. (2022). Decarbonisation of Energy 2022: Determining a robust mix of energy carriers for a carbon-neutral EU. Retrieved from: [https://www.europarl.europa.eu/RegData/etudes/STUD/2021/695469/IPOL\\_STU\(2021\)695469\\_EN.pdf](https://www.europarl.europa.eu/RegData/etudes/STUD/2021/695469/IPOL_STU(2021)695469_EN.pdf)
- Elkadeem, M., Wang, S., Azmy, A. M., Atiya, E. G., Ullah, Z., and Sharshir, S. W. (2020). A systematic decision-making approach for planning and assessment of hybrid renewable energy-based microgrid with techno-economic optimization: A case study on an urban community in Egypt. *Sustainable Cities and Society*, 54, 102013.
- Endo, F., Kanamitsu, M., Kojima, H., Hayakawa, N., and Okubo, H. (2007). *Optimum operation and maintenance of power grid based on equipment diagnoses*. Paper presented at the 2007 IEEE Lausanne Power Tech.
- Faiz, J., Ebrahimi, B. M., and Noori, T. (2008). Three- and two-dimensional finite-element computation of inrush current and short-circuit electromagnetic forces on windings of a three-phase core-type power transformer. *IEEE Transactions on Magnetics*, 44(5), 590-597.
- Fan, C., and Ding, Y. (2019). Cooling load prediction and optimal operation of HVAC systems using a multiple nonlinear regression model. *Energy and Buildings*, 197, 7-17.
- Fioriti, D., Pintus, S., Lutzemberger, G., and Poli, D. (2020). Economic multi-objective approach to design off-grid microgrids: A support for business decision making. *Renewable energy*, 159, 693-704.

- Flores, R. J., and Brouwer, J. (2018). Optimal design of a distributed energy resource system that economically reduces carbon emissions. *Applied Energy*, 232, 119-138.
- Florio, P., Peronato, G., Perera, A., Di Blasi, A., Poon, K. H., and Kämpf, J. H. (2021). Designing and assessing solar energy neighborhoods from visual impact. *Sustainable Cities and Society*, 71, 102959.
- Florio, P., Peronato, G., Perera, A. T. D., Di Blasi, A., Poon, K. H., and Kämpf, J. H. (2021). Designing and assessing solar energy neighborhoods from visual impact. *Sustainable Cities and Society*, 71.
- Fong, K., and Lee, C. (2015). Performance analysis of internal-combustion-engine primed trigeneration systems for use in high-rise office buildings in Hong Kong. *Applied energy*, 160, 793-801.
- Fontenot, H., and Dong, B. (2019). Modeling and control of building-integrated microgrids for optimal energy management – A review. *Applied Energy*, 254.
- Gang, W., Augenbroe, G., Wang, S., Fan, C., and Xiao, F. (2016). An uncertainty-based design optimization method for district cooling systems. *Energy*, 102, 516-527.
- Gang, W., Wang, S., Augenbroe, G., and Xiao, F. (2016). Robust optimal design of district cooling systems and the impacts of uncertainty and reliability. *Energy and Buildings*, 122, 11-22.
- Gang, W., Wang, S., Gao, D., and Xiao, F. (2015). Performance assessment of district cooling systems for a new development district at planning stage. *Applied Energy*, 140, 33-43.
- Gang, W., Wang, S., Xiao, F., and Gao, D. (2015). Robust optimal design of building cooling systems considering cooling load uncertainty and equipment reliability. *Applied energy*, 159, 265-275.
- Gang, W., Wang, S., Xiao, F., and Gao, D. C. (2015). Robust optimal design of building cooling systems considering cooling load uncertainty and equipment reliability. *Applied Energy*, 159, 265-275.
- Gang, W., Wang, S., Xiao, F., and Gao, D. C. (2016). District cooling systems: Technology integration, system optimization, challenges and opportunities for applications. *Renewable and Sustainable Energy Reviews*, 53, 253-264.
- Ganjehlou, H. G., Niaei, H., Jafari, A., Aroko, D. O., Marzband, M., and Fernando, T. (2020). A novel techno-economic multi-level optimization in home-microgrids with coalition formation capability. *Sustainable Cities and Society*, 60, 102241.
- Garcia, R. S., and Weisser, D. (2006). A wind–diesel system with hydrogen storage: Joint optimisation of design and dispatch. *Renewable Energy*, 31(14), 2296-2320.
- Garcia, R. S., and Weisser, D. J. R. e. (2006). A wind–diesel system with hydrogen storage: Joint optimisation of design and dispatch. 31(14), 2296-2320.

- Giraldez, J. (October 2018). Phase I Microgrid Cost Study: Data Collection and Analysis of Microgrid Costs in the United States. Retrieved from <https://www.nrel.gov/docs/fy19osti/67821.pdf>
- Giraldez Miner, J. I., Flores-Espino, F., MacAlpine, S., and Asmus, P. (2018). *Phase I microgrid cost study: Data collection and analysis of microgrid costs in the United States*. Retrieved from <https://doi.org/10.2172/1477589>
- Gómez-Hernández, D. F., Domenech, B., Moreira, J., Farrera, N., López-González, A., and Ferrer-Martí, L. (2019). Comparative evaluation of rural electrification project plans: A case study in Mexico. *Energy policy*, 129, 23-33.
- Gupta, S., and Kekatos, V. (2016). *Real-time operation of heterogeneous energy storage units*. Paper presented at the 2016 IEEE Global Conference on Signal and Information Processing (GlobalSIP).
- Hemmati, R., Mehrjerdi, H., and Nosratabadi, S. M. (2021). Resilience-oriented adaptable microgrid formation in integrated electricity-gas system with deployment of multiple energy hubs. *Sustainable Cities and Society*, 71.
- Henneaux, P. (2015). Probability of failure of overloaded lines in cascading failures. *International Journal of Electrical Power and Energy Systems*, 73, 141-148.
- Her, C., Sambor, D. J., Whitney, E., and Wies, R. (2021). Novel wind resource assessment and demand flexibility analysis for community resilience: A remote microgrid case study. *Renewable energy*, 179, 1472-1486.
- High-efficiency three-phase induction motors LSES-FLSES-PLSES. (2013). Retrieved from <https://suministrossercoin.com/pdf/catalogo-LS-LSES-FLSES-PLSES.pdf>
- Hwang, C. C., and Lou, J. N. (1998). Transient analysis of capacitance switching for industrial power system by PSpice. *Electric Power Systems Research*, 45(1), 29-38.
- IEA. (2020). An Energy Sector Roadmap to Carbon Neutrality in China <https://www.iea.org/reports/an-energy-sector-roadmap-to-carbon-neutrality-in-china>
- IPCC. (2014). Climate Change 2014: Mitigation of Climate Change. Retrieved from: <http://www.ipcc.ch/report/ar5/wg3/>
- Isatezde, E., Muhsindemir, M., Gurel, F., Ibrahimokumus, H., and Kahveci, H. (2018). *Two-Stage Power Converter Design and Control for Renewable Energy Systems*.
- Jia, X., Tso, C. P., Chia, P. K., and Jolly, P. (1995). A distributed model for prediction of the transient response of an evaporator. *International Journal of Refrigeration*, 18(5), 336-342.
- Jimada-Ojuolape, B., and Teh, J. (2020). Surveys on the reliability impacts of power system cyber-physical layers. *Sustainable Cities and Society*, 62, 102384.
- Jin, T., and Jimenez, J. A. (2010). *A review on planning and automation technologies for distributed generation systems*.
- Kang, J., and Wang, S. (2018). Robust optimal design of distributed energy systems based on life-cycle performance analysis using a probabilistic approach

- considering uncertainties of design inputs and equipment degradations. *Applied Energy*, 231, 615-627.
- Kang, J., Wang, S., and Gang, W. (2017). Performance of distributed energy systems in buildings in cooling dominated regions and the impacts of energy policies. *Applied Thermal Engineering*, 127, 281-291.
- Kharrich, M., Mohammed, O. H., Alshammari, N., and Akherraz, M. (2021). Multi-objective optimization and the effect of the economic factors on the design of the microgrid hybrid system. *Sustainable Cities and Society*, 65, 102646.
- Khederzadeh, M. (2010). Mitigation of the impact of transformer inrush current on voltage sag by TCSC. *Electric Power Systems Research*, 80(9), 1049-1055.
- Khodaei, A., and Shahidehpour, M. (2012). Microgrid-based co-optimization of generation and transmission planning in power systems. *IEEE Transactions on Power systems*, 28(2), 1582-1590.
- Khodaei, A., and Shahidehpour, M. J. I. t. o. p. s. (2012). Microgrid-based co-optimization of generation and transmission planning in power systems. 28(2), 1582-1590.
- Kiptoo, M. K., Lotfy, M. E., Adewuyi, O. B., Conteh, A., Howlader, A. M., and Senjyu, T. (2020). Integrated approach for optimal techno-economic planning for high renewable energy-based isolated microgrid considering cost of energy storage and demand response strategies. *Energy Conversion and Management*, 215.
- Kuznetsova, E., Li, Y.-F., Ruiz, C., and Zio, E. (2014). An integrated framework of agent-based modelling and robust optimization for microgrid energy management. *Applied energy*, 129, 70-88.
- Lasseter, R. H., and Paigi, P. (2004). *Microgrid: A conceptual solution*.
- Lee, S. T. (2008). *Estimating the probability of cascading outages in a power grid*.
- Li, G. (2000). Feasibility of large scale offshore wind power for Hong Kong - A preliminary study. *Renewable Energy*, 21(3-4), 387-402.
- Li, H., and Wang, S. (2019). Coordinated optimal design of zero/low energy buildings and their energy systems based on multi-stage design optimization. *Energy*, 189.
- Li, H., Wang, S., and Tang, R. (2019). Robust optimal design of zero/low energy buildings considering uncertainties and the impacts of objective functions. *Applied Energy*, 254, 113683.
- Li, X., Zhang, X., Wu, L., Lu, P., and Zhang, S. (2015). Transmission Line Overload Risk Assessment for Power Systems with Wind and Load-Power Generation Correlation. *IEEE Transactions on Smart Grid*, 6(3), 1233-1242.
- Liu, H. C., Liu, L., and Liu, N. (2013). Risk evaluation approaches in failure mode and effects analysis: A literature review. *Expert Systems with Applications*, 40(2), 828-838.
- Lu, L., Yang, H., and Burnett, J. (2002). Investigation on wind power potential on Hong Kong islands - An analysis of wind power and wind turbine characteristics. *Renewable Energy*, 27(1), 1-12.

- Lu, Y., Wang, S., Yan, C., and Shan, K. (2015). Impacts of renewable energy system design inputs on the performance robustness of net zero energy buildings. *Energy*, 93, 1595-1606.
- Lu, Y., Wang, S., Zhao, Y., and Yan, C. (2015). Renewable energy system optimization of low/zero energy buildings using single-objective and multi-objective optimization methods. *Energy and Buildings*, 89, 61-75.
- Luo, J., Li, H., and Wang, S. (2022). A quantitative approach and simplified generic transient motor startup power models for microgrids security assessment. *Sustainable Cities and Society*, 103998.
- Luo, J. T., Joybari, M. M., Panchabikesan, K., Haghghat, F., Moreau, A., and Robichaud, M. (2020). Parametric study to maximize the peak load shifting and thermal comfort in residential buildings located in cold climates. *Journal of Energy Storage*, 30.
- Luo, J. T., Joybari, M. M., Panchabikesan, K., Sun, Y., Haghghat, F., Moreau, A., and Robichaud, M. (2020). Performance of a self-learning predictive controller for peak shifting in a building integrated with energy storage. *Sustainable Cities and Society*, 60.
- Maleki, A., and Askarzadeh, A. (2014). Artificial bee swarm optimization for optimum sizing of a stand-alone PV/WT/FC hybrid system considering LPSP concept. *Solar Energy*, 107, 227-235.
- Mashayekh, S., Stadler, M., Cardoso, G., Heleno, M., Madathil, S. C., Nagarajan, H., . . . Wang, J. (2018). Security-Constrained Design of Isolated Multi-Energy Microgrids. *IEEE Transactions on Power systems*, 33(3), 2452-2462.
- Mehleri, E. D., Sarimveis, H., Markatos, N. C., and Papageorgiou, L. G. (2013). Optimal design and operation of distributed energy systems: Application to Greek residential sector. *Renewable Energy*, 51, 331-342.
- Mendes, G., Ioakimidis, C., and Ferrão, P. (2011). On the planning and analysis of Integrated Community Energy Systems: A review and survey of available tools. *Renewable and Sustainable Energy Reviews*, 15(9), 4836-4854.
- Mengelkamp, E., Gärttner, J., Rock, K., Kessler, S., Orsini, L., and Weinhardt, C. (2018). Designing microgrid energy markets: A case study: The Brooklyn Microgrid. *Applied energy*, 210, 870-880.
- Mohanty, P., Bhuvanewari, G., and Balasubramanian, R. (2012). *Optimal planning and design of distributed generation based micro-grids*.
- Morato, M. M., Vergara-Dietrich, J., Esparcia, E. A., Jr., Ocon, J. D., and Normey-Rico, J. E. (2021). Assessing demand compliance and reliability in the Philippine off-grid islands with Model Predictive Control microgrid coordination. *Renewable Energy*, 179, 1271-1290.
- Muhtadi, A., Pandit, D., Nguyen, N., and Mitra, J. (2021). Distributed energy resources based microgrid: Review of architecture, control, and reliability. *IEEE Transactions on Industry Applications*.
- Nedic, D. P. (2003). Simulation of large system disturbances. *the University of Manchester Institute for Science and Technology*.

- NY Prize, (2015), Microgrid 101. Retrieved from: <https://www.nyserda.ny.gov/All-Programs/NY-Prize/Resources-for-applicants/Microgrids-101>
- O'Shaughnessy, E., Cutler, D., Ardani, K., and Margolis, R. (2018). Solar plus: A review of the end-user economics of solar PV integration with storage and load control in residential buildings. *Applied Energy*, 228, 2165-2175.
- Obara, S., Sato, K., and Utsugi, Y. (2018). Study on the operation optimization of an isolated island microgrid with renewable energy layout planning. *Energy*, 161, 1211-1225.
- Pecenak, Z. K., Stadler, M., Mathiesen, P., Fahy, K., and Kleissl, J. (2020). Robust design of microgrids using a hybrid minimum investment optimization. *Applied Energy*, 276, 115400.
- Piwko, R., Meibom, P., Holttinen, H., Shi, B., Miller, N., Chi, Y., and Wang, W. (2012). Penetrating insights: Lessons learned from large-scale wind power integration. *IEEE Power and Energy Magazine*, 10(2), 44-52.
- Polleux, L., Guerassimoff, G., Marmorat, J.-P., Sandoval-Moreno, J., and Schuhler, T. (2022). An overview of the challenges of solar power integration in isolated industrial microgrids with reliability constraints. *Renewable and Sustainable Energy Reviews*, 155, 111955.
- Quashie, M., Marnay, C., Bouffard, F., and Joós, G. (2018). Optimal planning of microgrid power and operating reserve capacity. *Applied energy*, 210, 1229-1236.
- Rashid, M. H. (2011). *Power Electronics Handbook*: Elsevier Inc.
- Recalde, A. A., and Alvarez-Alvarado, M. S. (2020). Design optimization for reliability improvement in microgrids with wind-tidal-photovoltaic generation. *Electric Power Systems Research*, 188, 106540.
- Sabzehgar, R., Amirhosseini, D. Z., and Rasouli, M. (2020). Solar power forecast for a residential smart microgrid based on numerical weather predictions using artificial intelligence methods. *Journal of Building Engineering*, 32, 101629.
- Sabzehgar, R., Kazemi, M., Rasouli, M., and Fajri, P. (2020). Cost optimization and reliability assessment of a microgrid with large-scale plug-in electric vehicles participating in demand response programs. *International Journal of Green Energy*, 17(2), 127-136.
- Sarkar, S., and Ajjarapu, V. (2011). MW resource assessment model for a hybrid energy conversion system with wind and solar resources. *IEEE transactions on sustainable energy*, 2(4), 383-391.
- Sarkar, T., Bhattacharjee, A., Samanta, H., Bhattacharya, K., and Saha, H. (2019). Optimal design and implementation of solar PV-wind-biogas-VRFB storage integrated smart hybrid microgrid for ensuring zero loss of power supply probability. *Energy conversion and management*, 191, 102-118.
- Sekhar, P. C., Deshpande, R., and Sankar, V. (2016). *Evaluation and improvement of reliability indices of electrical power distribution system*. Paper presented at the 2016 National Power Systems Conference (NPSC).

- Shaaban, M. F., Ahmed, M. H., El-Fouly, T. H. M., and Salama, M. M. A. (2015). *Impact of integrating PEV and renewable sources on power system reliability assessment*.
- Shi, R., Li, S., Zhang, P., and Lee, K. Y. (2020). Integration of renewable energy sources and electric vehicles in V2G network with adjustable robust optimization. *Renewable energy*, 153, 1067-1080.
- Shuai, Z., Sun, Y., Shen, Z. J., Tian, W., Tu, C., Li, Y., . . . Reviews, S. E. (2016). Microgrid stability: Classification and a review. 58, 167-179.
- Siemens electric motors. (2021). Retrieved from <https://new.siemens.com/in/en/products/drives/electric-motors.html>
- Song, X., Zhao, Y., Zhou, J., and Weng, Z. (2019). Reliability varying characteristics of PV-ESS-based standalone microgrid. *IEEE Access*, 7, 120872-120883.
- Suman, G. K., Guerrero, J. M., and Roy, O. P. (2021). Optimisation of solar/wind/bio-generator/diesel/battery based microgrids for rural areas: A PSO-GWO approach. *Sustainable Cities and Society*, 67, 102723.
- Sun, S., Dong, M., and Liang, B. (2015). Distributed real-time power balancing in renewable-integrated power grids with storage and flexible loads. *IEEE Transactions on Smart Grid*, 7(5), 2337-2349.
- Sun, Y., Wang, S., Xiao, F., and Gao, D. (2013). Peak load shifting control using different cold thermal energy storage facilities in commercial buildings: A review. *Energy Conversion and Management*, 71, 101-114.
- Tayal, D. (2017). Achieving high renewable energy penetration in Western Australia using data digitisation and machine learning. *Renewable and Sustainable Energy Reviews*, 80, 1537-1543.
- Thomas, D., Deblecker, O., and Ioakimidis, C. S. (2016). Optimal design and techno-economic analysis of an autonomous small isolated microgrid aiming at high RES penetration. *Energy*, 116, 364-379.
- Tomin, N., Shakirov, V., Kozlov, A., Sidorov, D., Kurbatsky, V., Rehtanz, C., and Lora, E. E. (2022). Design and optimal energy management of community microgrids with flexible renewable energy sources. *Renewable energy*, 183, 903-921.
- Tomin, N., Shakirov, V., Kozlov, A., Sidorov, D., Kurbatsky, V., Rehtanz, C., and Lora, E. E. S. (2022). Design and optimal energy management of community microgrids with flexible renewable energy sources. *Renewable Energy*, 183, 903-921.
- Ton, D. T., and Smith, M. A. (2012). The US department of energy's microgrid initiative. *The Electricity Journal*, 25(8), 84-94.
- Venkateswari, R., and Sreejith, S. (2019). Factors influencing the efficiency of photovoltaic system. 101, 376-394.
- Wouters, C., Fraga, E. S., and James, A. M. (2016). Residential Microgrid Design Optimisation under Uncertain  $\mu$ CHP Characteristics. In *Computer Aided Chemical Engineering* (Vol. 38, pp. 1491-1496): Elsevier.

- Wu, H., Liu, X., and Ding, M. (2014). Dynamic economic dispatch of a microgrid: Mathematical models and solution algorithm. *International Journal of Electrical Power and Energy Systems*, 63, 336-346.
- Wu, R., and Sansavini, G. (2020). Integrating reliability and resilience to support the transition from passive distribution grids to islanding microgrids. *Applied Energy*, 272, 115254.
- Xu, X., Mitra, J., Wang, T., and Mu, L. (2014). Evaluation of operational reliability of a microgrid using a short-term outage model. *IEEE Transactions on Power Systems*, 29(5), 2238-2247.
- Xu, Z., Nthontho, M., and Chowdhury, S. (2016). Rural electrification implementation strategies through microgrid approach in South African context. *International Journal of Electrical Power and Energy Systems*, 82, 452-465.
- Yamchi, H. B., Shahsavari, H., Kalantari, N. T., Safari, A., and Farrokhifar, M. (2019). A cost-efficient application of different battery energy storage technologies in microgrids considering load uncertainty. *Journal of Energy Storage*, 22, 17-26.
- Yang, Z., Ghadamyari, M., Khorramdel, H., Alizadeh, S. M. S., Pirouzi, S., Milani, M., . . . Ghadimi, N. (2021). Robust multi-objective optimal design of islanded hybrid system with renewable and diesel sources/stationary and mobile energy storage systems. *Renewable and Sustainable Energy Reviews*, 148, 111295.
- Yin, M., Li, K., and Yu, J. (2022). A data-driven approach for microgrid distributed generation planning under uncertainties. *Applied Energy*, 309, 118429.
- Yu, J., Marnay, C., Jin, M., Yao, C., Liu, X., and Feng, W. (2018). Review of microgrid development in the United States and China and lessons learned for China. *Energy Procedia*, 145, 217-222.
- Yu, N., Kang, J.-S., Chang, C.-C., Lee, T.-Y., and Lee, D.-Y. (2016). Robust economic optimization and environmental policy analysis for microgrid planning: An application to Taichung Industrial Park, Taiwan. *Energy*, 113, 671-682.
- Zhang, B., Li, Q., Wang, L., and Feng, W. (2018). Robust optimization for energy transactions in multi-microgrids under uncertainty. *Applied Energy*, 217, 346-360.
- Zhang, G., Cao, Y., Cao, Y., Li, D., and Wang, L. (2017). Optimal energy management for microgrids with combined heat and power (CHP) generation, energy storages, and renewable energy sources. *Energies*, 10(9), 1288.
- Zheng, C., Wu, J., Zhai, X., and Wang, R. J. A. E. (2016). Impacts of feed-in tariff policies on design and performance of CCHP system in different climate zones. *175*, 168-179.
- Zheng, C. Y., Wu, J. Y., Zhai, X. Q., and Wang, R. Z. (2016). Impacts of feed-in tariff policies on design and performance of CCHP system in different climate zones. *Applied Energy*, 175, 168-179.
- Zhou, Y., and Cao, S. (2019). Energy flexibility investigation of advanced grid-responsive energy control strategies with the static battery and electric vehicles: A case study of a high-rise office building in Hong Kong. *Energy Conversion and Management*, 199, 111888.

- Zhuang, C., Shan, K., and Wang, S. (2021). Coordinated demand-controlled ventilation strategy for energy-efficient operation in multi-zone cleanroom air-conditioning systems. *Building and Environment*, 191.
- Zhuang, C., Wang, S., and Shan, K. (2020). A risk-based robust optimal chiller sequencing control strategy for energy-efficient operation considering measurement uncertainties. *Applied Energy*, 280, 115983.
- Zima, M., and Andersson, G. (2005). *On security criteria in power systems operation*.